Variation Analysis of Cold Rolled Steel Manufacturing

by

Kan Ota

B.S., Mechanical Engineering, Cornell University, 1997
M.Eng, Electrical Engineering, Cornell University, 1997

Submitted to the Department of Mechanical Engineering in
Partial Fulfillment of the Requirements for the Degree of

Doctor of Philosophy

at the

Massachusetts Institute of Technology
September 2000

Signature of Author: _____
Department of Mechanical Engineering
August 21, 2000

Certified By: _____
Kevin N. Otto
Robert Noyce Career Development Associate Professor of Mechanical Engineering
Committee Chairman

Accepted By: _____
Ain A. Sonin
Professor of Mechanical Engineering
Chairman, Departmental Graduate Committee

Variation Analysis of Cold Rolled Steel Manufacturing

by

Kan Ota

Submitted to the Department of Mechanical Engineering on August 21, 2000

in partial fulfillment of the Requirements for the Degree of

Doctor of Philosophy in Mechanical Engineering

Abstract

This thesis develops an integrated system model for a continuous cold rolling manufacturing process. Variation in the centerline strip thickness has been a major quality concern in the steel industry. Large variations can cause failure in downstream processes, such as jamming in stamping steps. The goal of this thesis is to determine the impact of the manufacturing system variation on output thickness, and to predict the strip thickness variation prior to production. Traditionally, statistical approaches have been adopted for such applications. A statistical model has also been developed in this thesis using the Principal Component Analysis. Even though it calibrates well, this model cannot be used as a predictive model. Output thickness variation is mapped to variations in process variables, which cannot be determined prior to production. To solve this problem, the concept of an Integrated System Modeling (ISM) is utilized in this thesis. ISM is a physics-based modeling technique, and it has been proven effective in determining sensitivity of the output to process variables in a manufacturing system consisting of multiple operations. This technique was originally developed for discrete manufacturing systems. Besides applying this technique to a continuous manufacturing system, other improvements have been made to this modeling technique. First, an algorithm is developed in this thesis to determine the frequency at which the model should be calibrated. Second, Monte-Carlo simulation is used to determine the sensitivity between output and process variables in the system. This avoids the limitation of Taylor series linearization around an operating point. Third, the controllers used in the manufacturing system are included in the model. This allows prediction of process variables, and hence a predictive model based solely on the input properties of the manufacturing system can be built. A virtual mill that predicts output thickness of the cold mill with geometric and material properties of the input steel strip is constructed. The model predicts output thickness variation to within 15% from that measured at 1Hz. Sensitivity analysis on this model identified that the input thickness variation is the largest contributor in exit thickness variation below 1Hz.

Thesis Committee: Prof. Kevin N. Otto, Chairman
Prof. David E. Hardt
Prof. Anna C. Thornton

Acknowledgements

First, I would like to thank my advisor, Professor Kevin Otto, for all his guidance and help throughout my doctoral program. I would also like to express thanks to my thesis committee, Professor Anna Thornton and Professor David Hardt, for their advice.

Second, I would like to thank my parents and my brother, Masu, for their encouragement and confidence in me. I would also like to thank Ivy for her support.

Third, I would like to express my gratefulness to the fellow students and professors at MIT who helped me during my doctoral program. Special thanks go to my lab mates at room 3-436 and 3-438, for making a friendly and comfortable environment, and especially to Rajiv Suri and Javier Gonzalez-Zugasti for their direction.

Finally, I would like to thank the sponsor of this thesis for providing the resources. I appreciate the people who spent time to explain their processes and provide me with the invaluable data for this project.

Table of Contents

Chapter 1: Introduction

Over the past few decades the expectations for quality in manufactured products has increased steadily. One important aspect of quality is the consistency of product specifications. Thus the manufacturing industry has responded by developing techniques to reduce the variations in products, leading to significant improvements in performance. Statistical approaches are one category of methods that have been successfully used to target and reduce variations in manufacturing processes. Examples of effective statistical approaches include the 6-sigma production and SPC. Implementation of SPC has resulted in significant improvements in quality. However, despite these advances in variation reduction, it has become increasingly difficult to identify the causes of quality loss, due to the growing complexity of manufacturing systems. Therefore, new techniques to detect and control variations in production are necessary.

One technique that has been introduced to specifically address complex manufacturing systems is the physics-based Integrated System Model (ISM). This model maps the system inputs and operating parameters to the system outputs. It has been successfully applied to various systems to identify major sources of variation and to evaluate different variation reduction strategies.

However, previous applications of ISM have been limited to discrete manufacturing, where each work piece is processed independently from the previous and successive pieces, and where the quality is defined by the performance of the individual work piece. In many situations, manufacturing systems are not discrete but rather the work piece is passed from one production line to another. There exist many opportunities for variations to accumulate. This research project proposes to expand ISM to a continuous manufacturing system in order to deal with the variations that are passed from one processing unit to the next. By applying ISM to continuous manufacturing systems, one can significantly increase the scope of the modeling capability. The specific continuous system that is studied in this thesis is cold rolled steel production.

The steel industry enjoyed phenomenal growth during the 1970's. However, due to fierce competition and over-capacity, steel companies must compete heavily on price and quality. The most important determinant of quality of cold-rolled steel is the centerline exit thickness variation. Reducing this variation would lead to a considerable improvement in product performance.

This thesis performs variation analysis to identify the sources of variation in centerline exit thickness of cold rolled steel strips, the prime component of steel strip quality. The sensitivity between the total output variation and the variations in each processing step are investigated, in order to assess the contribution of each step toward the overall variation. Furthermore, a model is constructed to predict output thickness variation without actual processing of the strip. In this way, variables that can potentially affect the output thickness can be identified before the strip is processed. An ultimate application for this variation prediction model is to avoid processing steel strips that are likely to have high output thickness variation. The overall quality of the steel strips would therefore be improved.

The achievements in this thesis are:

1. Developed Monte Carlo methods to analyze variation on continuous manufacturing processes. (Chapter 7)
2. Included the influences of on-line controllers in a variation prediction model. (Chapter 6)
3. Developed sufficient sampling frequency criteria for process variables to capture data stream variance. (Chapter 4)
4. Built a statistical variation model of cold rolling stand with Principal Component Analysis. (Chapter 2)
5. Performed sensitivity analysis using the Monte-Carlo simulation of the large manufacturing system (cold mill). (Chapter 7)

1.1 Flat-Rolled Steel Production

About half of the rolled steel products made in the United States are flat-rolled. (Roberts 1987) The flat rolling manufacturing of steel has been developed since the nineteenth century and has evolved into a complex series of processes. The processes include blast furnace, hot rolling, pickling, cold rolling, and galvanizing.

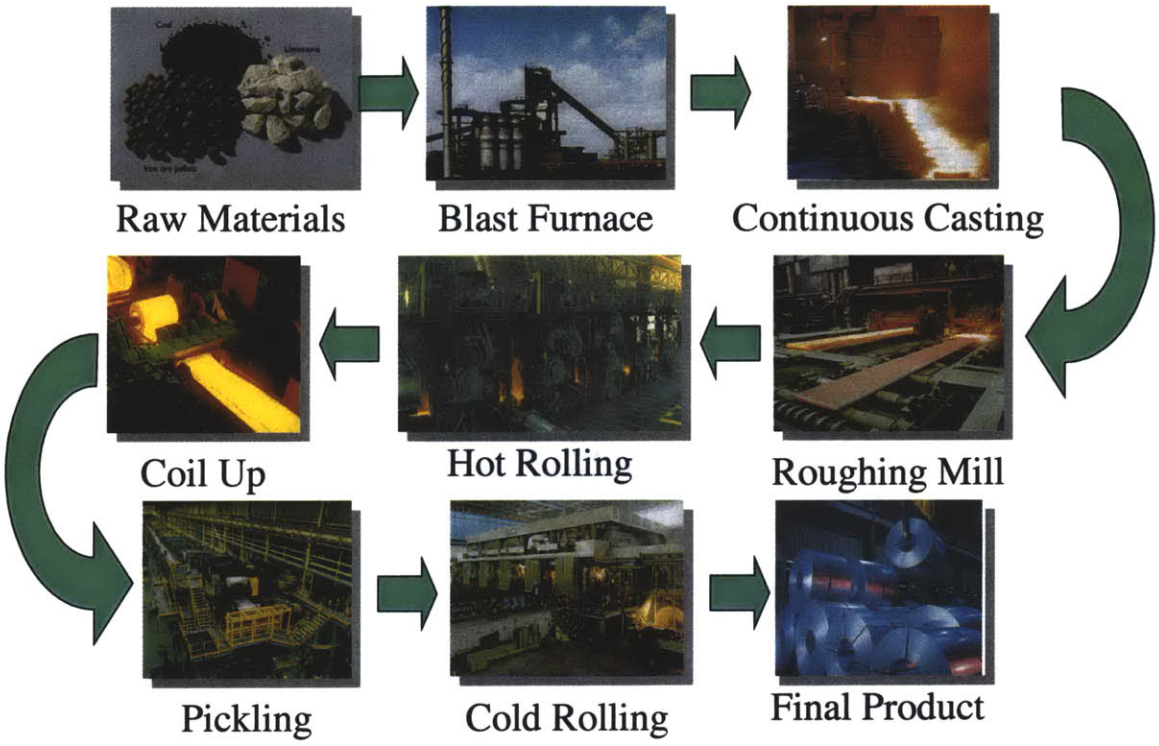

Figure 1.1 Flat Rolled Steel Manufacturing Process[1]

To produce steel, first iron ore pellets are melted in a blast furnace. Coke and oil are used to generate the energy in the furnace and limestone is used to remove impurities. Proper chemicals are then added to the molten iron at specific temperatures to produce the desired alloys in ladle metallurgy facilities. This stage determines the material properties and the grade of the product. Low-carbon steel has less than 0.1% of carbon and 0.2% to 0.5% of manganese, Carbon steel has a carbon content of 0.1% to 0.8%, and HSLA steel is low-carbon steel microalloyed with niobium, vanadium and titanium.

---

[1] Figure from "Steel Manual" by Bolbrinker (Bolbrinker 1992)

The molten alloy is then poured into either a slab caster or a continuous caster. The alloy is cast into about 20-ton steel slabs, with thicknesses ranging from 2 to 12 inches and widths ranging from 27 to 72 inches. The slabs from continuous casters enter hot rolling mills directly and the energy loss is minimized. On the other hand, the slabs from slab casters are often reheated in reheat furnaces to raise the temperature to about 2200°F, a practice called hot charging. In both cases, the temperatures of the slabs are carefully controlled to ensure consistent material properties of the product.

After the slabs reach the proper temperature and are relatively easy to deform, they are fed into the hot-rolling mills. The hot-rolling mills usually consist of several reduction stands. The most common form of reduction stand is the 4-high stand, which is made of two work rolls and two back-up rolls. (Figure 1.2)

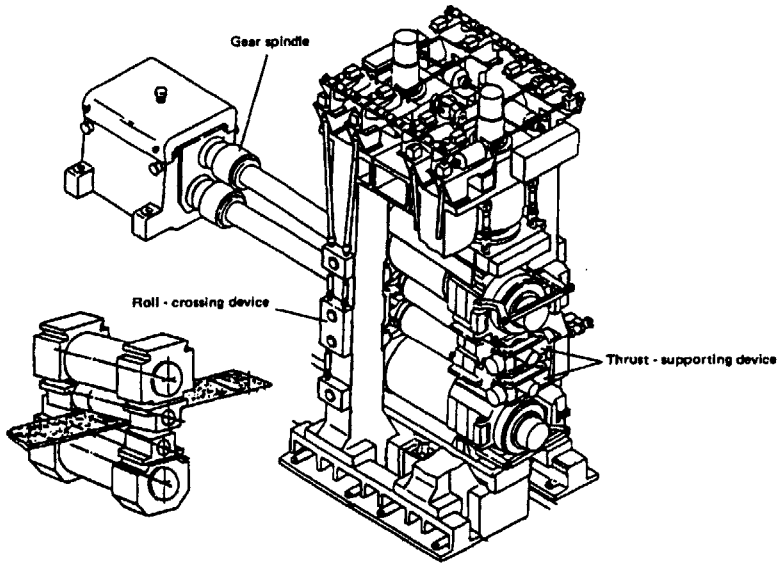

Figure 1.2 4-High Reduction Stand[2]

The multiple reduction stands enable the mill to reduce the slabs into strips with thickness of around 0.06 to 0.5 inches progressively. Some mills, in addition to the multiple stands, use alternating forward and reverse rolling to achieve the same result. At the end of the

[2] Figure from "Flat Processing of Steel", Roberts, W. 1987 (Roberts 1987)

hot-rolling mill, each steel strip is rolled into coils for easy transportation. Therefore, a steel strip is also referred to as a steel coil.

Due to the high temperature, a layer of oxides, also known as mill scales, form on the surface of steel. There are three types of oxides: ferrous oxide (FeO), ferrous-ferric oxide (Fe_3O_4) and ferric oxide (Fe_2O_3). Ferrous oxide, which occurs at the layer next to the metal surface, constitutes about 85% of the scale thickness, the ferrous-ferric oxide about 10% to 15%, and the ferric oxide about 0.5% to 2%. These oxides must be removed prior to the cold-rolling mills to ensure finishing quality and to lengthen equipment life.

These scales are removed in the pickling process. The strips are submerged in acidic solutions such as sulfuric acid (H_2SO_4) or hydrochloric acid (HCl). The pickling lines are usually equipped with mechanical scale-braking devices to facilitate the process. The chemical reaction produces water-soluble salt and hydrogen. The temperature and the concentration of the solutions are carefully calibrated. The time that the strip stays in the solution, which is determined by the strip's speed, also determines the amount of the metal that dissolves in the pickling solution.

The pickled strip is then trimmed to the desired width and sent to the cold-rolling mill to be reduced to the final desired thickness. There are many different types of cold-rolling stands. For example, a 2-high is a stand with only two work rolls, a 4-high is a stand with two work rolls and two back up rolls, and there are also 6-high stands, with two work rolls and four back up rolls. There are also 12-high 20-high, and Z-high designed to provide higher rigidity to the mill and produce higher reduction. The 4-high mill stands are the most commonly used type of stand for cold reduction. They are usually used in a series of four to six stands to apply progressive thickness reduction. The multiple stand mills enable the output thickness to have different finishes, bright or matted, by changing the rollers on the last stand.

The cold rolling process is intended to produce strips of specific thickness. However, this process also work-hardens the strips and leaves residues of the lubricant on the surface. The residual stress in the material creates complications in the downstream process, such as stamping, on the strip. The cleanliness of the strip is important because it significantly affects the corrosion resistance of the product. The annealing process not only removes the residual stress in the steel, but also vaporizes the lubricants remaining on the surface.

The annealed steel strips can be shipped as a final product or galvanized to increase rust resistance of the product. Rust resistance of a steel product is very important in consumer products such as automobiles and food cans. Chromium oxide has been used for coating since the 1960's, but zinc is the most commonly used coating material. The zinc coating is usually deposited on a steel surface either electrolytically or by the traditional hot-dip method. Another way to form this metallic coating is by the vapor-deposition process.

1.2 Cold Rolling Mill of Thesis

The cold rolling mill discussed in this thesis consists of five reduction stands. All stands are 4-high stands, with two work rolls and two back-up rolls. The work rolls of the last stand can be changed to make products with different surface finishes. The data used in this thesis are all collected from coils with smooth finishing.

Sophisticated controllers called automated gauge controllers (AGC) are installed in this mill. There are two types of AGC's: Force AGC and Mass-Flow AGC. The Force AGC monitors the gap between rollers and adjusts the roll forces accordingly. The Mass-Flow AGC predicts the output thickness at the next stand based on the assumption of conservation of volume flow. Based on the prediction, the Mass-Flow AGC changes the roll speed to achieve the target thickness. The control system constantly monitors the process by measuring entry tension, exit tension, roll force, roll torque, and roll speed for all five stands. The entry strip thickness, along with strip thickness at the exit of stands 1, 4, and 5 are also measured. The sampling rate currently in use for each process variable was decided based on failure monitoring criteria, not gauge variation monitoring.

Chapter 4 will discuss an algorithm that determines a sampling frequency at which variation in each variable can be observed sufficiently.

1.3 Quality Concerns of Cold Rolling Process

Even with the sophisticated control systems, cold rolling mills are constantly under strong pressure to meet the increasingly stricter customer requirements. There are several modes of quality loss that cold rolling mills suffer from. These modes are profile, flatness, and centerline thickness of the strip. The profile is the cross section of the strip. A common, and often tolerated, problem is the thickening in the center of the strip, a phenomenon known as crown. This is due to work roll deformation as its ends are pushed toward the strip while the reaction force is concentrated in its center. The flatness measures the warp of the strip. A flat strip lies in a two-dimensional plane, without wavy edges or curled ends. Poor flatness is caused by residual stress in the strip, which might be caused by temperature history of the strip or uneven placement of the rolls. Strips with severe curl can damage the cold rolling mill.

The most important quality of the steel strips is the consistency of the output centerline thickness. Large variations in centerline thickness can cause catastrophic failures in downstream processes, such as jamming in stamping steps. Unlike the flatness, it is difficult to compensate for large thickness variation. The requirements for low centerline thickness variation has raised so much that the industry standard for the allowable variation is now a quarter of the tolerance set by ASTM. For a thin steel strip with target thickness less than $600\mu m$, the tolerance set by ASTM is $\pm 80\mu m$ from the target thickness (Ginzburg 1993).

1.4 Related Works

Shewhart, Deming and Juran describe variation in processes through separation into two basic categories: special causes and common causes (DeVor 1992). The special causes are problems that arise unpredictably, and they interfere with routine operation. On the

other hand, the common causes are the problems that are inherent in all manufacturing systems. Special causes are correctable locally while common causes will influence all of the production until found and removed.

Shewhart introduced the concept of statistical control. A process is in a state of statistical control when a phenomenon's future variance can be predicted within certain limits, by using the history of the phenomenon. The resulting technique, SPC, detects special causes in a manufacturing system by monitoring the mean shifts or changes in variation. Chen has applied SPC to control IC fabrication processes (Chen 1998), and Sachs has combined SPC and Feedback Control and developed the concept of Run by Run process control (Sachs 1995).

Another technique that is commonly used to monitor quality loss in manufacturing processes is the Exponentially Weighted Moving Average (EWMA) (Crowder 1989). This tool helps visualize the shift in manufacturing states. Smith and Boning have applied this technique to control semiconductor processes (Smith).

Response Surface Modeling (RSM) is an established tool that helps engineers to statistically model variations in manufacturing systems. The output variation is fit to that of process variables. The resulting surface is useful for identifying the relationships between system variation and variation in each process variable. The data space, to which the response surface is fit, can be actual process data or the result of Design of Experiment, DOE (Boning 1993). Lei has used a quadratic equation to model variance in statistical circuits (Lei 1998). Evolutionary Operation (EVOP) technique is a continuous form of RSM. It involves performing several designs of experiments and determining a new operating point using the accumulated data (Box 1957).

Several techniques have been developed to identify the elements in a system that have the most significant impact on output quality. Frey and Otto have defined key inspection characteristics that identify the subset of quality characteristics required to identify yield

(Painter). Thornton defines key characteristics as the product features that are most sensitive to the existing process variation (Thornton 1996). Hu has introduced the Stream-of-Variation theory, which is a fault diagnosis technique for assembly plants (Hu 1997).

Some research on variation in manufacturing systems is based on physical models of the system. Mantripragada and Whitney use state Transition models to calculate variation propagation in assembly lines (Mantripragada 1999). Wei and Thornton have investigated the variation stack-up in tube bending process (Wei 2000). Frey et al has developed the concept of capability matrix along with a modeling technique using block diagrams to optimize manufacturing procedures (Frey). The physics-based Integrated System Model (ISM), developed by Suri and Otto, maps system output variation to variations in process variables for manufacturing systems with multiple operations. The variation model is derived through linearization of the nominal model for the manufacturing system (Suri and Otto).

Numerous studies have focused on the rolling process. Lubrano and Bianchi have developed a finite element model to predict the behaviors of the elastic and plastic deformation of both steel and rolls (Lubrano 1996). Edwards has developed an energy balance model that is useful for mill setup. (Carlton, Edwards et al.) A model that is suitable for rolling thin gauge strips is developed by Fleck et al (Fleck 1992). MacAlister has developed a framework to use rolling models for manufacturing system automation (MacAlister 1989). Orowan constructed a model to closely calculate the roll pressure distributions in a roll bite (Orowan).

To improve the quality of cold rolled steel many researchers have tried to identify the sources of disturbances in the cold rolling mill. Pinkowski focuses on the sources and causes of mill roll marks (Pinkowski 1996). Nessler, Richard, and Nieb tried to identify the sources for the vibration and chatter in rolling processes (Nieb 1991; Richards 1992; Nessler 1993). Cory focuses on monitoring the vibration due to roll eccentricitiy (Cory

1990). Since disturbances in rolling processes tend to be periodic, Shim performed frequency analysis on strip thickness (Shim and Park 1998).

Some researchers have developed control algorithms in production to reduce the thickness variations in cold rolled steel. Lynn has utilized the statistical process control methodology (Lynn 1991), and John et al developed an H^{∞} control loop on a cold rolling mill to improve the thickness quality of cold rolled steel (John 1998). Other than the centerline thickness, flatness and shape of steel strip is also a quality concern for steel industry. There are many shape control devices to adjust the crown of steel strip, such as CVC rolls, and inflatable crown back-up roll (Guo 1996). Egan has developed a flatness model for steel rolling (Egan 1996), and Kamada uses pair cross mill to control the edge profile of steel strips (Kamada 1996).

1.5 Thesis Goal

The goal of this research is to use the concept of ISM on a continuous manufacturing system. This task leads to many major challenges. One of the challenges is to determine a sampling frequency at which sufficient variations in the systems are observed. To illustrate the importance of sampling frequency, two extreme cases can be considered. First, if the sampling rate is once per production, there will be no information on the quality of each product other than a bias value from other products. On the other hand, if there are infinite samples in a production, the data will contain too much high frequency system dynamics such as sensor noise and vibrations. It is important to determine an optimum sampling-rate that returns the proper amount of information in the data.

Another challenge in this research is to include the controllers in the manufacturing system. Modern manufacturing systems rely heavily on automatic controllers to attenuate errors occur in manufacturing systems. These controllers create further complication in modeling variations because the variation observed in a signal may be a control action, a disturbance in the system, or a combination of both. It is necessary to separate the variation due to control actions from that due to system noise.

A cold rolling mill simulator will be constructed in this thesis as an application of the solutions for these two challenges. The simulator predicts output thickness based on geometric and material properties of input steel strip. The control models combine with physical models, predict the values of process variables for each stand at the sampling frequency that is sufficient to observe the variations in the system.

Monte-Carlo simulation is used to determine the sensitivity coefficients between the system output and the process variables. These sensitivity coefficients can also be determined from an approximation of the system model, which is derived by linearizing the physical model at an operating point. The shortcoming of this method, other than being an approximation, is that the linearized model is only valid at a vicinity of the operating point. On the other hand, a linearization provides rapid information, often by mere inspection of the coefficients.

Scenarios with various input variations will be simulated with the cold rolling mill simulator. The simulation outcomes are used to confirm the sensitivity values obtained from Monte-Carlo simulations. From these simulation results, optimum improvement of the system can be identified.

1.6 Thesis Overview

This thesis is composed of eight chapters. This chapter serves as the introduction of the field of variation analysis and cold rolling. The outline of this thesis is shown in Figure 1.3. Chapter 2 discusses the statistical approaches to predict variations. SPC and PCA have been applied to this thesis and the results and the limitations of statistical approaches to predict output variation are presented in this chapter. The limitations lead to the need for physical modeling of the manufacturing system.

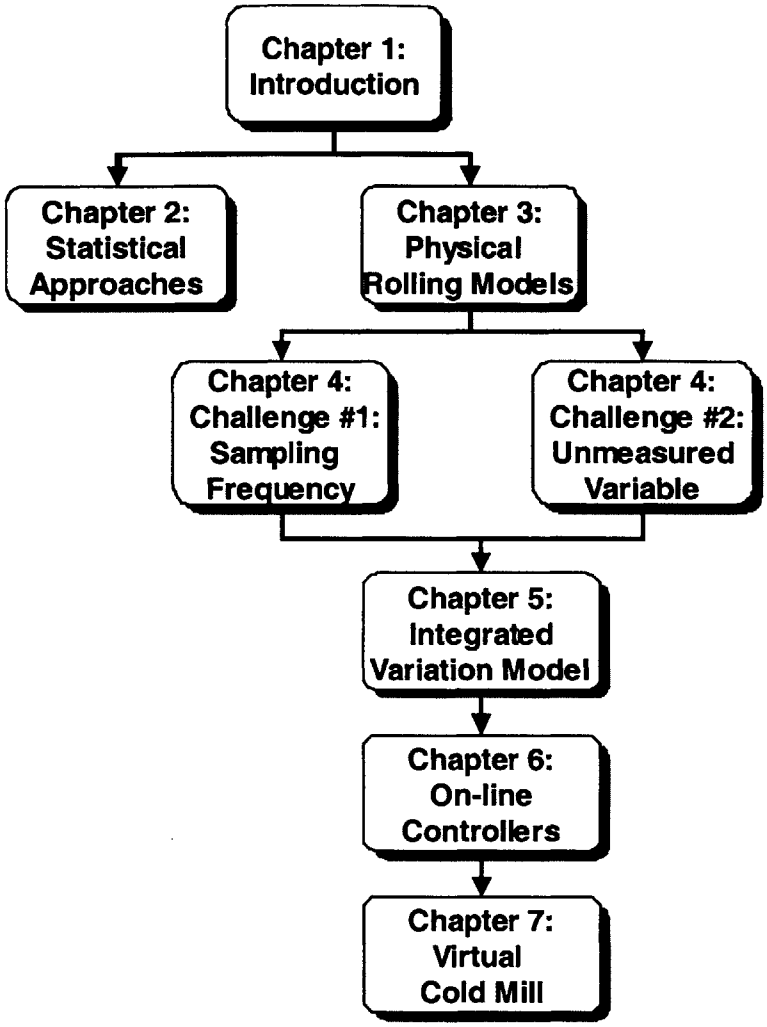

Figure 1.3 Thesis Overview

In Chapter 3, the physical models for cold rolling process are discussed. This chapter presents well-established models such as Roberts' model, Stone's model, and Carlton's energy balance model. This chapter also lists the assumptions and variables used by each model. The pros and cons of these models are also discussed. This provides the underlying physical model for the integrated system model.

Two challenges are encountered when applying a rolling model to study the variation in output of a continuous steel rolling process. The first challenge is to define a sampling frequency at which the model should be calibrated and explored. The second challenge is

that yield strength and the hardening coefficient of steel, which are required by the physical model to predict output thickness, are not measured. These challenges and their solutions of are discussed in Chapter 4.

Once the sampling frequency is determined and the unmeasured variables are modeled, an integrated model can be constructed by linking models for each process. A variation analysis is performed on this integrated model through Monte-Carlo simulation to determine the sensitivity between output thickness variation and process variations. The details are presented in Chapter 5.

This integrated model at that point cannot be used to predict output thickness variation because it requires the values of process variables such as force and velocity of each stand. Since the values of these variables are determined by the controllers, the models of these controllers should be combined into the integrated physical model. The resulting model will predict output thickness purely based on the geometric and material properties of the input steel strip. Chapter 6 discusses about modeling these controllers, including feedforward and feedback control algorithms. A model for each controller is determined, with statistically fit coefficients.

In Chapter 7, the predictive model constructed by integrating controller models and physical models is discussed. This is a cold rolling mill simulator that predicts output thickness from geometric and material properties of input steel strips. The mean and standard deviation of predicted thickness distributions are compared with that of measured values. Sensitivity analysis is performed on this model to study the impact of variation in each process variable on the output thickness variation.

This thesis is concluded in Chapter 8. The values and limits of this simulation model are discussed.

Chapter 2: Statistical Techniques

Variation in processes can be separated into two basic categories: special causes and common causes (DeVor 1992). The special causes are problems that arise unpredictably, and they interfere with routine operation. Special causes are the sources of variations that can be detected and removed. On the other hand, the common causes are the problems that are inherent in all manufacturing systems. The common causes are the variations whose sources cannot be identified.

Special causes are correctable locally while common causes influence all of the production until found and removed. In this chapter, statistical tools for understanding variations in a manufacturing system, such as SPC and RSM, are discussed. A statistical model that maps output thickness variation to the variation in process variables is constructed at the end of this chapter.

This chapter focuses on the statistical approaches to identify the sources of output thickness variation for a cold rolling mill. The techniques used are statistical process control and principal component analysis. The statistical process control is used to identify the correlation among the spikes in each process variable. A high correlation will suggest high sensitivity between variables. The principal component analysis is used to regression fit a equations that maps output thickness variations of steel strips to the mean and standard deviations of process variables. This model predicts output thickness variation of the cold rolled steel strip once the values of process variables are known.

2.1 Statistical Process Control (SPC)

Shewhart developed Statistical Process Control in the 1950s. Shewhart states that processes under *statistical control* are driven solely by common causes of variation. A system showing instability or a lack of control is afflicted with assignable special causes. The state of being in statistical control is when the process is free of special causes of

variation. This allows the operator to state the probability that the observed phenomenon (output production) will fall within given limits.

The SPC method is based on two time-varying control charts, which plot process mean and range over time. Each chart has an upper and a lower control limit drawn at ±3 standard deviation of the mean and a range of observed data points. These charts enable operators to observe mean shifts in the process and determine if corrective action is necessary. However, the control charts identify the presence of a problem, but does not aid in determining the cause. Statistical detection of correlation between input and output variables is attempted in this thesis to trace the sources of variations.

2.1.1 Application of SPC on Continuous Cold Rolling

A goal of this thesis was to determine the sensitivity of output thickness to each process variable. However, a straight calculation of the correlation among variables resulted in low correlation values. Table 2.1 is the correlation coefficient between each variable and exit thickness. The variable that has the largest correlation to the exit thickness is roll force at Stand 4, with value of 51%.

Correlation with Exit Thickness			
Entry Thickness	6%	Stand 3 Roll Force	5%
Entry Tension	18%	Stand 3 Roll Speed	-19%
Tension btw Stand 1-2	2%	Tension btw Stand 4-5	-3%
Stand 1 Force	-5%	Stand 4 Roll Force	-2%
Stand 1 Roll Speed	16%	Stand 4 Roll Speed	51%
Stand 1 Exit Thickness	-23%	Stand 4 Exit Thickness	37%
Tension btw Stand 2-3	-8%	Exit Tension	7%
Stand 2 Roll Force	4%	Stantd 5 Roll Force	5%
Stand 2 Roll Speed	-8%	Stand 5 Roll Speed	2%
Tension btw Stand 3-4	8%	Exit Thickness	100%

Table 2.1 Correlation between Process Variables and Exit Thickness

Even though the correlation can be easily calculated, it does not explain the causality between variations in process variables and the output thickness variation. The variation in a process variable may be control efforts trying to remove thickness variation.

Therefore, high correlation may only show that the output thickness is effectively influenced by control efforts, instead of suggesting sources of variations. Therefore, it is necessary to exclude the impact of controller in the computation of correlation. In this thesis, SPC is used separate the controlled variation from the noise that adds variation to the exit thickness. The SPC analysis is a side project in this thesis, done to first see if such a simplistic approach was possible.

SPC is effective in identifying the existence of mean shifts in both output thickness and process variables. A sudden mean shift is considered outside the bandwidth of the controllers. If sudden mean shifts in output thickness coincided with that in another variable, their correlation suggests causality. The SPC techniques found in the literatures were modified to apply to a continuous system with controllers to identify sudden mean shifts. Each data point is compared with the mean and standard deviation of a window of past production. The data point is determined to be a sudden mean shift, or a spike, if it lies outside of ±3 standard deviation range of the previous window. The determination of the mean and ±3 standard deviation is shown in Figure 2.1. The size of the window can be experimentally determined to ensure that a reasonable number of data points fall outside the control limits.

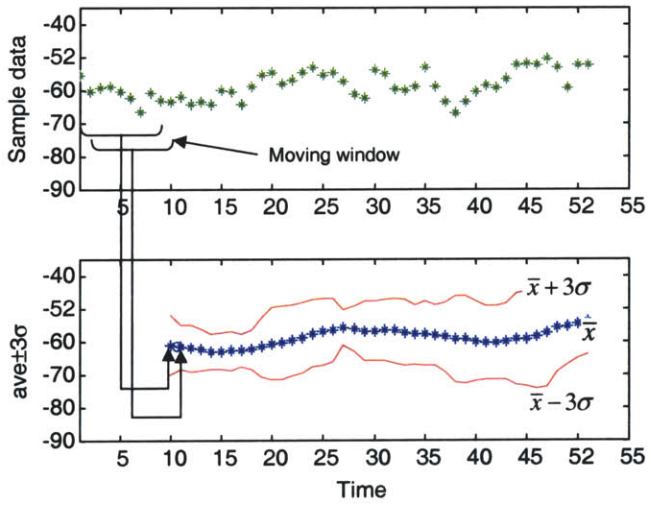

Figure 2.1 Average and ± 3 Standard Deviations of a Signal

The moving average, $\bar{x}$, and standard deviation, σ, is expressed in Equation 2.1 and 2.2; w is the number of data points in the moving window.

$$\bar{x}_{i+w} = \frac{\sum_{k=i}^{i+w} \bar{x}_k}{w} \tag{2.1}$$

$$\sigma_{i+w} = \sqrt{\frac{\sum_{k=i}^{i+w} (x_k - \bar{x}_{i+w})^2}{w-1}} \tag{2.2}$$

After the average and $\pm 3\sigma$ range is determined, the original data were overlaid on the control chart. The data points that lay outside the $\pm 3\sigma$ range are identified as spikes (Figure 2.2).

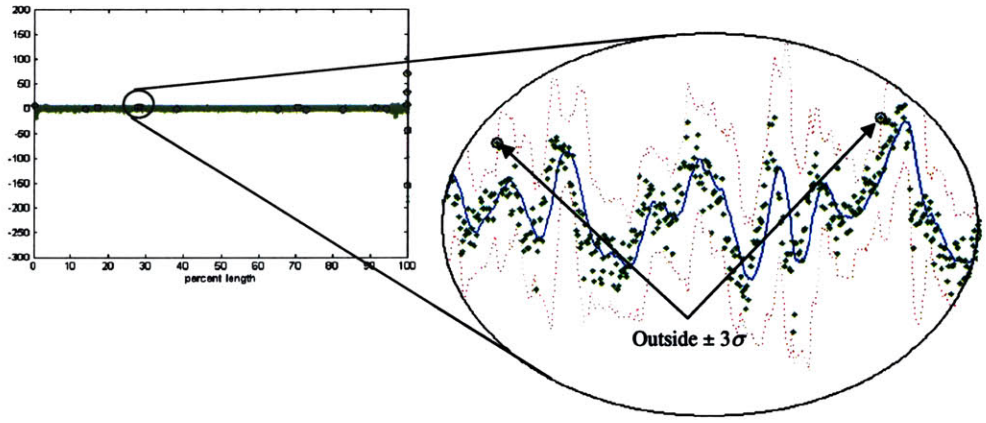

Figure 2.2 Determination of Spikes in a Data Stream

This procedure was performed on all process variables and thickness measurements from the cold rolling mill. The spikes in all data streams were then compared based on its location on the coil. The strip was split into M sections and the number of spikes in each section was determined for each data stream. A spike matrix, S, was generated to show the locations of the spikes (Equation 2.3).

$$S = \begin{bmatrix} s_{1,1} & s_{1,2} & \cdots & s_{1,N} \\ s_{2,1} & \ddots & & \\ \vdots & & \ddots & \\ s_{M,1} & & & s_{M,N} \end{bmatrix} \tag{2.3}$$

Each element $s_{i,j}$ was the number of spikes, M was the number of the sections down the strip, and N is the number of data streams. A symmetric correlation matrix, C, is then calculated based on each column, $\bar{s}_j$, in S (Equation 2.4).

A typical spike matrix, S, is shown in Figure 2.3.

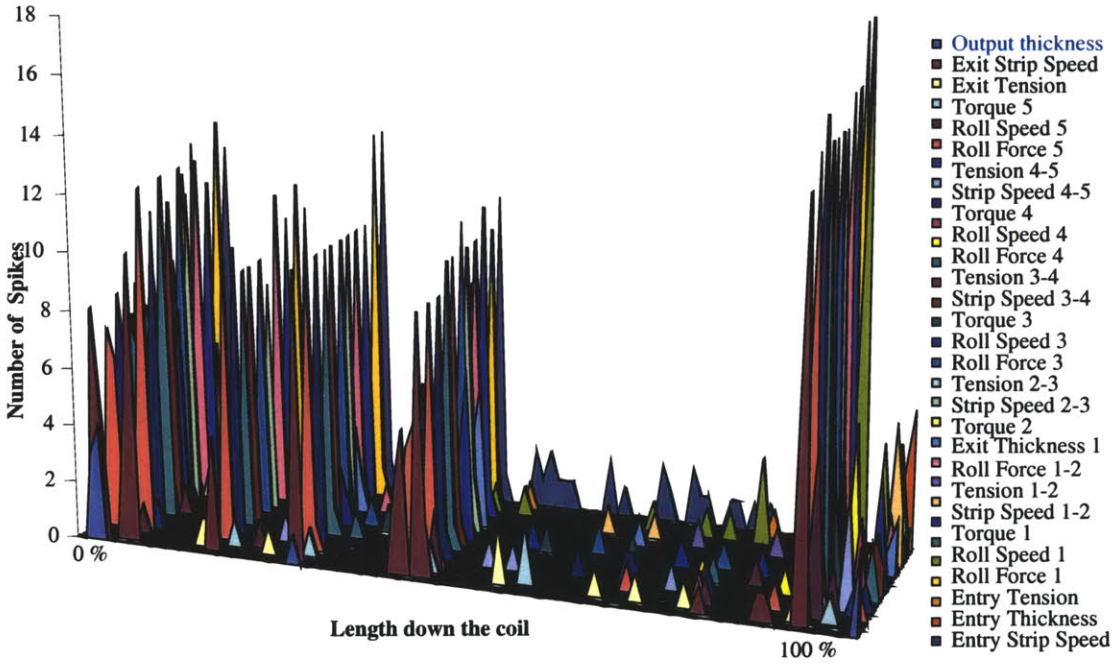

Figure 2.3 Typical Spike Analysis Result

$$C = \begin{bmatrix} 1 & c_{2,1} & \cdots & c_{N,1} \\ c_{2,1} & 1 & & \vdots \\ \vdots & & \ddots & c_{N,N-1} \\ c_{N,1} & & c_{N,N-1} & 1 \end{bmatrix} \tag{2.4}$$

where

$$c_{i,j} = \frac{COV(\bar{s}_i, \bar{s}_j)}{\sigma_{\bar{s}_i} \cdot \sigma_{\bar{s}j}} \tag{2.5}$$

$$COV(\bar{s}_i, \bar{s}_j) = \frac{1}{M} \sum_{k=1}^{M} (s_{k,i} - \mu_{\bar{s}_i})(s_{k,j} - \mu_{\bar{s}_j}) \tag{2.6}$$

A typical result of the correlation matrix is shown in Appendix A.

As would be expected, correlation matrix showed that there was high correlation between speed changes and process variables such as torque. This observation was confirmed when Figure 2.3 was overlaid with the roll speed data for the production of the strip (Figure 2.4).

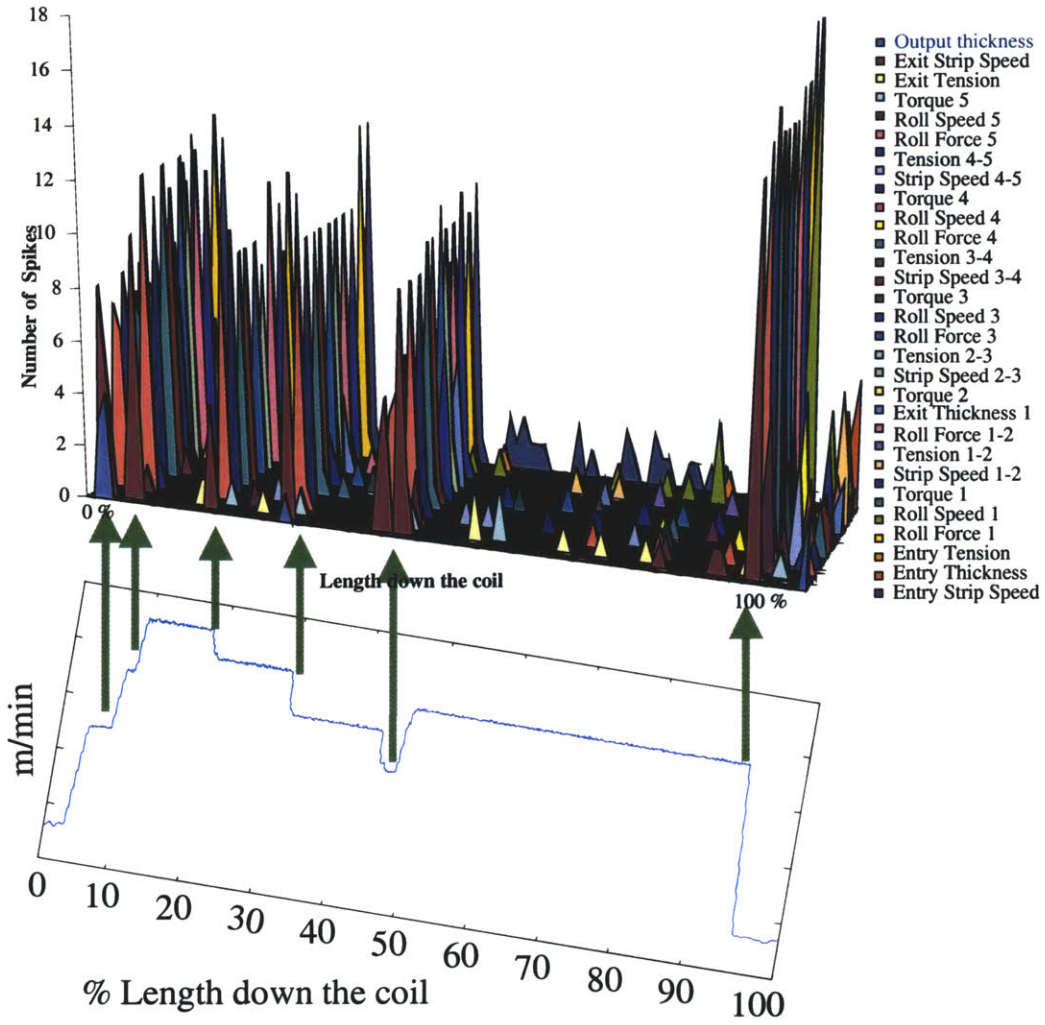

Figure 2.4 Spikes in Data Streams and Roll Speed Data

The operators conducted the speed changes upon observing surface stains entering the cold rolling mill. The SPC and correlation analysis also showed, however, that the correlation between the output thickness variation and speed changes was 30%. When operator made speed changes, there was reasonable likelihood that thickness perturbations result on the strip, even with the sophisticated control system employed.

The analysis above indicated that speed changes caused by the operator introduced spikes in most of the process variables, and somewhat on output thickness. A recommendation was to minimize speed changes, which is obvious, but also to limit the rate of change of speed. Speed should be raised and lowered as slowly and continuously as possible, to enable the on-line controllers to work.

A further analysis was then employed to examine the smaller regions of steady velocity, outside of where the operators make speed changes. A typical result of spike analysis on steady state region is shown in Figure 2.5. No clear correlations among process variables were observed.

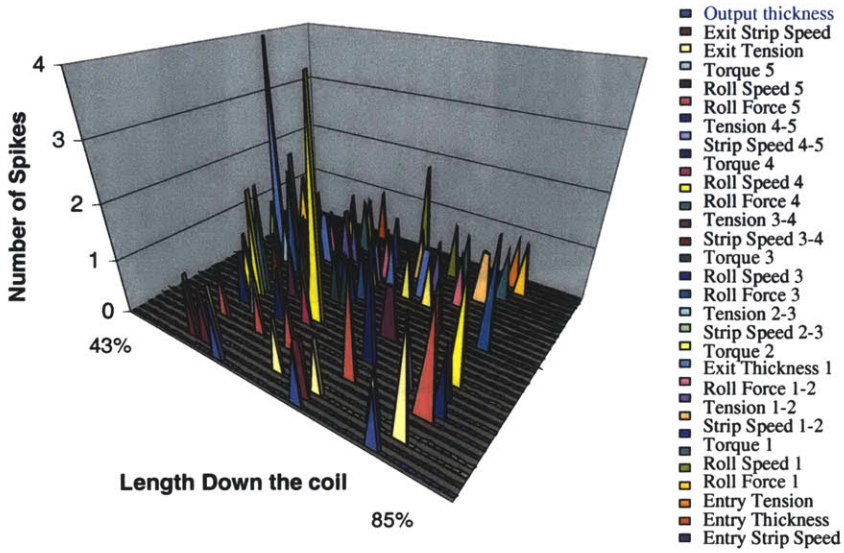

Figure 2.5 Typical Spike Analysis in Steady Velocity Section

The correlation coefficients of the spike data in the constant velocity section suggested the sensitivity of output thickness variation to each process variable. For example, stand 5 torque's spike correlation with output thickness was 0.57; that of stand 1 torque was only 0.04. Other process variables that had significant spike correlation with output thickness were stand 3 roll- force, stand 4 torque, and stand 4 exit-tension. Their spike correlation coefficients with output thickness were 0.24, 0.30 and 0.30 respectively.

SPC was helpful in identifying the problems, and spike correlation was effective in determining the relative impacts of each process variable spikes to the output thickness spikes. Even though these analyses provided interesting insights about the system, they did not provide information on the causalities between the variations. For example, the observed fluctuations in a process variable may be a result of control actions. Therefore, high correlation between output thickness and a certain variable might suggest an effective control action instead of identifying a source of quality loss.

2.2 Parameter Fitting

Another statistical approach to identify sensitivity between output thickness variation and process variation is fitting parameters of an equation that maps variation in output thickness to statistical characteristics of process variables. In this thesis, the form of the equation is a linear combination of the mean and standard deviation of process variables. This would make for a very simple analysis of variation, should it prove effective.

$$\sigma_{out} = \beta_0 + \sum \beta_i \mu_i + \sum \beta_i \sigma_i \tag{2.8}$$

Second order terms such as μ_i^2, σ_i^2, and $\mu_i \sigma_j$ can be included in the model. They are not included in here in the attempt to keep the number of fitting variable small relative to the number of data points. This model is based on two assumptions. The first is that the operation was stable and varied in a small region around an operating point. The second assumption is that the data streams are independent. The first assumption of modeling complex manufacturing systems has been applied widely. However, the second assumption is not true in the case where a controller is present. The controller's function is to reduce output variation based on the observed process variables by constantly changing the process. Therefore, the measured σ_i's in the system are not independent. Therefore, principal component analysis is required to construct a data space without statistical dependence. A statistical model that predicts output thickness variation can then be fit with this new data.

2.3 Principal Component Analysis

Principal component analysis, originally developed by Pearson, is often used to address these multicollinearity problems in regressio (Dunteman 1989) (Wold, Esbensen et al. 1987). Principal component analysis is used in the situation where there is coupling among the inputs which appeared as a co-linearity in the data space. It rotates the data space to generate a new set of input variables that are linearly independent while also determining the insignificant modes for simplifying the regression process. It searches for a new set of uncorrelated linear combinations of the original variables that describes the most of the information in the original variables. The new set of variables is generated by assigning weights to the original variables. Principal component analysis transforms a data matrix with p data streams, $X = \{x_1, x_2, \cdots, x_p\}$ into a new q-dimensional space $Y = \{y_1, y_2, \cdots, y_q\}$ while each vector y_i is calculated by multiplying a weight vector, a_i, to X (Equation 2.9).

$$y_i = a_{i1}x_1 + a_{i2}x_2 + \cdots a_{ip}x_p \tag{2.9}$$

The weight a_{ij}'s are determined mathematically with the method discussed later.
Geometrically, the first principal component is the closest linear fit to the observed outputs, minimizing the squared difference between the observation and the prediction. The second principal component adds more information to describe the behavior of the observed outputs, being the closest fit to the residuals from the first principal component. The first principal component carries the most information in original data set, X, and each additional principal component will provide diminishing information. The number of principal components is chosen based on the information contained in them. The maximum number of principal component is the number of data streams in the original data set. The procedures for calculating principal components are described as follows.

To determine the transfer function, the first step is to determine the eigenvalues, λ, of the matrix X (Equation 2.10) .

$$Xa = \lambda a \tag{2.10}$$

The number of λ should be the same as the rank of X, and the matrix a is composed of the respective eigenvectors (Equation 2.11, 2.12).

$$a = \{a_1, a_2, \cdots, a_k\} \tag{2.11}$$

$$Xa_i = \lambda_i a_i \tag{2.12}$$

Each eigenvector is also normalized so that the length is unity (Equation 2.13).

$$\sum_{j=1}^{p} {a_{ij}}^2 = 1 \tag{2.13}$$

In the case where X is not square, singular value decomposition can be used to calculate the matrix a. For example, a $m \times n$ matrix X with rank r can be decomposed into three matrices involving eigenvectors and eigenvalues (Equation 2.14).

$$X_{m \times n} = U_{m \times m} \Sigma_{m \times n} V_{n \times n}^{-1} \tag{2.14}$$

Σ is a diagonal matrix formed by the singular values, σ_i, which are equivalent to the eigenvalues in the case with a square X (Equation 2.15). The singular values are the square roots of the real positive eigenvalues of XX^H (Equation 2.16).

$$\Sigma = \begin{bmatrix} \sigma_1 & 0 & \cdots & 0 \\ 0 & \sigma_2 & & 0 \\ & & \ddots & \vdots \\ \vdots & & \ddots & \\ & & & \sigma_r \\ 0 & 0 & \cdots & 0 \end{bmatrix} \tag{2.15}$$

$$\sigma_i \equiv \sqrt{\lambda_i} \quad i = 1,2,3,\cdots,r \tag{2.16}$$

The singular values are arranged in the order that $\sigma_1 \geq \sigma_2 \cdots \geq \sigma_r$.

The U matrix is composed of left singular vectors, u_i, and V is of right singular vectors, v_i.

$$U = \{u_1, u_2, \cdots, u_m\} \tag{2.17a}$$

$$V = \{v_1, v_2, \cdots, v_n\} \tag{2.17b}$$

The right singular vectors are equivalent to the eigenvectors in the case with a square X, and they are calculated with the following equation.

$$X^{-1} H v_i = \sigma_i^2 v_i \tag{2.18}$$

Once each principal component is calculated, different criteria can be used to determine the number of principal components that simplifies the problem while maintaining sufficient information of the original data. Kaiser recommends dropping those principal components with associated eigenvalues less than one for a normalized X. On the other hand, Jolliffe has argued that Kaiser's rule tends to discard too much information and suggested the cutoff to be 0.7. Cattell proposed a "scree" graph, which plots the eigenvalues and determines a proper number of principal components based on the change in the slope. Another criterion that was suggested by Duntman is to retain enough principal components to account for a given percentage of variation.

All of these rules are arbitrary and involves some personal judgements. As a general rule, the more principal components that are retained, the more complete the description of the data. Furthermore, as suggested by Duntman, smaller principal components are harder to interpret than larger ones.

2.3.1 Application of Principal Analysis Regression on Cold Rolling Model

This regression and principal component analysis technique was applied in this thesis to modeling the cold rolling mill. It was assumed that the model for the five reduction stands are repeatable; therefore, it was applied to a single stand instead of the connected five stands.

Data streams for 21 coil productions were available at the time of analysis. 14 of them were used for calibration, and the obtained equation was validated against the remaining seven coils. For each data set, six process variables were available for Stand 1, on which

the analysis was performed. They were input thickness, roll force, entry tension, exit tension, roll speed, and roll torque. Mean, μ_i, and standard deviation, σ_i, were calculated for each data stream, and the output of the model was output thickness variation, represented by its standard deviation. A 14×12 matrix X was then generated with these observations. (Equation 2.19)

$$X = \begin{bmatrix} \mu_{1,1} & \sigma_{1,1} & \mu_{2,1} & \sigma_{2,1} & \cdots & \sigma_{6,1} \\ \mu_{1,2} & \sigma_{1,2} & \mu_{2,2} & \vdots & & \sigma_{6,2} \\ \mu_{1,3} & \sigma_{1,3} & \vdots & & & \sigma_{6,3} \\ \mu_{1,4} & \vdots & & & & \vdots \\ \vdots & & & & & \vdots \\ \mu_{1,14} & \sigma_{1,14} & \cdots & \cdots & \cdots & \sigma_{6,14} \end{bmatrix} \tag{2.19}$$

This data matrix is highly correlated, with coefficients of correlation ranging from -0.60 to 0.94. Principal component analysis was therefore applied to address this problem. First, the matrix X was normalized and the singular values and singular vectors were calculated. Kaiser's criterion was then used to determine the number of principal components. It turned out that there were ten singular values that were bigger than unity, so ten principal components were calculated using Equation 2.9. Second, regression was performed to map observed outputs to the principal components. In addition, *t-test*, with $\alpha = 0.05$, was included in the regression analysis to ensure each that component was significant. As the result, five principal components were significant and the output was regenerated and the equation predicted the output thickness variation with r^2 of 0.85 and RSME of $0.11 \mu m$ (Figure 2.6). Since the principal components were difficult to interpret, the resulting equation was converted into the original set of variables (Equation 2.20).

$$\begin{aligned} \sigma_{out\_thick} = {} & 2.867 + 0.159\mu_{\text{entry thickness}} + 0.0687\sigma_{\text{entry thickness}} + 0.209\mu_{\text{roll force}} \\ & - 0.085\sigma_{\text{roll force}} - 0.269\mu_{\text{entry tension}} + 0.144\sigma_{\text{entry tension}} \\ & - 0.166\mu_{\text{roll speed}} + 0.133\sigma_{\text{roll speed}} + 0.0269\mu_{\text{torque}} - 0.02155\sigma_{\text{torque}} \\ & - 0.0483\mu_{\text{exit tension}} + 0.0271\sigma_{\text{exit tension}} \end{aligned} \tag{2.20}$$

The equation was then validated with another seven sets of production data streams. The model predicted the output thickness variation with r^2 of 0.81 and RSME of 0.08μm (Figure 2.7). This result is quite good in fit.

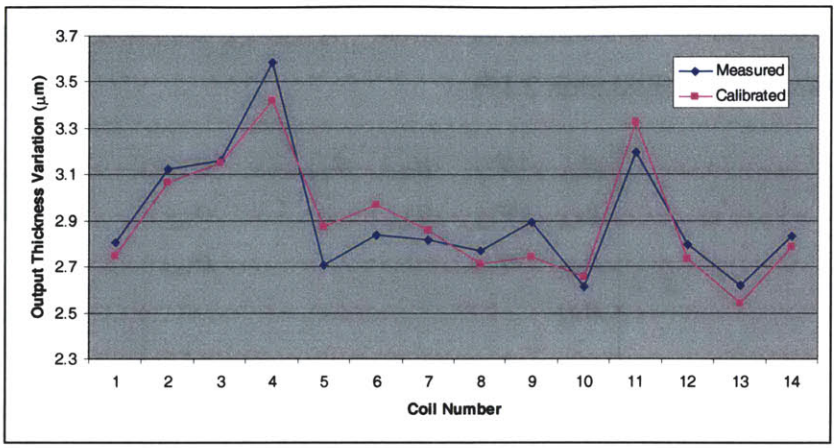

Figure 2.6 Calibration of Equation 2.20

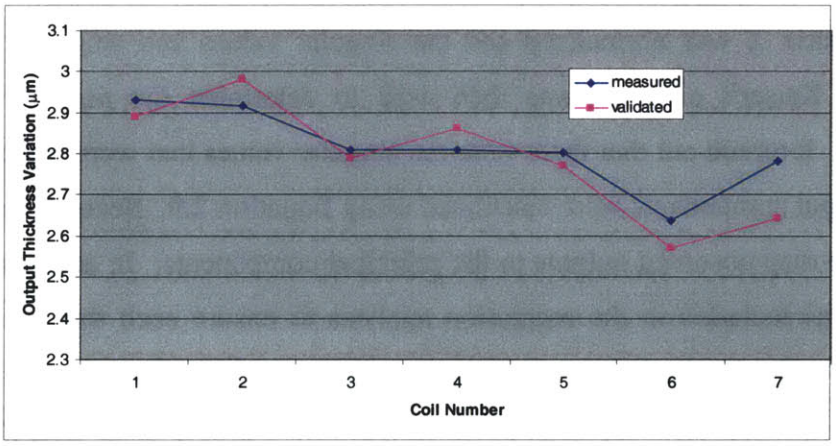

Figure 2.7 Validation of Equation 2.20

2.4 Limitations of Statistical Approach

As demonstrated in the previous section, the principal component analysis in conjunction with regression was effective for building a statistical model for a complex system with correlated data streams. However, there were limitations to this approach. The observed variations in process variables are composed of the actions of controllers and noises in

the system. The control actions attenuate disturbances in the manufacturing system and the noises contribute to the output variation. Equation 2.20 does not reflect this phenomenon. This meant that we could not perform sensitivity analysis with this equation. The result would show whether thickness variation is highly sensitive to, for example, force, but not force errors. Most of the force variation is "good" variation, requested by the control system to take out variations in thickness.

An attempted solution was to split the data streams into high-frequency and low-frequency components based on the observed transfer function, and then to perform the same analysis on these new set of data. One could interpret the low-frequency part of the data as control actions, and the high-frequency component as system noise. The cutoff for high and low frequency was determined based on the transfer function between the process variable and the output thickness. For example, the transfer function from normalized stand 1 roll force to the normalized output thickness was shown in Figure 2.8. In this figure, the dashed line was the ratio between the magnitude of normalized force and the magnitude of the normalized output thickness. Since the plot was too noisy in the high frequency region, a moving average line, drawn in black, was added to the plot. It was observed that the magnitude of the transfer function was below 0db at the low frequency range. This suggested that the change in the force observed at those frequencies did not contribute to the variation of output thickness. On the other hand, the magnitude of the transfer function was above 0db in the higher frequency range, and this meant that the change in force resulted in increased output thickness variation. Based on these observations, the cutoff frequency was defined as the frequency where the plot crossed the 0db line.

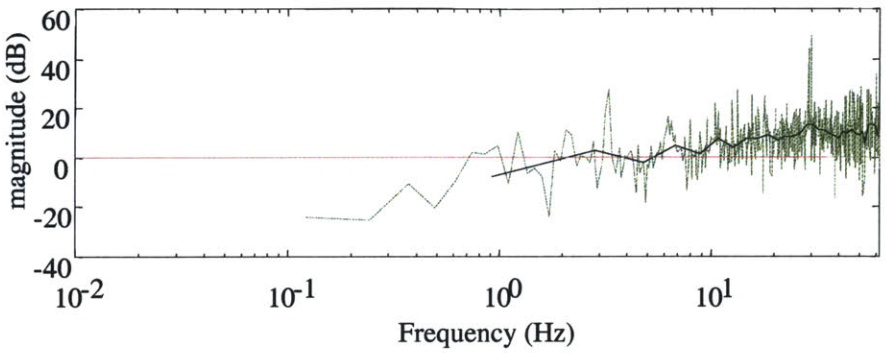

Figure 2.8 Transfer Function From Roll Force to Exit Thickness

After the cutoff frequency for each variable was determined, each data stream was filtered into high frequency and low frequency components. The mean and standard deviation for each component was then calculated as performed in the previous analysis. This time, the principal component analysis resulted in 15 principal components using Kaiser's criterion. The regression analysis and *t-test* identified 4 of them to be significant. The new model calibrated to a statistical fit with r^2 of 0.85 and RSME of 0.11, which roughly equaled to the result obtained without filtering the data. (Figure 2.9)

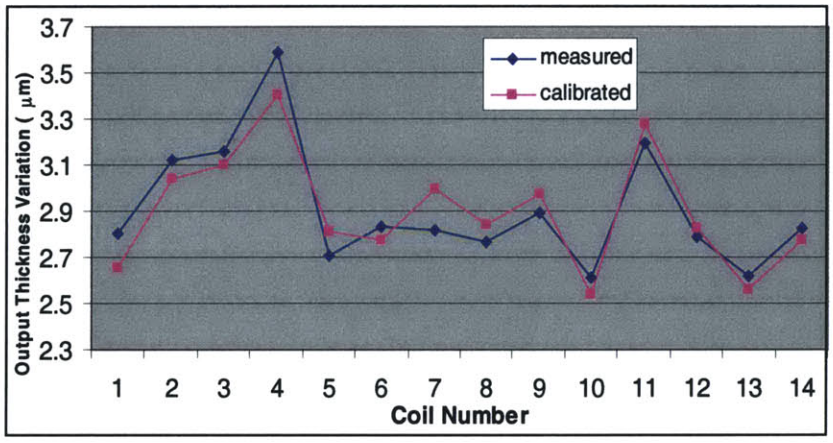

Figure 2.9 Calibration of Equation 2.21

However, the new equation only validated to r^2 of 0.46 and RSME of 0.12. (Figure 2.10)

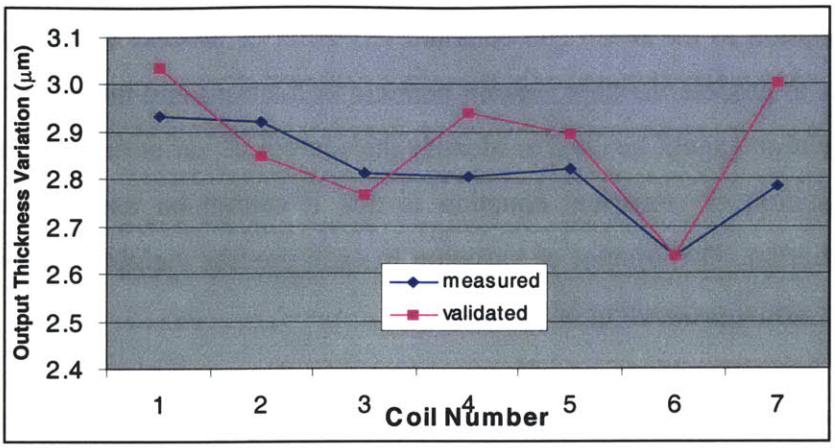

Figure 2.10 validation of Equation 2.21

It was possible that the filtering had introduced error into the model. In addition, even if the model were able to validate to the same correctness, it would still be difficult to interpret the model. (Equation 2.21)

$$\begin{aligned}\sigma_h = {} & 3.391 - 0.0585\sigma_{\text{entry tension control}} + 0.216\sigma_{\text{entry tension noise}} + 0.0136\sigma_{\text{exit tension control}} \\ & + 0.212\sigma_{\text{exit tension noise}} - 8.47\times10^{-4}\sigma_{\text{roll force control}} - 2.419\times10^{-6}\sigma_{\text{roll force noise}} \\ & - 0.0743H_{\text{low frequency}} - 0.0789H_{\text{high frequency}} - 0.0586\mu_{\text{roll speed}} - 0.0118(\text{width})\end{aligned} \tag{2.21}$$

The signs for some of the variables did not make physical sense. For example, according to the equation, the noise in roll force reduced the output variation, and this was counterintuitive. Regression analysis only searches for a set of β_i's that minimize error between model prediction and measurements regardless the actual relationships between the variables. Therefore, the physical insight that could be drawn from the statistical model was limited.

2.5 Chapter Summary

This chapter has shown two statistical approaches to determine the sensitivity of variation in output thickness to that in process variables. The SPC spike analysis has identified that spikes in process variables strongly correlate to speed change, but it cannot explain

the causality between the variation in thickness and that in process variables. The second statistical approach, principal component regression, successfully maps output thickness variation to the mean and standard deviation of process variables. However, the variations in process variable contain both control actions and noises. Therefore, this statistical equation cannot be used to identify the sources of variation in output thickness. Another limitation of statistical equation is that it cannot be used to predict output thickness variation. The amount of variation in each process variable can be determined only after the actual processing of the strip.

Because of the reasons discussed above, it is clear that a physic-based model is necessary for predicting output thickness. The development of such a model is discussed next.

Chapter 3: Cold Rolling Models

Chapter 2 has shown that the information obtained from a statistical equation is limited despite the fact that it can predict the output. On the contrary, equations derived from physical principals provide strong confidence that it correctly reflects the system once it is properly validated. The challenges in constructing such a model are to make realistic assumptions and to identify the correct variables.

The approach for building a physics-based model that predicts output thickness variation based only on the characteristic properties of input strip is as follows. The first step is constructing a physical model that explains the behavior of a reduction stand. This model will be expanded to all five reduction stands, and the five models can be integrated as one model that predicts output thickness based on the values of process variables. The second step is to predict the values of process variables. This is performed by constructing models of the on-line controllers, since the values of process variables are results of control actions. The target values of each controller are functions of characteristic properties of the input strip and the process variables in previous stands. The last step linking the controller models with the physical models of reductions stands. With this, sensitivity analysis can be performed to identify the sources of variation and their impacts on the output thickness.

Chapter 3 focuses on the physical models for an individual reduction stand that have been developed over the years: plane strain force balance model, Roberts' Model, Stone's Model, and Carlton's energy balance model. These models are studied and a suitable model for predicting the behavior of an individual reduction is selected.

Modeling of the cold rolling process is a very mature field of study. Stone, Roberts, Orowen, Ford, and Ekelund have derived models for predicting roll force or torque based on the desired thickness reduction (Wusatowski 1969). Hitchcock has derived an well-accepted model to predict the deformation of work rolls (Roberts 1978). Numerous

studies have focused on the deformation of steel under rolling conditions (Lindholm 1965).

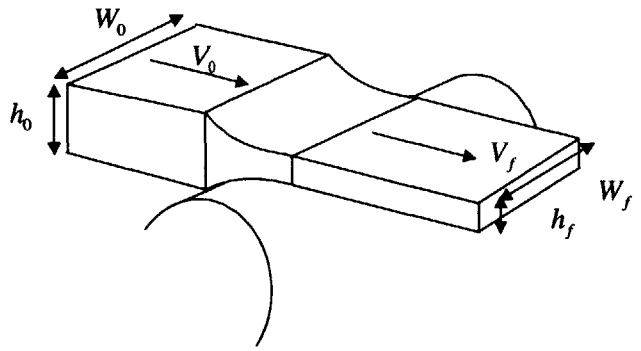

Figure 3.1 Strip Deformation in a Cold Rolling Stand

Figure 3.1 is a schematic of the rolling process. The top roller is not shown in the figure for better visualization of the strip. From conservation of mass and the assumption that the density is constant, the volume flow is conserved.

$$h_0 \times W_0 \times V_0 = h_f \times W_f \times V_f \tag{3.1}$$

The change in width is insignificant compared to the thickness and length change during the rolling process. Therefore, plane strain is usually assumed in the models and only dimensional changes in the vertical and transverse directions are considered in the models.

The region where the rolls touch the strip is called the roll bite. Both elastic and plastic deformations of the strip take place in this region. However, the elastic deformation is insignificant compared to the plastic deformation and is ignored in this model. The point where the strip first touches the roll is called the entry point while the point where the strip leaves the roll bite is called the exit point.

The entry speed is the strip speed at the entry point, and the exit speed is that at the exit point. Since the width is relatively constant, the reduction in thickness causes the exit velocity to accelerate to higher than the roll speed, while the entry velocity is slower than the roll speed. The point where the strip speed equals the roll circumference speed is

defined as the neutral point (Figure 3.2). The region between the entry point and the neutral point is called the entry zone, where the strip speed is slower than the roll peripheral speed. On the other hand, the region between the neutral point and the exit point is called the exit zone, and the strip speed is faster than the roll peripheral speed.

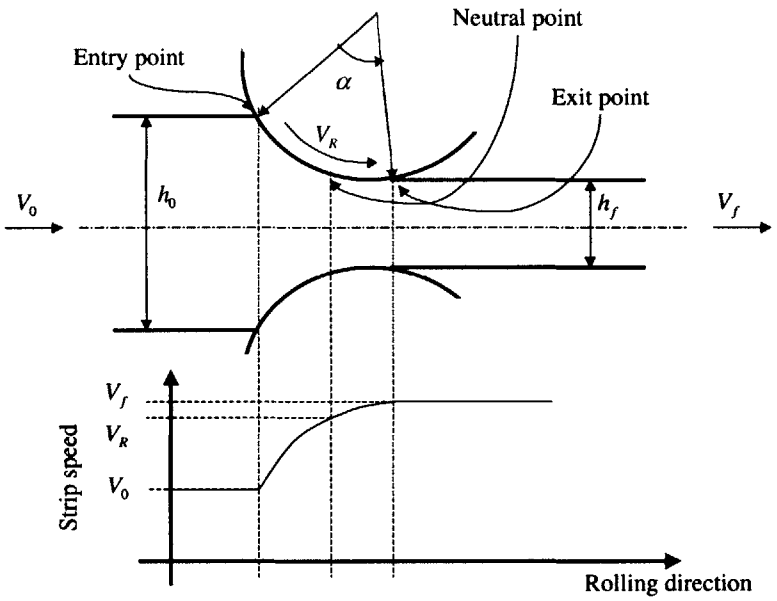

Figure 3.2 Strip Speed Change during Deformation

3.1 Plane Strain Force Balance Model

This simple model assumes plane stress in rolling process and models the rolling process in a 2-dimensional model (Kalpakjian 1995). The assumptions of this model are listed as follows:

1. Conservation of volume is assumed.
2. The work roll radius is assumed to be rigid.
3. Strip width is constant before and after the rolling process.
4. The effect of entry and exit tension is ignored effective yield strength.
5. The effect of roll speed is neglected.

6. Work hardening occurs during the rolling process and the effective yield strength is assumed to be the average.
7. The coefficient of friction is assumed to be constant in the roll bite.
8. The rolling angle, α, is within a couple of degrees; therefore, the angle of reduction, ϕ, is small. $(\sin\phi = \phi, \cos\phi = 1)$

Nomenclature for Force Balance Model

α : roll angle
h_0 : entry thickness
h_f : exit thickness
μ : friction coefficient
L : contact arc length
ϕ : angle of reduction
σ : effective yield strength
F : roll force
p : roll pressure
R : roll radius
W : strip width
T: tension in transverse direction

Figure 3.3 shows a section of the strip that is under deformation. The roll peripheral speed is faster than the strip speed in the entry zone; therefore, the frictional pressure, μp, is in the forward direction. The situation is opposite in the exit zone, so the force is pointing backwards.

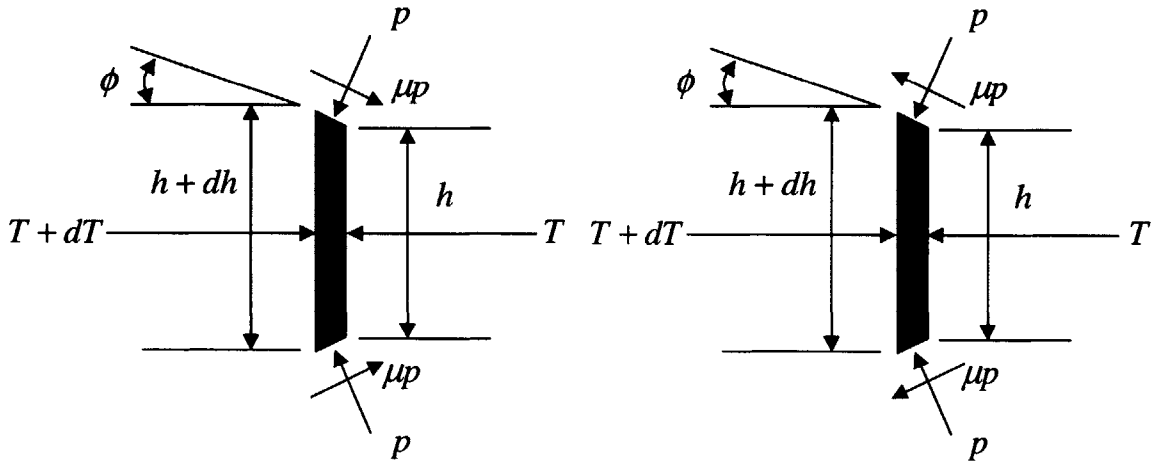

Figure 3.3 Force Balance on a Section of Strip under Deformation

From the force balance, the following equation is derived. The ± sign is due to the opposite directions of frictional forces in the entry and exit zones.

$$(T+dT)(h+dh)-2FRd\phi\sin\phi-Th\pm 2\mu FRd\phi\cos\phi=0 \tag{3.2}$$

The second order terms are dropped since their magnitudes are insignificant relative to the others. The equation is then reorganized into a differential equation.

$$\frac{d(Th)}{d\phi}=2FR(\sin\phi\mp\mu cons\phi) \tag{3.3}$$

Since ϕ is small, the following is assumed: $\sin\phi=\phi$ and $\cos\phi=1$. This assumption resulted in the following differential equation.

$$\frac{d(Th)}{d\phi}=2FR(\phi\mp\mu\phi) \tag{3.4}$$

From the geometry and the assumption that the roll is rigid, the following equation is derived.

$$h=h_f+2R(1-\cos\phi)\approx h_f+2R\phi^2 \tag{3.5}$$

This equation is combined with Equation 3.3, and integrating the resulting differential equation results in the following expression for roll pressure, p.

$$p=\sigma\frac{h}{h_0}e^{\mu\left(h_0-2\sqrt{\frac{R}{h_f}}\tan^{-1}\left(\sqrt{\frac{R}{h_f}}\phi\right)\right)} \tag{3.6a}$$

$$p=\sigma\frac{h}{h_f}e^{\mu\left(2\sqrt{\frac{R}{h_f}}\tan^{-1}\left(\sqrt{\frac{R}{h_f}}\phi\right)\right)} \tag{3.6b}$$

Equation 3.6a is for the roll pressure in the entry zone, and Equation 3.6b is that for the exit zone. Figure 3.4 shows the general shape of these two curves, and the area under the curve is the rolling force per unit width.

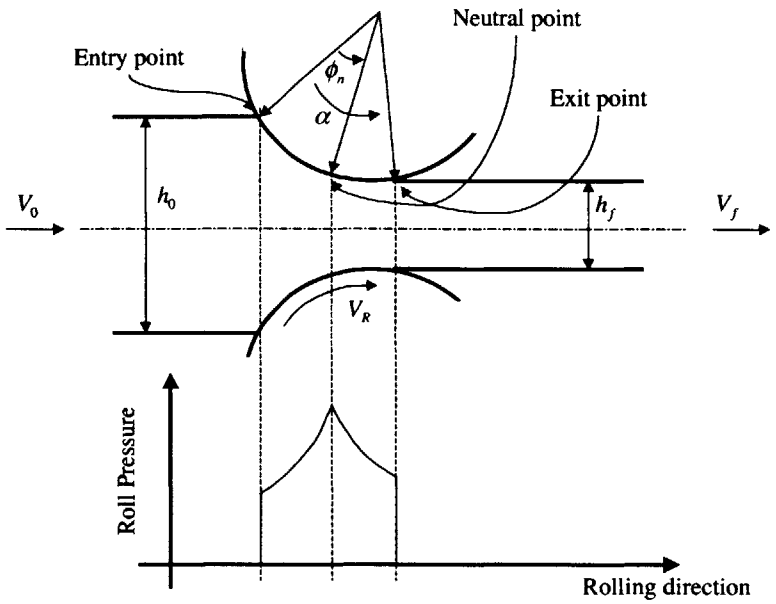

Figure 3.4 Pressure Distribution in Roll Bite

With the knowledge of roll pressure, the roll force can be calculated by integrating the pressure along the contacting arc.

$$F = \int_0^{\phi_n} WpRd\phi + \int_{\phi_n}^{\alpha} WpRd\phi \tag{3.7}$$

The angle ϕ_n can be calculated by equating Equation 3.6a and 3.6b, and the solution is shown below.

$$\phi_n = \sqrt{\frac{h_f}{R}} \tan\left(\sqrt{\frac{h_f}{R}}\frac{1}{4}\left(2\sqrt{\frac{R}{h_f}}\tan^{-1}\left(\sqrt{\frac{R}{h_f}}\alpha\right) - \frac{1}{\mu}\ln\frac{h_0}{h_f}\right)\right) \tag{3.8}$$

This equation is useful for determining the roll force when the thickness reduction is known. However, it is very difficult to use this equation to predict output thickness based on measured roll force. The determination of roll force, F, requires the knowledge of the entry and exit pressure profiles, to calculate which requires the location of neutral point, ϕ_n. Both of these values are function of exit thickness, h_f, as shown in Equation 3.7 and

3.8. It will be a set of simultaneous equations with integration. One crude solution is to use the average pressure, p_{ave}, to describe the pressure profile, resulting in Equation 3.9.

$$F = LWp_{ave} \tag{3.9}$$

Since the average force is a function of thickness, an expression of thickness can be derived as a function of force, coefficient of friction, roll radius, input thickness, and effective yield strength.

The effective yield strength, σ, is used in place of yield strength because the strip hardens during deformation. One model that predicts the work hardening of steel is the exponential function of true stress (Ginzburg 1989).

$$\sigma = K\varepsilon^n \tag{3.10}$$

where ε is the true strain. The parameter n is called strain-hardening exponent, and the parameter K is the strength coefficient. Both parameters are material properties of steel. The effective stress is also called the flow stress, which is the required stress to continue plastic deformation. For plane stress compression, this number has been shown to be 1.15 times the annealed yield strength of the material.

This plane stress force balance model over simplifies the rolling process. Neglecting the impact of tension, roll speed, and roll deformation is not a reasonable assumption when accurate prediction of output thickness is desired. This model is useful when rough estimation is desired, but not suitable for the tasks of this thesis.

3.2 Roberts' Model

Roberts' model is a more sophisticated model than the force balance model. The assumptions that it is based on are as follows.

1. The volume of the strip remains constant.
2. The friction effect is neglected.

3. Elastic deformation of the strip is negligible compared to the plastic deformation of the strip under rolling.
4. The work roll deforms elastically during the rolling process, with a constant deformed roll radius.
5. Tensile stress applied on the strip reduces the effective compressive yield strength of the strip as predicted by Tresca's maximum shear theory.
6. Plane strain conditions are assumed. In other words, width is assumed to be constant through the production.
7. The process conditions are symmetrical about the pass-line of the mill stand.
8. Forward slip is neglected, i.e., the strip exit speed equals the roll circumference speed.

Nomenclature for Roberts Model

h_0 : entry thickness
h_f : exit thickness
F : roll force
L : contact arc length
$\dot{e}$: strain rate
σ_p : minimum deformation pressure
f_R : specific roll force
D : roll radius
A : strain rate sensitivity coefficient
E : Young's modulus
V : roll circumference speed
σ_0 : annealed yield strength
σ_a : effective tensile stress in roll bite
σ_c : dynamic constrained yield strength
D': deformed roll diameter
r : reduction ratio
W : width
σ_1 : entry tension
σ_2 : exit tension
β : roll deformation conatant
C_L : Lode's constant

Since the reduction ratio is defined by Equation 3.11, h_f can be determined once r is calculated with Equation 3.12.

$$r = \frac{h_0 - h_f}{h_0} \tag{3.11}$$

$$h_f = -h_0(r-1) \tag{3.12}$$

From the geometry of the roll bite, the following equation can be derived such that

$$r = \frac{2L^2}{D'h_0} \tag{3.13}$$

where D' is the deformed diameter of the roll, which can be predicted with Hitchcock's equation (Equation 3.14).

$$D' = D(1 + \beta(f_R/(Eh_0 r))) \tag{3.14}$$

The specific roll force, which is defined as the roll force per unit strip width, is used to simplify the model. This is valid because geometrical symmetry and plane strain are assumed.

L, the length of the contact arc, is also necessary to determine the reduction ratio. It is known that the specific force is the product of deformation pressure and contact arc length.

$$f_R = \sigma_p L \tag{3.15}$$

The deformation pressure is a function of material yield strength, tensile stress in the strip, and strain rate. Von Mises and Tresca have developed different criteria to predict yield stress under compressive deformation with tension. (Kalpakjian 1991) In Roberts' model, Tresca's criterion has been recommended.

$$\sigma_a = (\sigma_1 + (1-r)\sigma_2)/(2-r) \tag{3.16}$$

While many complex relationships between yield strength and strain rate are proposed, Roberts propose a statistical model.

$$\sigma_c = C_L(\sigma_0 + A\log_{10}(1000\dot{e})) \tag{3.17}$$

The Lode's constant, C_L, is multiplied because of the plane strain condition (Khan 1995). The strain rate, $\dot{e}$, can be calculated geometrically (Figure 3.5).

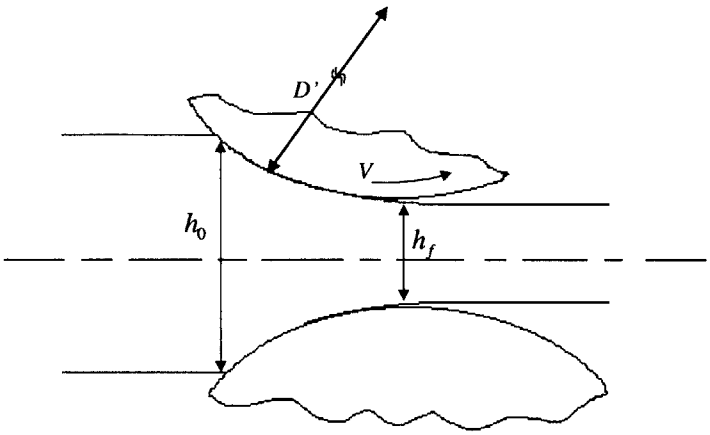

Figure 3.5 Variables used in Roberts' Model

$$\dot{e} = V\sqrt{\frac{2r}{D'h_0}} \tag{3.18}$$

The deformation pressure is the difference between the dynamic constrained yield strength and the effective tensile stress in the roll bite.

$$\sigma_p = \sigma_c - \sigma_a \tag{3.19}$$

This results in eight simultaneous equations that can be used to model a cold mill stand. The Roberts' model is often used in the steel industry for its accuracy and simplicity. This thesis used this model to describe the thickness reduction of the steel strip in the first four stands.

3.3 Stone's Roll Force Model

Even though Roberts' model returns reasonably good results, some assumptions are not always applicable. First, neglecting friction in rolling model leads to underestimation of strip hardness. Second, the neutral point shifts toward the middle of roll bite when exit tension is decreased. The assumption of no slippage ignores this phenomenon. Stone derived a roll force model that does not assume the exit speed to be the same as roll circumference speed from the pressure distribution in the roll bite. This enables the

rolling models to be applied to a wider range of productions. The assumptions of Stone's force model are listed below.

1. The volume of the strip remains constant.
2. Elastic deformation of the strip at the start and the end of the roll bite.
3. Tensile stress applied on the strip reduces the effective compressive yield strength of the strip as predicted by Von Mises' shear theory.
4. Plane strain conditions are assumed. In other words, width is assumed to be constant through the production.
5. The process conditions are symmetrical about the pass-line of the mill stand.
6. The neutral point, where the strip speed equals the roll circumference speed, occurs at the midpoint of the contact arc.
7. The pressure distributions in the roll bite are symmetrical about the neutral point.
8. The friction coefficient is constant in the roll bite.

Nomenclature for Stone's Force Model

h_0 : entry thickness
h_f : exit thickness
F : roll force
L : contact arc length
σ_p : minimum deformation pressure
μ : coefficient of friction
r : reduction ratio
σ_1 : entry tension
σ_2 : exit tension
f_R : specific roll force
V : roll circumference speed
x_L : distance betwen neutral point and exit point

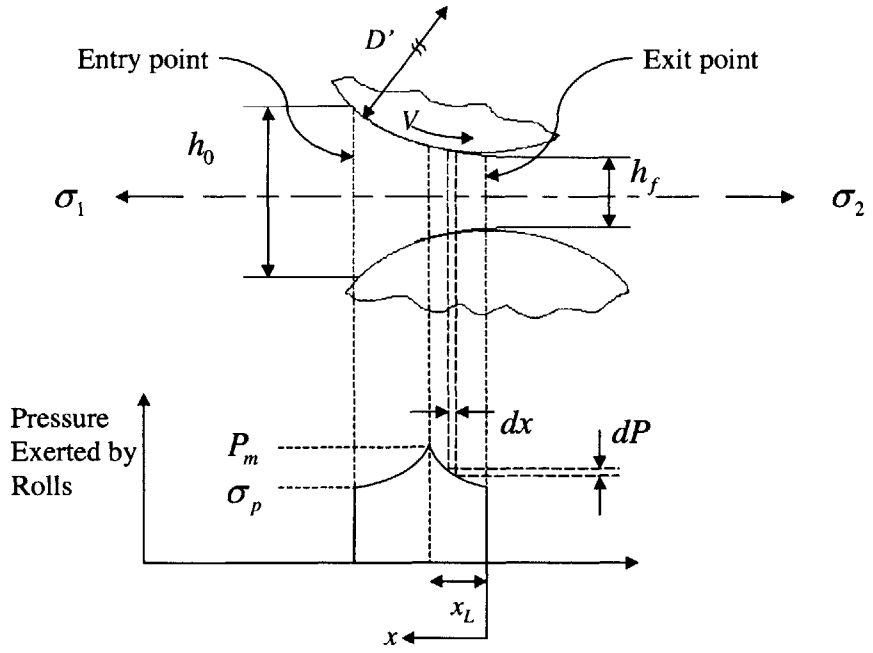

Figure 3.6 Schematic for Stone's Model

Similar to the force balance model, Stone's model is derived based on the force balance of a finite piece of the strip. First, an element with length dx at distance x from the exit point is identified. The point where roll speed equals the strip speed is defined as the neutral point, and it is located at distance x_L from the exit point. While Roberts assumes the pressure distribution within the roll bite is uniformly distributed, Stone assumes the following equations to describe the incremental change of pressure.

$$dp = \frac{2\mu p dx}{h_0(1-r)} \tag{3.20}$$

where p is the normal pressure on the strip, m is the coefficient of friction, and $h_0(1-r)$ is the exit thickness of the strip, h_f.

Since it is assumed that no deformation occurs during plastic deformation, the pressure at distance x from the exit point, P_x, can be expressed by the following integral.

$$p_x = \int_{\sigma_p}^{P_x} \frac{dp}{p} = \sigma_p e^{\frac{2\mu x}{h_0(1-r)}} \tag{3.21}$$

Once the pressure at each location x is determined, the force exerted by the roll on the strip between the exit point and the neutral point is as follows.

$$f_R = \int_0^{x_L} p_x dx = \int_0^{x_L} \sigma_p e^{\frac{2\mu x}{h_0(1-r)}} = \frac{\sigma_p h_0(1-r)}{2\mu}\left[e^{\frac{2\mu x_L}{h_0(1-r)}} - 1 \right] \tag{3.22}$$

The assumption that x_L occurs at the middle of the contact arc and the geometrical similarity with respect to the pressure distribution on each side of the neutral point leads to the final equation for the specific force equation.

$$f_R = \frac{\sigma_p h_0}{\mu}\left[e^{\frac{\mu L}{h_0}} - 1 \right] \tag{3.23}$$

This force model can be rewritten to calculate the contact arc length in the cases that the roll force is known.

One major difference between Stone and Roberts' model is the location of neutral point. Stone has derived a model for the rolling conditions that neutral point is near the center of the roll bite. While Roberts' assumption that neutral point is near the exit or roll bite is reasonable for Stand 1 through 4, Stone's assumptions is valid for the last stand because the exit tension of the last stand is much less than its entry tension. In this thesis, Stone's Force model is used in combination with Roberts' model to express the behavior of the last stand in the mill.

3.4 Carlton's Energy Balance Model

Carlton, et al, has developed a model based on energy balance instead of force balance, in the 1970s (Carlton, Edwards et al.). This model is intended to predict the necessary roll force to achieve the target exit thickness. The assumptions that this model is based on are listed below, and the schematic drawing of the model is shown in figure 3.7.

1. The energy from mechanical shafts and tension goes to friction and steel plastic deformation.

2. Plane strain conditions are assumed. All deformation of the strip is in transverse and vertical direction.
3. Negligible elastic recovery and constant pressure distribution is assumed when calculating the location of the neutral point.
4. For calculation of frictional energy, the forward slip is ignored, and the pressure distribution in roll bite is assumed to be linear.
5. 50% of the frictional heating energy is assumed to transmit to the strip.

Nomenclature for Carlton's Energy Balance Model

a_i : specific roll force coefficients

b_i : frictional heating coefficients

c_i : forward slip ratio coefficients

c : elasticity constant

C_P : specific heat of strip

E : Young's modulus of roll

E_s : Young's modulus of strip

E_f : specific frinction energy

E_m : specific shaft energy

E_r : specific reduction energy

E_t : specific tension energy

f : forward slip ratio

h_0 : entry thickness

h_f : exit thickness

h_m : minimum strip thickness in roll bite

$\overline{h}$: average strip thickness

$k(r)$: plane strain yield stress at reduction r

k_θ : sensitivity of yield stress to temperature

k_i : yield stress coefficients

Δk : yield stress offset

$\Delta k_{\dot{\varepsilon}}$: strain rate component of yield stress

Δk_θ : temperature component of yield stress

k^*: effective yield stress

L : contact arc length w/o roll deformation

L_p : contact arc length with roll deformation

F : total specific force

F_e : elastic recovery component of roll force

F_P : plastic compresstion component of roll force

r : thickness reduction ratio

R : work roll radius

R': deformed work roll radius

T : shaft torque

T_1, T_2 : entry, exit tension force

σ_1, σ_2 : entry, exit tension stress

σ_2': tensile stress at boundary between plastic and elastic deformation

V_1, V_2 : entry, exit roll speed

x_n : normalized neutral angle

α : strain rate constant

δ : strip thickness reduction

ε : true strain

$\dot{\varepsilon}$: true strain rate

θ_1, θ_2 : entry, exit strip temperature

λ : dimensionless parameter

μ : coefficient of friction

ν : Possion's ratio

ρ : strip density

ϕ_n : neutral angle

ϕ_1 : angle of entry point

ω : work roll angular speed

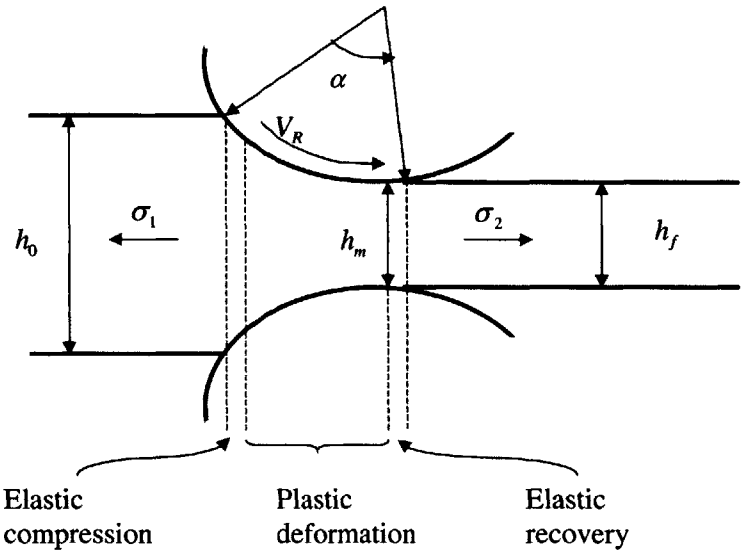

Figure 3.7 Schematics for Carlton's Model

From the first assumption, an energy balance equation can be written (Equation 3.24).

$$E_r + E_f = E_m + E_t \tag{3.24}$$

where specific energy is defined as energy per unit volume of strip rolled.

The mechanical energy, E_m, is a function of torque, deformed roll radius, exit strip thickness, and forward slip ratio. Therefore, the previous equation can be re-written as the following.

$$T = R'h_f f\left(E_r + E_f - E_t\right) \tag{3.25}$$

Torque can be measured from the current supplied to the motor and each term in this equation is calculated with the following models.

The deformed roll radius, R', is another form of Hitchcock's equation.

$$R' = R\left(1 + c\,P/\delta_1\right) \tag{3.26}$$

where c is the elasticity constant in Hitchcock's equation and δ_1 is a fictitious thickness change.

$$c = 16\left(1-\nu^2\right)/\pi E \tag{3.27}$$

$$\delta_1 = \left(\sqrt{h_o - h_m} + \sqrt{h_f - h_m}\right)^2 \tag{3.28}$$

The minimum thickness h_m, shown in figure 3.7, is given by Equation 3.29.

$$h_m = h_f\left[1-\left(1-\nu_s^{\,2}\right)\left(k\left(h_f\right)-\sigma_2\right)/E_s\right] \tag{3.29}$$

The variable, $k\left(h_f\right)$, is the plane strain yield stress of the strip at thickness h_f. Roberts has suggested a polynomial equation, has developed an exponential expression. The equation recommended by Carlton is the following.

$$k\left(h_f\right) = k\left(r\left(h_0, h_f\right)\right) = k_1\left(k_2 + r\right)^{k_3} + \Delta k \tag{3.30}$$

where r is a function of h_f. The k_i's are statistically fit constants and are material properties of each strip. The yield stress offset term, Δk, allows the inclusion of temperature and strain rate effect in the calculation of effective yield stress of the strip.

$$\Delta k = \Delta k_{\dot{\varepsilon}} + \Delta k_\theta \tag{3.31}$$

The effect of strain rate on the yield strength is a very active area of research (Manjoine 1944; Marsh 1963; Ishikawa 1996). An example is Fuller's equation, which is obtained statistically from empirical data (Fuller 1969).

$$\Delta k_{\dot{\varepsilon}} = 0.164\left[1 - 0.33\varepsilon + 0.7e^{(-11.8\varepsilon)}\right]\left[\frac{\dot{\varepsilon}}{100}\right]^{0.15} \tag{3.32}$$

The temperature's impact on the yield strength is assumed to be linear to the medium temperature of the strip.

$$\Delta k_\theta = -k_{\theta 1}\left(\theta_1 - \theta_2\right)/2 \tag{3.33}$$

While the entry strip temperature can be measured, the output strip temperature has to be calculated on-line with the following equation.

$$\theta_2 = \theta_1 + \left(E_r + 0.5E_f\right)/\rho C_P \tag{3.34}$$

The strip density, ρ, and specific heat, C_P, and the statistically determined coefficient, $k_{\theta 1}$, are material properties. The forward slip ratio, f, is defined as the ratio between strip exit speed and the roll peripheral speed, $f \equiv V_2/R\omega$. A dimensionless x_n, $0 \le x_n \le 1$, is introduced to calculate the slip ratio. x_n is defined as the normalized distance from the end of the plastic compression zone to the neutral point. Besides x_n, f is also a function of the entry strip thickness, minimum strip thickness in roll bite, and the exit strip thickness.

$$f = \left[1 + x_n{}^2 \left(h_0 - h_m\right)/h_m\right] \, h_m/h_f \tag{3.35}$$

Prior to calculating x_n, it is necessary to know the location of the neutral point in the roll bite. Assuming constant pressure in the compression zone, the location of x_n is calculated as follows, using the force equilibrium condition in the transverse direction.

$$x_n = 0.5\left[1 - \frac{\delta}{2\mu L_p} + \frac{\sigma_2{}' h_f - \sigma_1 h_0}{2\mu\left(F_P\right)}\right] \tag{3.36}$$

Carlton then modifies the equation to compensate for modeling error by adding arbitrary statistical variables, c_i, which are fit statistically.

$$x_n = c_1\left[1 - \frac{c_3\delta}{2\mu L_p} + \frac{c_2\left(\sigma_2{}' h_f - \sigma_1 h_0\right)}{2\mu\left(F_P\right)}\right] \tag{3.37}$$

The horizontal stress at the exit edge of the plastic zone, derived by Ford et al, is calculated with the following equation. (Ford 1951)

$$\sigma_2{}' = \sigma_2 - 2\mu F_e/h_f \tag{3.38}$$

where the elastic recovery force, F_e, is

$$F_e = \frac{2}{3}\sqrt{R'h_f}\left(k(h_f) - \sigma_2\right)^{1.5}\sqrt{\left(1-\nu^2\right)/E_s} \tag{3.39}$$

The force in the plastic deformation zone is calculated with the following equation.

$$F_P = \left[a_1 k(\bar{r}) - a_2(\sigma_1 + a_3\sigma_2')\right]L_P\left(h_f/\bar{h} + a_4\lambda^{a_5}\right) \tag{3.40}$$

The coefficients a_i's are statistically fit, and λ is a dimensionless parameter (Equation 3.41).

$$\lambda = \mu L_P/\bar{h} \tag{3.41}$$

The term $k(\bar{r})$ is the mean yield stress of the strip in the plastic deformation zone (Equation 3.42), calculated by substituting the average reduction in the plastic deformation zone, $\bar{r}$, in Equation 3.30. The average strip thickness in plastic deformation zone, $\bar{h}$, can be calculated with $\bar{r}$ or the following equation if a circular contact arc is assumed.

$$\bar{r} = 1 - 0.4\frac{h_0}{h_0} - 0.6\frac{h_f}{h_0} \tag{3.42}$$

$$\bar{h} = \frac{h_0}{3} + \frac{2h_f}{3} \tag{3.43}$$

The amount of energy per volume used to reduce the strip thickness, E_r, in Equation 3.44 is a function of yield strength at the original thickness, medium thickness, and the exit thickness of the strip, along with the amount of reductions.

$$E_r = \frac{\delta}{6}\left[\frac{k(h_0)}{h_0} + 8\frac{k\left(\frac{h_0+h_f}{2}\right)}{h_0+h_f} + \frac{k(h_f)}{h_f}\right] \tag{3.44}$$

The frictional energy per unit volume, E_f, is a function of the speed of the strip relative to the roll and the normal force along the two contacting arcs. The function $p(x)$ is the pressure at the location x.

$$E_f = \frac{2}{\mu V}\int_0^{L_P} |\Delta V| \mu p(x) dx \tag{3.45}$$

By neglecting the forward slip and assuming linear pressure distribution in the roll bite, the integral for calculating frictional energy in the rolling process can be expressed by the following equation.

$$E_f = \frac{\beta_0 \mu L_P}{h_f}\left\{\left[1 - 2\sqrt{\frac{h_f}{\delta}}\tan^{-1}\sqrt{\frac{\delta}{h_f}} + \frac{h_f}{\delta}\ln\left(1+\frac{\delta}{h_f}\right)\right]\left(\frac{2F}{L_P} - p_1\right) + \left[1 - \frac{h_f}{\delta}\ln\left(1+\frac{\delta}{h_f}\right)p_1\right]\right\} \tag{3.46}$$

The term p_1 is the difference between the yield strength of the strip at the elastic recovery zone and entry tension stress.

$$p_1 = k(h_e) - \sigma_1 \tag{3.47}$$

The thickness of the strip at the elastic recovery zone is statistically determined with a coefficient β_1.

$$h_e = \beta_1 h_0 + (1-\beta_1)h_f \tag{3.48}$$

The last term in Equation 3.* is the specific tension energy supplied by the mill. This energy is simply the difference between exit and entry tension.

$$E_t = \sigma_2 - \sigma_1 \tag{3.49}$$

It has been shown to predict the roll force with reasonable accuracy, and it has been adapted in commercially available software for simulating the cold rolling process. This model is useful for predicting the necessary roll torque based on the desired reduction. However, this model requires many statistical parameters that need to be fit from process data. Furthermore, this model is very computationally intensive.

3.5 Chapter Summary

This chapter has discussed the rolling models that have been developed for decades. Roberts' model and Stone's model are used in this thesis to model individual stands in the cold rolling mill. This is the first step for constructing a model that predicts output thickness from the characteristic properties of input strips. In next chapter, these models can be linked as an integrated model. The inter-stand models that predict the input material properties of strip for each stand will also be discussed.

Chapter 4: Cold Mill Modeling

In the previous chapter, the model for each reduction stand was developed. As will be argued, Roberts' model is used to model the behavior of Stand 1 through 4, while Stone's model is suitable for Stand 5. In this chapter, the five individual stand models are integrated. The material equations that describe the hardening of steel after each reduction stand are discussed in Chapter 4.

However, two problems need to be solved before the integrated model can be used to predict output thickness variation based on process variables. The first problem is to determine at what frequency the model should be calibrated and explored. This frequency determines the amount of variation that will be observed. The second problem is that two critical process variables required by the integrated model are not measured. These variables are the yield strength, s_0 and the hardening coefficient a_1. This chapter will also discuss the solutions for these two problems.

Once these two problems are resolved and an integrated physical model of the cold rolling mill is constructed, output thickness can be calculated given the values of process variables. Models of controllers can be developed to predict these values. A model that predicts output thickness based on characteristic properties of input strip will be constructed by combining these controller models with the integrated physical model.

4.1 Stand Model

As discussed in the previous chapter, the force balance model over-simplifies the rolling process. Neglecting the tensions in the strip leads to errors in estimating the yield strength of the strip. Also, the deformation of work roll, which is ignored in the model, has a significant impact on the strip production. On the other hand, Carlton's energy model, while sophisticated, has too many variables that are unmeasured in the system.

Given this, Roberts's model is a good model for this system. It addresses the basic physical phenomenon that takes place in the rolling process, such as roll deformation and effective yield strength. It has been successfully applied in this thesis to describe the behavior of the rolling stands 1 through 4. Stone's model is utilized in the last stand for the reason discussed in section 4.4. This model includes friction and is based on slightly different assumptions, but it has manageable complexity and has been shown to have reasonable accuracy. (Lin 1996)

4.2 Inter-stand Model

In the entire cold-mill system model, the outputs of each stand model become the inputs of the next model. These variables are the geometrical characteristics and material properties of the steel. The geometrical characteristics include the thickness and width, which is assumed to be constant throughout the entire production. The thickness can be calculated based on the models discussed above. This section discusses the material model, as it relates to inter-stand connectivity of the individual stand models.

The material properties that propagate down the production line are the yield strength, σ_i, and the sensitivity to strain rate, A (Equation 3.17). The yield strength increases as the strain in the workpiece increase, a phenomenon known as work hardening. It has been shown that work hardening takes place after deformation in each stand (Bentz and Roberts 1966). Two models are explored to predict the yield strength of the steel strip entering each stand. The first is an exponential model,

$$\sigma_1 = \sigma_0 \varepsilon^n ; \tag{4.1}$$

where n is the material property known as the strain-hardening exponent and ε the real strain that has been applied to the strip (Khan 1995). The second model is a polynomial equation (Equation 4.2).

$$\sigma_1 = \sigma_0 + a_1 r_x + a_2 r_x^{\,2} + a_3 r_x^{\,3} \tag{4.2}$$

where a_1, a_2, and a_3 are material properties, and r_x is the total reduction prior to the stand (Roberts 1978). Both have been applied and the polynomial model returned a better result in the integrated model developed in this thesis.

Another material property that propagates down the production is the strain rate sensitivity coefficient, A. Figure 4.1 shows the relationship between yield strength, strain, and strain rate for steel. The slope indicated on the curve is the strain rate sensitivity. The slope decreases as the strain in the workpiece increases. A linear model is proposed to describe the change in A (Equation 4.3).

$$A_1 = A_0 - cr_x \tag{4.3}$$

where c is a constant.

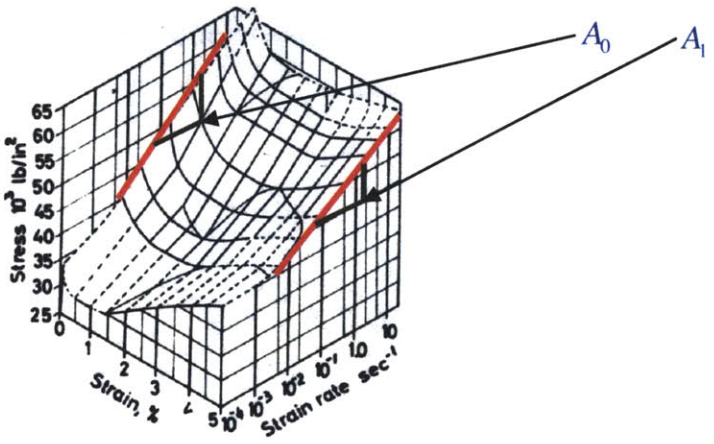

Figure 4.1 Strain and Strain-Rate Hardening Surface of Steel[3]

With the models discussed in this section, input variables for each rolling stand can be calculated from the process of the previous stands. The stand models can be then linked and generate an integrated model.

[3] Figure from "Strain Rate Effects in Dynamic Loading of Structures" by Bodner (Bodner 1965)

4.3 Sampling Frequency Determination

Before calibrating the models, it is important to identify the data stream to be used. Series of sampled points are used to describe each variable in continuous manufacturing processes. The model can be calibrated at each sampled point if all data streams are synchronized. In the actual system, sensors have different response times and the sampled data for the variables are stored at different rates. In this thesis, raw data from the sensors are averaged into data streams with identical numbers of bins for two reasons. The first is to block out the high frequency sensor noises and the high frequency dynamics of the mill, such as vibrations, that cannot be modeled. Taking the average of data over a time period has a similar effect as a low-pass filter. The second reason for splitting sensor data into bins of averaged values is the asynchronization among data. If the size of each bin is significantly larger than the offsets among data storage devices, the impact of these offsets in time is reduced. Figure 4.2 is a schematic of the averaging process, with the bin size 5 times the original sampling period.

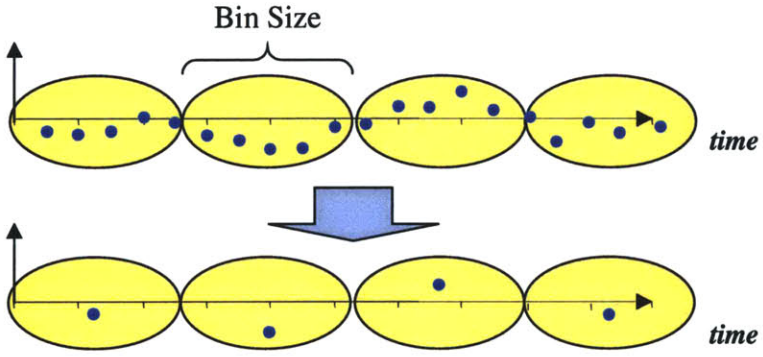

Figure 4.2 Averaging of a Data Stream

The averaging process reduces the variation that is observed in each variable. It is necessary to determine how much information is contained in the averaged data stream, and what a sufficient sampling rate would be. From this point forward in the thesis, the sampling rate of a data stream will refer to the inverse of the duration of a bin. For example, a data stream with bin size of 0.5 second has a sampling rate of 2Hz.

In this thesis, the strip thickness standard deviation is the direct concern. Therefore, a ratio between standard deviations, r, is proposed in this thesis as an indicator for the amount of variation retained in a sampled data stream. (Equation 4.4)

$$r = \frac{\sigma_{\text{sampled}}}{\sigma_{\text{actual}}} \tag{4.4}$$

Of course, σ_{actual} can never be known, only sampled measurements. For any measured stream of data, one can consider its sampling rate adequate to represent σ_{actual} if halving its data causes no reduction in information on σ. Therefore, the quantity in Equation 4.5 is considered.

$$r = \frac{\sigma_{\text{reduced sampling}}}{\sigma_{\text{original sampling}}} \tag{4.5}$$

One can show r is monotone with the information content in the signal, and so is theoretically a good measure, while yet practically remaining focused on σ. From information theory, the information content of a continuous random variable, Y, is expressed as

$$H(Y) = -\int_{-\infty}^{\infty} p(y) \ln p(y) dy \tag{4.6}$$

where $p(y)$ is the probability density distribution of Y. If $p(y)$ is a Gaussian distribution with mean of $\bar{y}$ and standard deviation of σ, the information in Y can be represented as a function of σ, as shown in Equation 4.7 (Blahut 1987).

$$\begin{aligned} H(Y) &= -\int_{-\infty}^{\infty} \frac{1}{\sqrt{2\pi\sigma^2}} e^{\left(\frac{(y-\bar{y})^2}{2\sigma^2}\right)} \ln\left(\frac{1}{\sqrt{2\pi\sigma^2}} e^{\left(-\frac{(y-\bar{y})^2}{2\sigma^2}\right)}\right) dy \\ &= \frac{1}{2}\ln 2\pi\sigma^2 + \frac{1}{2} \\ &= \frac{1}{2}\ln\left(2\pi e\sigma^2\right) \end{aligned} \tag{4.6}$$

The difference between information from the new and the original data streams is represented in Equation 4.8.

$$\Delta H = H(Y_2) - H(Y_1) \tag{4.8}$$

where 1 denotes the original data and 2 denotes the new data obtained through taking averages of data in bins.

The probability density distribution associated with each Y_2 is narrower than that with Y_1 due to the averaging effect. As an example, a normally distributed random signal, shown in Figure 4.3, is sampled at Ω_0 Hz, $\frac{\Omega_0}{2}$ Hz, and $\frac{\Omega_0}{4}$ Hz. The standard deviation decreases as the sampling rate slows. The resulting probability density functions of Y are shown in Figure 4.4 and they vary as the sampling frequency changes.

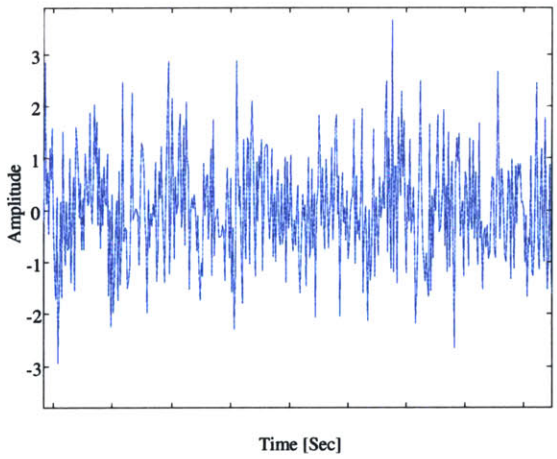

Figure 4.3 Normally Distributed Signal

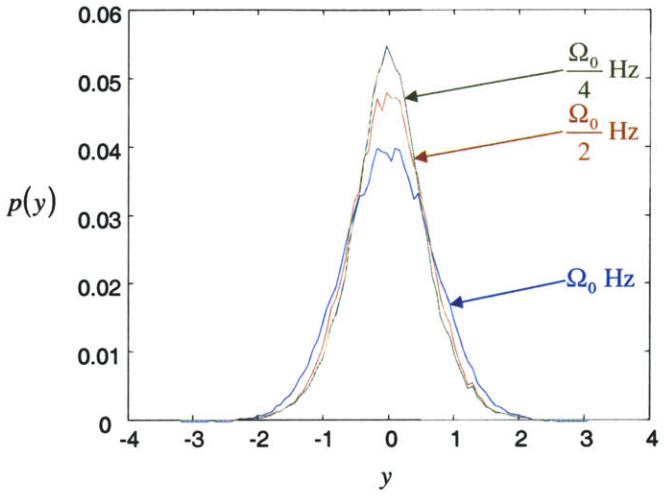

Figure 4.4 *pdf* Calculated from Samples with Different Frequencies

The ratio *r*, defined as the ratio between standard deviations between the original and the averaged data streams, can be derived. Equation 4.7 is substituted in Equation 4.8 to represent the difference in the information content between the two data streams only with their standard deviations.

$$\begin{aligned} -\Delta H &= H(Y_1) - H(Y_2) = \frac{1}{2}\ln\left(2\pi e\sigma_1^{\,2}\right) - \frac{1}{2}\ln\left(2\pi e\sigma_2^{\,2}\right) \\ &= \frac{1}{2}\ln\left(\frac{2\pi e\sigma_1^{\,2}}{2\pi e\sigma_2^{\,2}}\right) \\ &= \ln\left(\frac{\sigma_1}{\sigma_2}\right) \end{aligned} \tag{4.9}$$

Equation 4.9 is then rearranged to express *r* in terms of information content in the original and new distributions.

$$\begin{aligned} r &= \frac{\sigma_2}{\sigma_1} \\ &= e^{\Delta H} \end{aligned} \tag{4.10}$$

Therefore, ensuring the ratio *r* remains adequate is the same as ensuring the information loss ΔH is not excessive. However, r is practically a better measure, as it has ready interpretation.

In this thesis, an empirical approach is introduced to express r based on the sampling frequency, Ω (Equation 4.1).

$$r = \beta_0 + \beta_1 \ln(\Omega + \beta_2) \tag{4.11}$$

The values of r are calculated for various Ω, and the coefficients β_i are regression fit over these r and Ω.

This expression is valuable not only because it gives an indication of the amount of variation that is observed at a given sampling rate, but it also allows determination of a sampling rate that is sufficient for observing variations in a data stream. The derivative of Equation 4.10 represents the gain in r per unit increase in Ω. Since the derivative is a monotonically decreasing function, a threshold can be set to define a sufficient sampling rate, beyond which faster sampling returns little additional information.

4.3.1 Examples

Two examples are used to demonstrate the validity of Equation 4.10. The first example is a normally distributed random signal sampled at 100Hz for 10 seconds (Figure 4.5). The power spectrum density of this signal is shown in Figure 4.6.

The standard deviation of this normally distributed signal is 1.0313. As the sampling rate falls, the averaging effect washes out the variations in the high frequency regions. The standard deviation is calculated for each down-sampled data stream, and the ratio between the new standard deviation and the original standard deviation is calculated (Table 4.1).

Sampling Frequency (Hz)	*r*
100	1.00
50	0.71
25	0.48
12.5	0.34
6.3	0.22
3.1	0.12
1.6	0.08
0.8	0.05

Table 4.1

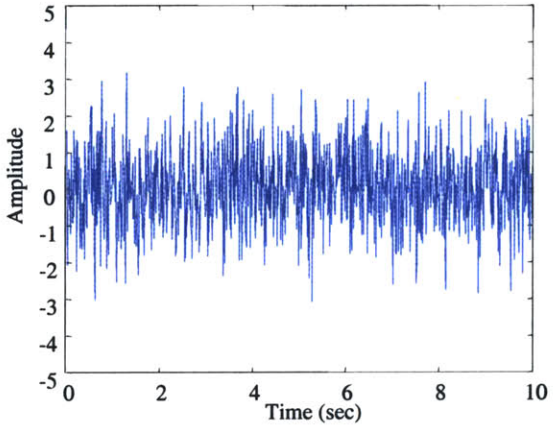

Figure 4.5 A Random Signal

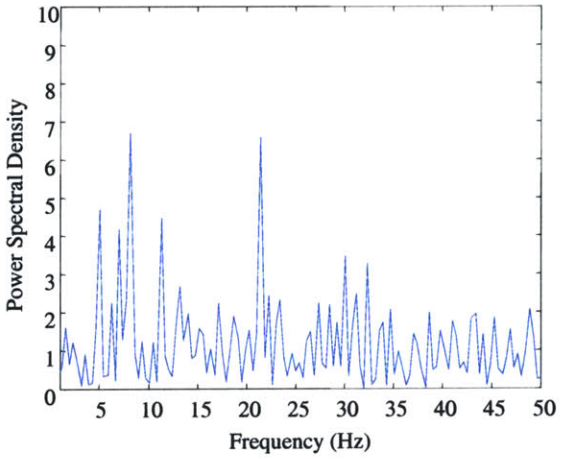

Figure 4.6 Power Spectrum of the a Random Signal

An equation is fit to trace these series to predict r as a function of sampling frequency (Equation 4.12)

$$r = -1.2021 + 0.4623(\ln(\Omega + 14.5141)) \tag{4.12}$$

This curve and its derivative are plotted in Figure 4.7. The left y-axis is the ratio r, and the right y-axis is its derivative. The values from Table 4.1 are plotted on the same graph, shown as red circles.

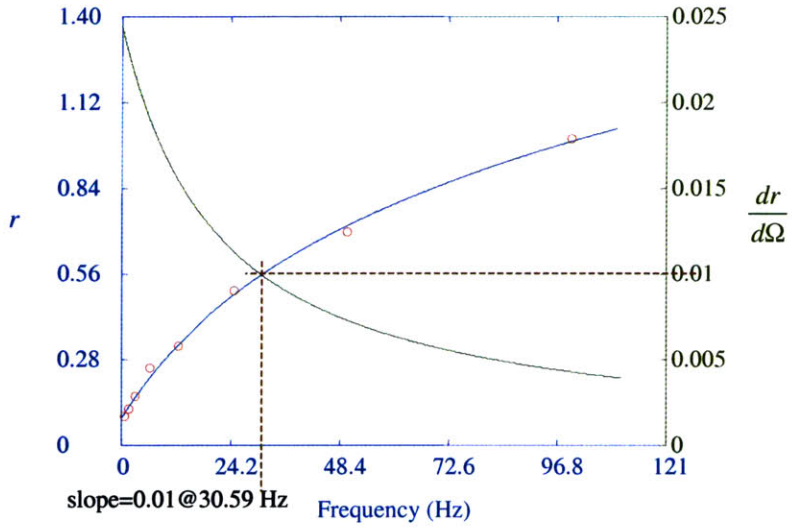

Figure 4.7 r Calculated by Averaging the Random Signal

This model predicts that the higher the sampling rate, the more variation will be observed (Equation 4.13).

$$\lim_{\Omega \to \infty} r = -1.20 + 0.46(\ln(\infty + 14.51)) = \infty \tag{4.13}$$

However, since the derivative monotonically approaches zero, a sufficient sampling frequency beyond which the increase in r is negligible can be determined from the derivative. In this example, a threshold for the derivative is set arbitrarily at 1%. This leads to the conclusion that increasing the sampling rate beyond 31Hz results in less than 1% gain in the observed variation.

The first example has shown that Equation 4.11 can describe the amount of information that is contained in a normally distributed random signal sampled at different frequencies. However, most manufacturing systems contain more than these kinds of random noises. Instead, vibrations or noises at certain resonance frequencies are often observed. The second example is designed to mimic such situations.

In this example, a 2Hz sine wave is added to the previous signal. The resulting data stream in time domain is plotted in Figure 4.8, and its power spectrum density is shown in Figure 4.9.

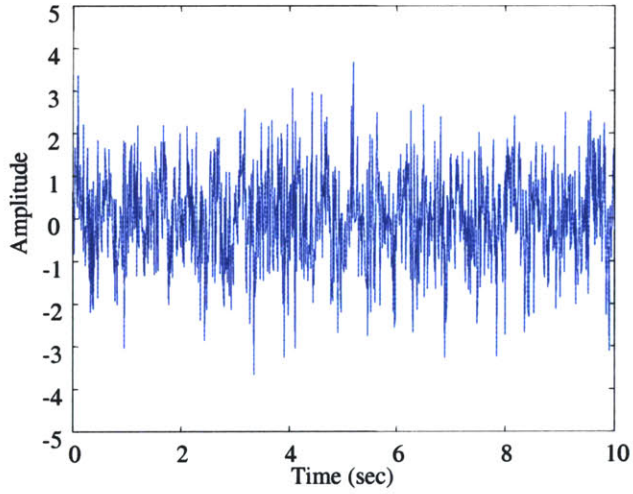

Figure 4.8 Random Signal with a Superimposed 2Hz Wave

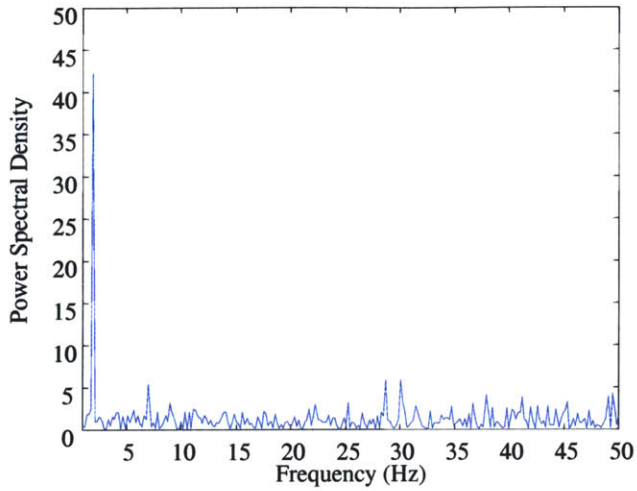

Figure 4.9 Power Spectrum of the Random Signal with a Superimposed 2Hz Wave

The ratio between the standard deviation of the new signal to that of the original signal is listed in Table 4.2. An equation is regression fit based on these numbers and is plotted in Figure 4.10 along with its derivative. It is observed that this curve increases faster than the curve in the previous example, but it flattens at lower frequencies also.

Sampling Frequency	*r*
100	1.00
50	0.76
25	0.59
12.5	0.46
6.3	0.41
3.1	0.20
1.6	0.13
0.8	0.09

Table 4. 2

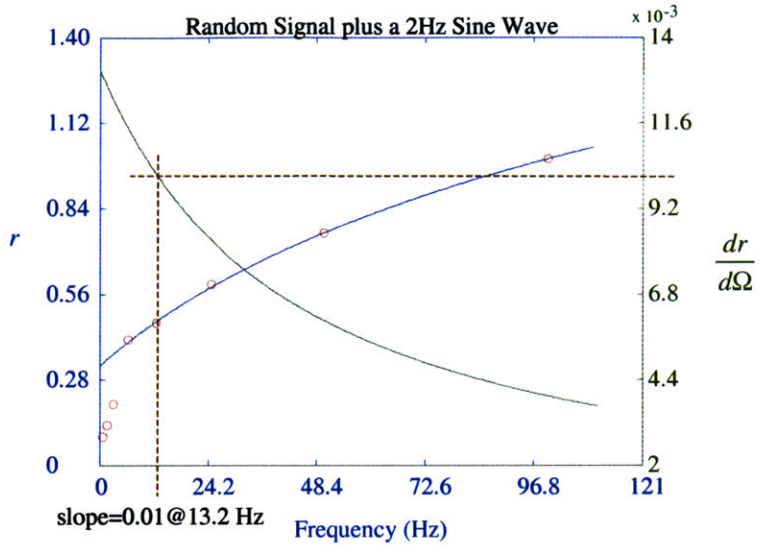

Figure 4.10 *r* Calculated by Averaging the Random Signal with a Superimposed 2Hz Wave

In the case that a periodic pattern is linearly imposed on the random noise, Equation 4.11 is used to fit the points that are above the periodic pattern's Nyquest frequency. A sufficient sampling frequency for that signal can then be determined based on the curve's derivative.

4.3.2 Application to the Cold Rolling Mill

This technique for identifying sampling rate was applied in this thesis for each variable measured in the cold rolling mill. Some of the variables had most of their variations in low frequencies. An example is the entry strip thickness, whose power spectrum is shown in Figure 4.11. In such cases, curves similar to that of the first example were observed (Figure 4.12).

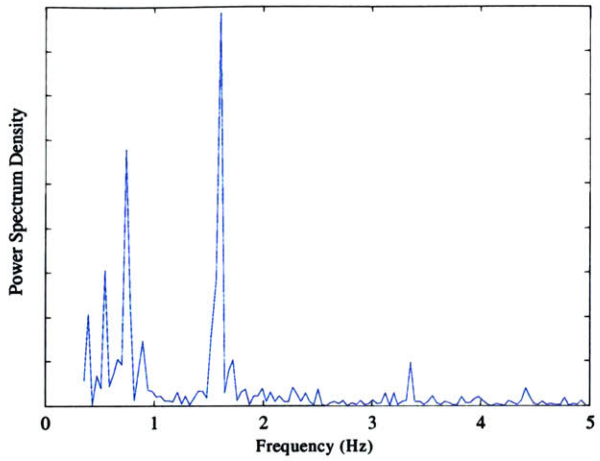

Figure 4.11 Power Spectrum of Entry Thickness

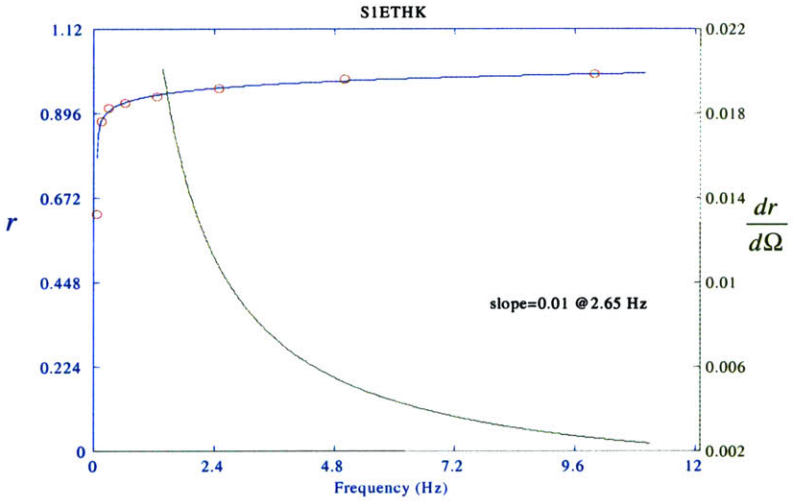

Figure 4.12 *r* Calculated by Averaging Entry Thickness Data

On the other hand, some variables contain variations at certain frequencies. An example is the stand 1 roll force, whose power spectrum is shown in Figure 4.13. Due to the variations in certain frequencies, curves similar to that in the second example is observed (Figure 4.14).

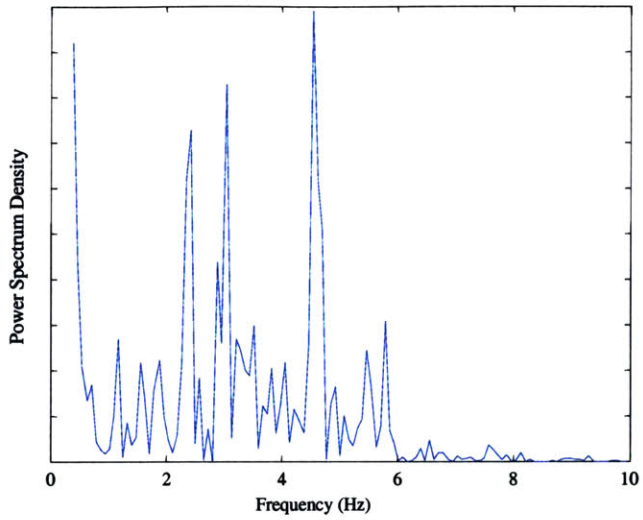

Figure 4.13 Power Spectrum of Stand 1 Force

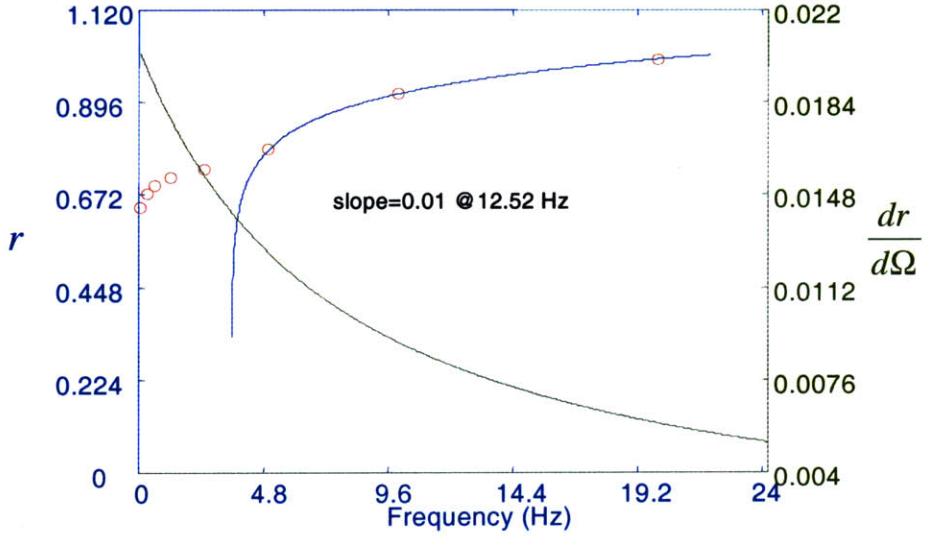

Figure 4.14 *r* Calculated by Averaging Stand 1 Force

The technique discussed was applied to each process variable to identify the sufficient sampling frequency. The sufficient sampling rate for output thickness was found to be 9.8Hz. However, it was not possible to calibrate the model at that sampling rate for two reasons. The first reason was the hardware limitation. Most sensors in this mill were designed to operate at 5Hz; this meant that the model could be calibrated at 5Hz at best without needing to interpret the data. The second reason was the data storage synchronization. The multiple streams of data were stored in different storage devices and they were only synchronized to within a few tenths of a second. Therefore, all signals

were re-sampled at 1Hz to reduce the effect of the lack of synchronization. This reduced the amount of variation that was observed. The standard deviation of output thickness measured at 1Hz is 43% of that measured at 5Hz, and 36% of that measured at 10Hz.

While the model is only explored at 1Hz, the algorithm can be easily expanded to explain 10Hz data streams should an adequate sensor system become available. This can be seen in Figure 8.1, which is the waterfall chart of the exit thickness. It plots the power spectrum density of output thickness in a vertical plane at each location down the strip.

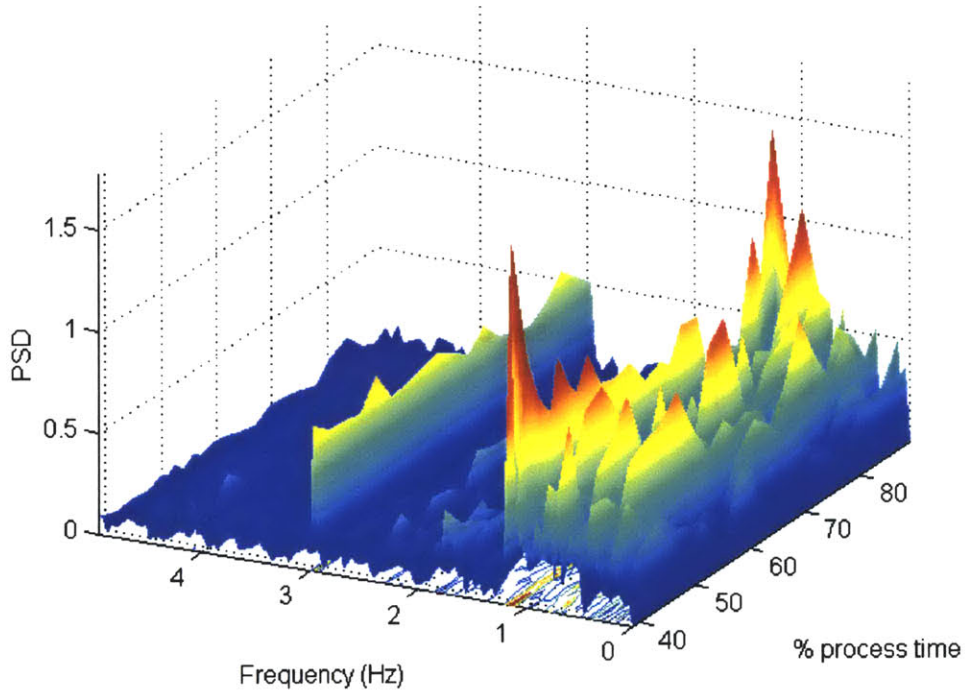

Figure 4.15 Waterfall plot of Stand 1 Exit Thickness

The impact of input strip thickness disturbances and the control actions concentrate in low frequencies (up to about 1.5Hz). Above 1.5Hz, the added variations can be seen to be roll eccentricities, such as at 3Hz in Figure 4.15. Other variations are insignificant and can be modeled as random noise in the simulation model. The eccentricity of rolls can be included in the current model by adding a periodic gain to the roll radius variable, with the observed frequency.

4.4 Model Calibration

The first problem in implementing the physical model to describe the behavior of the cold mill is determining at which sampling frequency to calibrate the model in order to observe the output thickness variation sufficiently. This problem has been addressed in the previous section. The second problem is that both the yield strength and hardening coefficient of the strip are not measured. To solve this problem, the values of these variables are modeled in terms of known process variables. The details are presented in this section.

In the cold rolling mill, entry and exit tensions, roll speed, and roll force are measured at each stand. Thickness measurements are only available at the entry of the mill, the exit of the 1st stand, the exit of 4th stand, and the exit of the 5th stand (Figure 4.16). As such, the cold rolling model is split into three models: Stand 1, Stand 2-3-4, and Stand 5 models. This allows each model to be calibrated to the nearest measured output thickness.

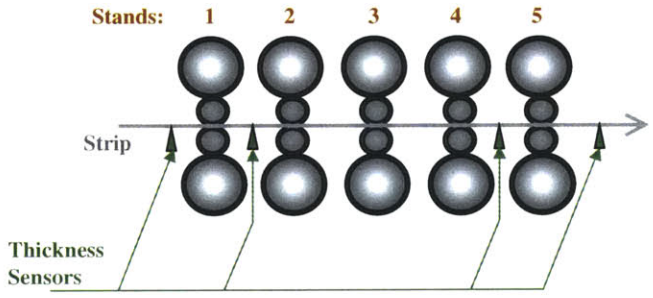

Figure 4.16 Thickness Sensors at the Cold Rolling Mill

It has been shown in previous chapters that a physical model is required to model the behavior of the cold rolling mill. However, there are unmeasured material properties σ_0, a_1, a_2, and a_3. Therefore, before one can construct a model for each stand and use the output of one stand model as the input of the next, statistical expressions for σ_0 and a_i must be determined. The simplest approach is to attempt a single, constant value for each

strip. It is a poor fit, since the material properties substantially vary down the strip, and a single constant best-fit value is not adequate. Figure 4.17 shows the result of a model fit of Stand 1 exit thickness with constant material properties.

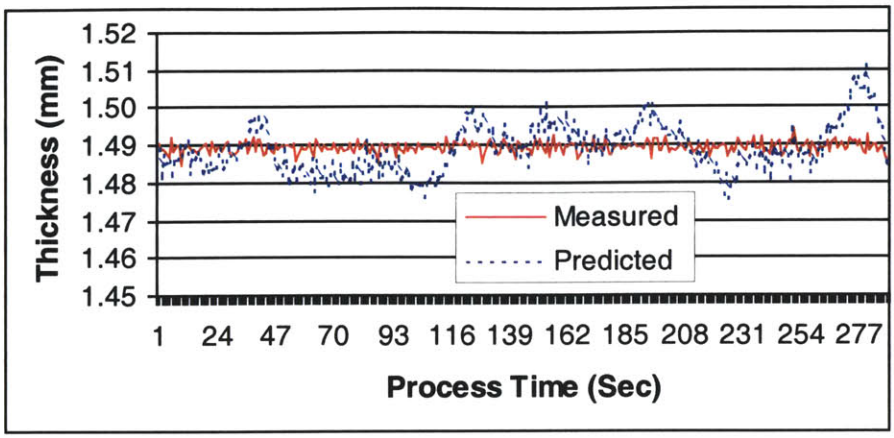

Figure 4.17 Model Stand 1 Exit Thickness with Constant Material Properties

4.4.1 Calibration Theory

Since σ_0 and $\bar{a}$ significantly impact the rolling process, their changes should be reflected in the process variables. In this thesis, they are expressed in terms of measured variables as shown in Equation 4.14.

$$\sigma_0 = \alpha_0 + \sum_j \alpha_j p_j \tag{4.14.a}$$

$$a_i = \beta_0 + \sum_j \beta_j p_j \tag{4.14.b}$$

Now the task is to find regression coefficients α_i, β_i that minimize least square error between thickness prediction of the model and actual measurement for the entire strip, while satisfying the equations in Roberts' model that describe the physical behaviors of the mill. That is, a single set of constants (α_i, β_i) is sought for each strip. Figure 4.18 illustrates the setup of this minimization problem for Stand *i*.

$$\text{Find } \varepsilon^2 = \min_{\vec{\alpha},\vec{\beta}} \left(h_{i,\text{measured}} - h_{i,\text{predicted}}\right)^2$$

such that

$$D'_i = D_i\left(1+\beta\left(f_{Ri}/Eh_{i-1}r_i\right)\right)$$
$$\sigma_{p_i} = km_i - \sigma_{ai}$$
$$L_i = f_{Ri}/\sigma_{p_i}$$
$$\dot{e}_i = V_i\sqrt{\left(r_i D'_i\, h_{i-1}\right)}$$
$$\sigma_{ai} = \left(\sigma_{1i} + \left(1+r_i\right)\sigma_{2i}\right)/\left(2-r_i\right)$$
$$r_i = 2L_i^{\,2}/D'_i\, h_{i-1}$$
$$h_i = h_{i-1}\left(1-r_i\right)$$
$$r_{xi} = \left(h_0 - h_i\right)/h_0$$
$$\sigma_i = \sigma_0 + a_1 r_{xi} + \bar{a}_2 r_{xi}^{\,2} + \bar{a}_3 r_{xi}^{\,3}$$
$$\sigma_0 = \alpha_0 + \sum \alpha_j p_j$$
$$\vec{a} = \vec{\beta}_0 + \sum \vec{\beta}_j p_j$$

Figure 4.18 Calibration Technique

Note this is a very difficult problem, maintaining $11 \times N$ simultaneous nonlinear equations while minimizing over $\vec{\alpha}$ and $\vec{\beta}$ for each Stand *i*. *N* is the number of samples for a strip, and is typically over 200.

Given this, the minimization is split into two steps.

1. Solve nonlinear simultaneous equations for the necessary $(\sigma_0, \vec{a})_{\text{Required}}$.
2. Fit $(\sigma_0, \vec{a})_{\text{Required}}$ to process variables, $\vec{p}$.

That is, first solve for the necessary $(\sigma_0, \vec{a})$ such that output thickness of each stand h_i predicted by the model is exactly as measured, as illustrated in Figure 4.19.

$\forall$ sample point n, Find $(\sigma_0, \bar{a})_{\text{Required}}$

such that $\forall$ Stand i

$$D'_i = D_i\left(1 + \beta\left(f_{Ri} / Eh_{i-1} r_i\right)\right)$$
$$\sigma_{p_i} = km_i - \sigma_{ai}$$
$$L_i = f_{Ri} / \sigma_{p_i}$$
$$\dot{e}_i = V_i \sqrt{\left(r_i D'_i h_{i-1}\right)}$$
$$\sigma_{ai} = \left(\sigma_{1i} + (1 + r_i)\sigma_{2i}\right)/(2 - r_i)$$
$$r_i = 2L_i^{\,2} / D'_i h_{i-1}$$
$$h_i = h_{i-1}(1 - r_i)$$
$$r_{xi} = (h_0 - h_i)/h_0$$
$$\sigma_i = \sigma_0 + a_1 r_{xi} + \bar{a}_2 r_{xi}^{\,2} + \bar{a}_3 r_{xi}^{\,3}$$

Figure 4.19 Split Calibration Technique – Step 1

Next, determine expressions for $(\sigma_0, \bar{a})_{\text{Required}}$ by regression fitting them to process variables, $\bar{p}$. The regression for σ_0 is illustrated in Figure 4.20, where n is the index for each sample point, and N is the number of sample points. The setup of regression for $\bar{a}$ is shown in Figure 4.21.

Find $(\bar{\alpha})$ $\qquad \varepsilon^2 = \min_{\bar{\alpha}} \left(\sum_n^N \left(\sigma_{0\,n,\text{Required}} - \sigma_{0\,n,\text{Regression}}\right)^2 \right)$

such that

$$\sigma_{0\,n,\text{Regression}} = \alpha_0 + \sum \alpha_j p_{n,j}$$

Figure 4.20 Split Calibration Technique – Step 2, σ_0 equation

Find $(\bar{\beta})$ $\qquad \varepsilon^2 = \min_{\bar{\beta}} \left(\sum_n^N \left(\bar{a}_{n,\text{Required}} - \bar{a}_{n,\text{Regression}}\right)^2 \right)$

such that

$$\bar{a}_{n,\text{Regression}} = \bar{\beta}_0 + \sum \bar{\beta}_j p_{n,j}$$

Figure 4.21 Split Calibration Technique – Step 2, $\bar{a}$ equation

4.4.2 Step 1: Determination of Values of Unmeasured Variable Values

In the first stand, there are 17 variables where 15 of them are either described by an equation or measured. There are two degrees of freedom, which are fit over two unknown variables, yield strength, σ_0, and the strain rate sensitivity coefficient, A. If there is no degree of freedom, all values need to be exact for the simultaneous equations to solve. With any error, that is not possible. It is therefore desired to have just one degree of freedom so that any and all errors in the model will be pushed into one variable. Therefore, we hold A constant at an expected value of 32N/mm^2. The remaining unknown variable, σ_0, is then the only unmeasured variable, which is adjusted to make the model's thickness prediction equal to that measured while satisfying all Roberts' equations at each sampled point. The degree of freedom ensures that the model's output can be made same as the measurement while pushing all modeling and measurement errors into the unknown variable. Figure 4.22 is an example of calibrated σ_0.

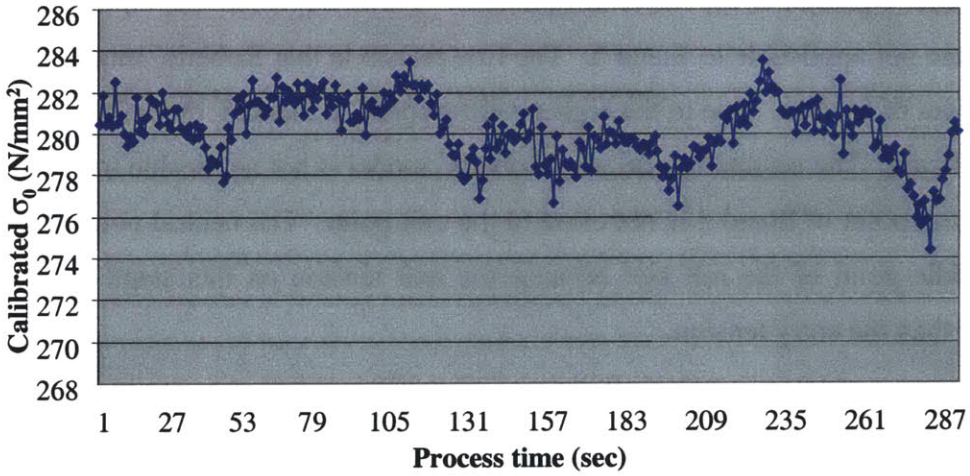

Figure 4.22 Calibrated σ_0

Since there is no thickness measured at the second or third stand, the middle three stands are combined into one model. There are 71 variables in this three-stand model where 68 of them are either described by an equation or known. The unknowns are a_1, a_2, and a_3 in Equation 4.2. For the same reason discussed above, two constraints are added to reduce the degree of freedom to one by fixing a_2 and a_3 constant. a_1 becomes the only

unmeasured process variable in the Stand 2-3-4 model. It is adjusted to make the predicted thickness of stand 4 equal to that measured through the simultaneous equations of Roberts' model. An example of calibrated a_1 is shown in Figure 4.23.

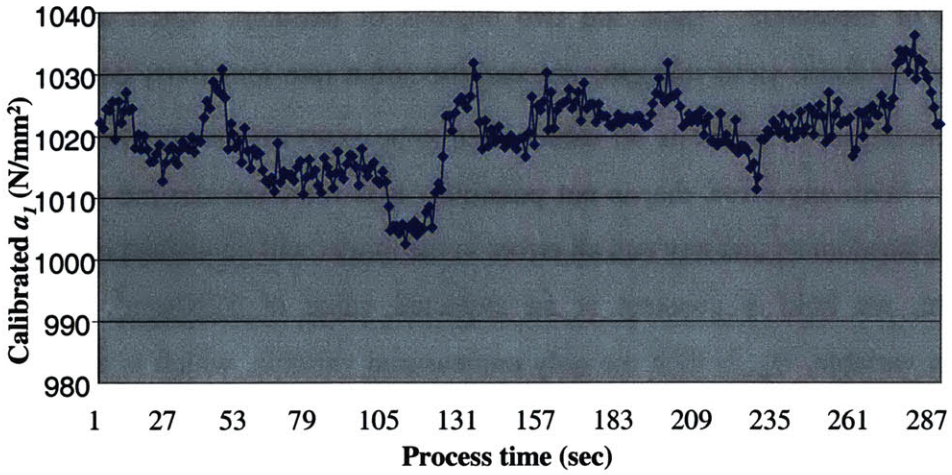

Figure 4.23 Calibrated a_1

The stand 5 model has 16 variables where all variables are either measured or calculated by Roberts' equation or the material equations. However, some assumptions in Roberts' model are not applicable to Stand 5. The first reason is that Roberts' model neglects the coefficient of friction. Due to the higher rolling speed in Stand 5, the influence of friction is significant. The second reason why Roberts' model is not applicable to Stand 5 is that the neutral point of Stand 5 is not close to the exit point. The neutral point shifts toward the middle point of the roll bite because the exit tension on this stand is significantly smaller than the entry tension.

Stone's force model is used for the fifth stand instead of Roberts'. This results in a set of simultaneous equations with 17 variables, and the coefficient of friction, μ, in this model provides one degree of freedom. The coefficient of friction is also an unmeasured variable, whose value is searched so that the model's thickness prediction equals the measured output at each sampled point. Same as σ_0 and a_1, the value of μ will be mapped to measured process variables. Figure 4.24 is an example of calibrated μ.

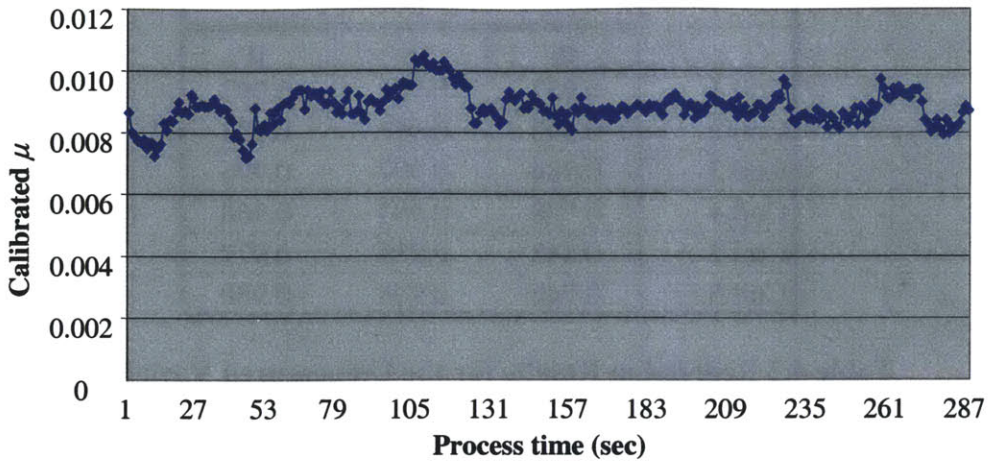

Figure 4.24 Calibrated μ

This analysis provides the required (σ_0, a_1, μ) to make the simultaneous equations produce the measured h using the measured process variable values. In effect, this is a transformation from h to (σ_0, a_1, μ) for regression fitting purposes. We can now find a single set of regression parameters, for the entire strip to predict the (σ_0, a_1, μ) we have just calculated, and thereby find the regression parameters that minimize h error through the simultaneous equations.

4.4.3 Step 2: Modeling Unmeasured Process Variables

The required values of σ_0 and $\bar{a}$ that allow the model predictions to match the measured values are the calibrated values. Once these values are determined, they are regression fit over the available process variables. The yield strength is fit to the measured process in Stand 1, such as entry thickness, entry tension, exit tension, roll force, and roll speed. This analysis is performed over six coil productions. The r^2 values for the regression is shown in Table 4.2.

	r^2		
	σ_0	a_1	μ
Coil 1	0.957	0.998	0.987
Coil 2	0.893	0.997	0.983
Coil 3	0.984	0.997	0.996
Coil 4	0.928	0.994	0.968
Coil 5	0.848	0.987	0.977
Coil 6	0.946	0.998	0.980

Table 4.2 Regression Results for the Unmeasured Variables

The relationship between the calibrated σ_0 and its ideal values for Coil 1 is shown in Figure 4.25. The number of sample points in Coil 1 is 288.

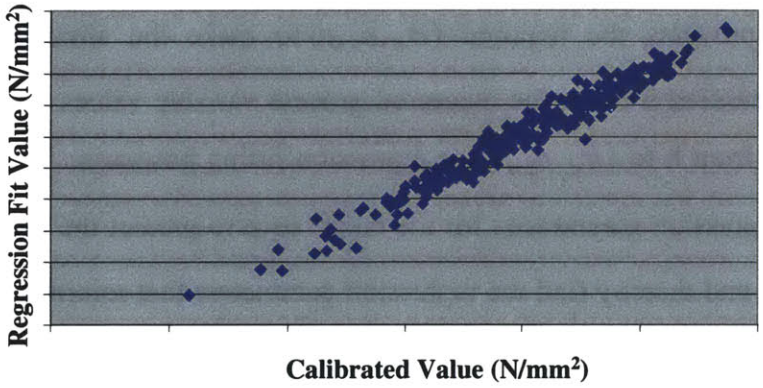

Figure 4.25 Regression Result for σ_0

The strain-hardening coefficient, a_1, for the first coil is calibrated to r^2 of 0.99. Its regression result is shown in Figure 4.26. The unmeasured variable a_1 is fit over entry tension, exit tension, roll force, roll speed, in Stand 1 through 4, along with entry thickness, exit thickness at Stand 1.

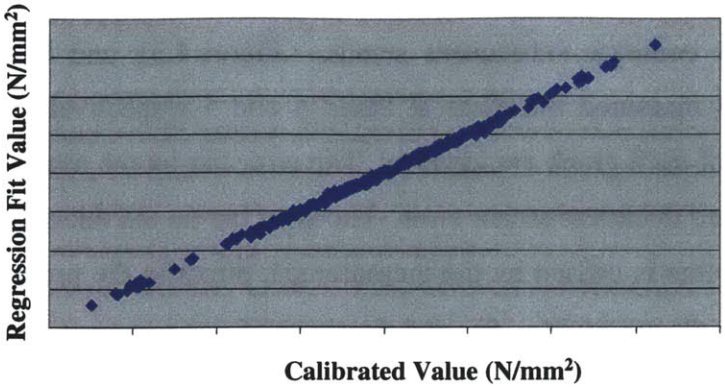

Figure 4.26 Regression Result for a_1

In addition to all variables that are used to fit a_1, the coefficient of friction in Stand 5 is fit over exit thickness at Stand 4, plus roll force, entry tension, exit tension, and roll speed of Stand 4. The regression result is shown in Figure 4.27.

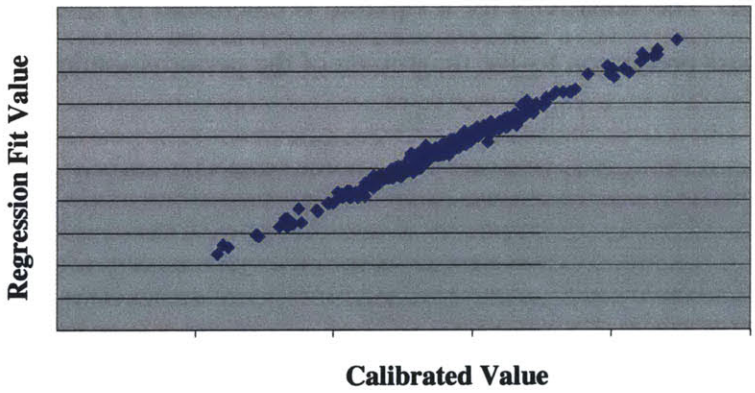

Figure 4.27 Regression Result for μ

4.4.4 Thickness Predicted from Measured Variables Only

In the previous section, the ideal values of unmeasured variables σ_0, a_1, and μ were modeled with measured process variables. By substituting these models into the corresponding locations in Roberts' model, a mapping of output thickness from solely the measured process variables can be constructed.

Figure 4.28 compares the measured Stand 1 exit thickness to the prediction of the model using only measured variables as inputs. Figure 4.29 plots the predicted versus the

measured Stand 1 exit thickness. The horizontal and vertical axes are identical. Figure 4.30-4.34 compare subsequent stands. Figure 4.31 and Figure 4.34 plot the predicted versus measured thickness at Stand 4 and 5 respectively. The vertical and horizontal axes of each graph are identical. The error bar on the measurement plot is the magnitude of rated thickness sensor error. The error bar on the thickness prediction is the amount of error that is caused by the measurement errors in the process variables. It is determined from the sensitivity, $S_{\bar{p}}$, and the range of measurement error, $\Delta\bar{p}$, of process variables. The mathematical expression is shown in Equation 4.15.

$$\Delta h_S = \sqrt{\sum S_{p_i}^2 \cdot \Delta p_i} \tag{4.15}$$

The sensitivity is determined from the ratio of an artificially introduced small perturbation in each process variable and the resulting thickness prediction in a Monte Carlo simulation. The sensitivity for a variable *is* calculated by dividing the differences in output thickness prediction by the magnitude of the perturbation in the variable.

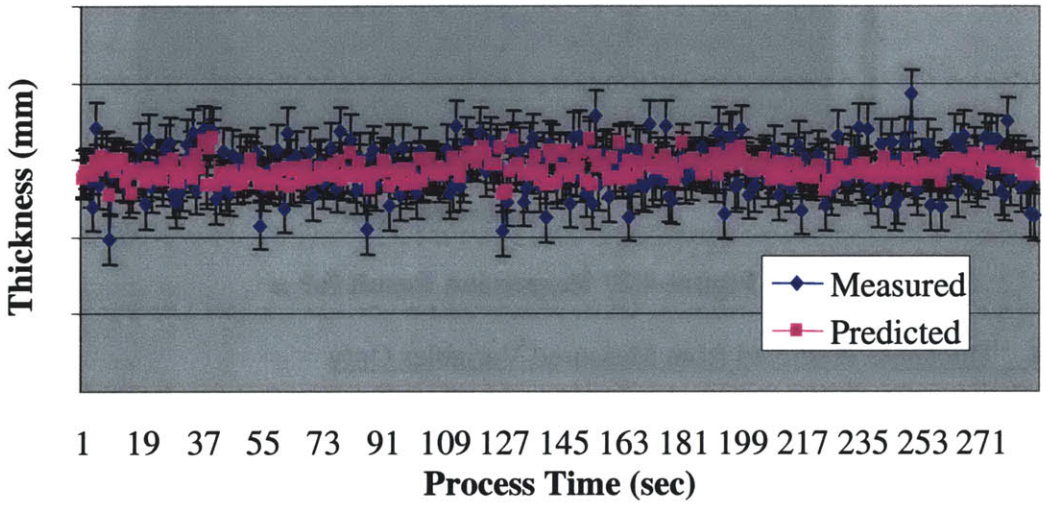

Figure 4.28 Stand 1 Exit Thickness Prediction with Error Bars

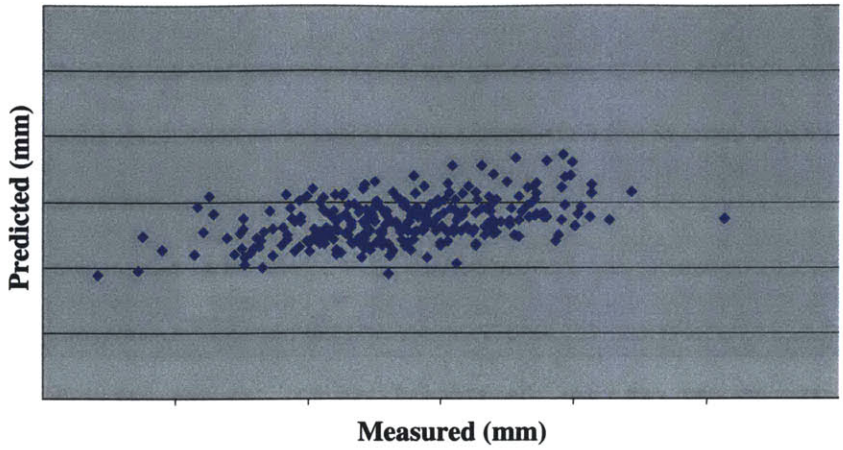

Figure 4.29 Stand 1 Exit Thickness Prediction

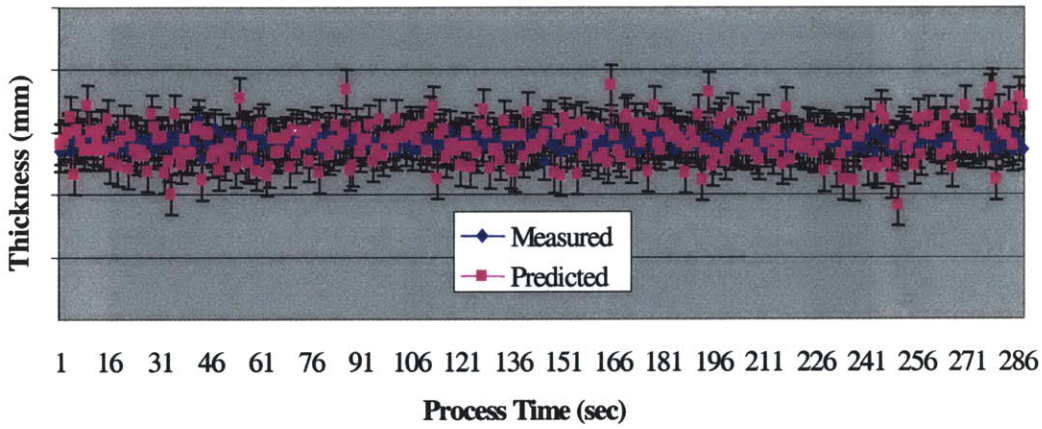

Figure 4.30 Stand 4 Exit Thickness Prediction with Error Bars

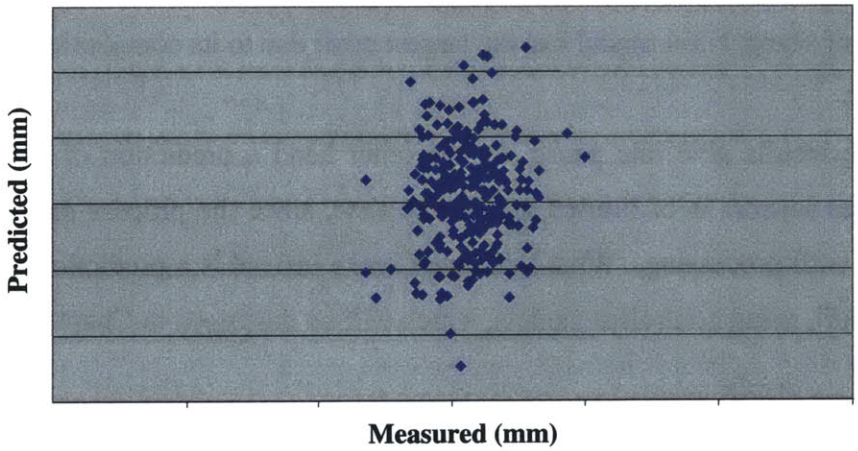

Figure 4.31 Stand 4 Exit Thickness Prediction

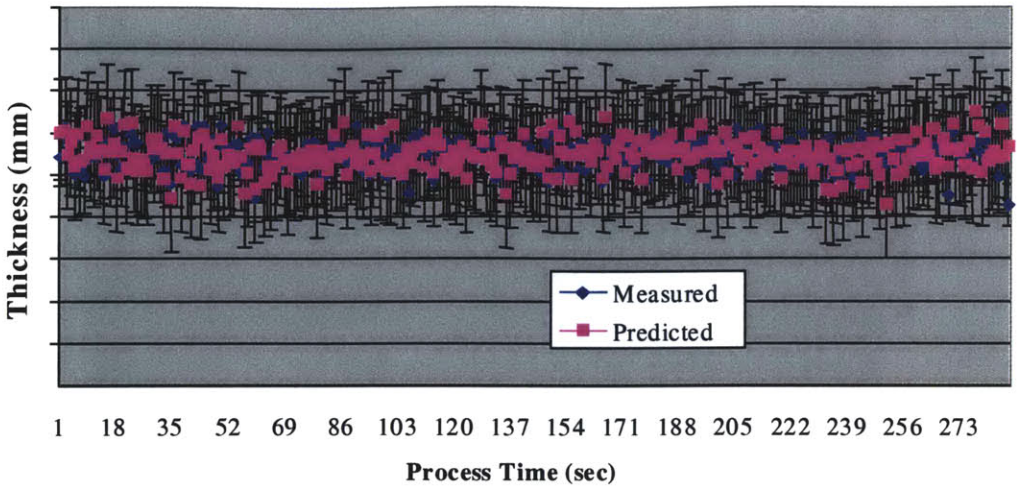

Figure 4.32 Stand 5 Exit Thickness Prediction with Error Bars

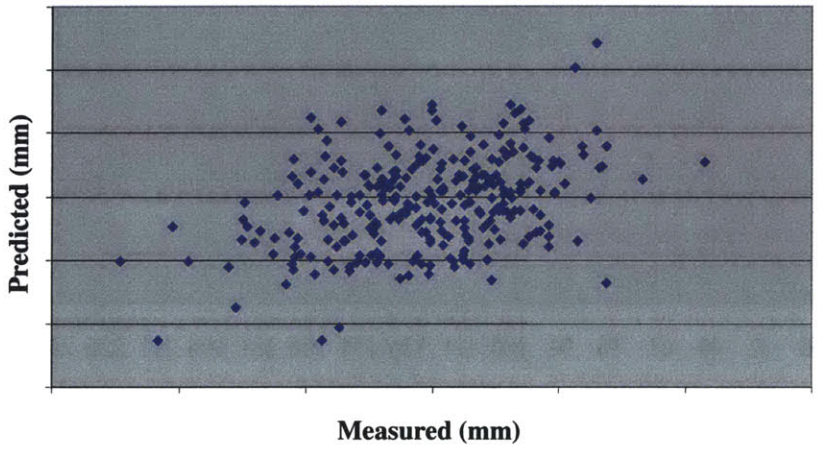

Figure 4.33 Stand 5 Exit Thickness Prediction

The output of Stand 2-3-4 model has the largest error due to its complexity.

While these results give one pause, on the other hand a prediction of thickness based upon process sensors is of limited use in any case, since the process measurements are not known until processing. What this thesis seeks instead is a prediction of the process values a priori, using controller models, which will be discussed in Chapter 6.

Figure 4.28 through Figure 4.33 show substantial error, r^2 are generally below 0.6. This demonstrates the difficulty in attainment of a predictive model capable of sample-by-

sample down-the-strip thickness prediction using process measurements. There is substantial error due to the accuracy of the measurement sensors on the system. One can compare the thickness sensor error to the error in predicted thickness caused by process input sensor errors. For Stand 1 model, the ratio between the error due to thickness sensor uncertainty and the process input sensor errors propagated through the model is 92%. This ratio for Stand 4 and Stand 5 model are 65% and 355% respectively. This is one strong cause of the large discrepancies between the predicted and measured thickness: sensor errors are preventing agreement between the input and output measurements in the extremely small range of variations being analyzed.

Therefore, the large measurement error in all sensors prevents prediction of output thickness using the variables currently being measured using the current sensors. However, the goal of this thesis is to predict the variation parameters of the exit thickness, not the actual thickness profile down the strip. For example, as shown in Chapter 3, the mean thickness of a strip can be easily predicted. The issue is whether other strip parameters, such as variance, can be also predicted. Furthermore, the mill simulation model developed in this thesis will include a controller model that predicts the values of process variables that were measured with sensor error. The simulation model's thickness prediction will not be influenced by the sensor errors in the process variables.

4.5 Chapter Summary

In this chapter, the five individual stand models were integrated by linking the outputs of one stand with the inputs of subsequent stand. The models that describe the material property changes of the steel strip during the rolling process were introduced. In addition to constructing an integrated model for the cold rolling mill, two topics were covered in this chapter. The first was developing a method to determine a sampling frequency that allows sufficient observation of variations in the rolling mill data stream. The variation in exit thickness can be sufficiently when sampled at 9.8Hz. Due to synchronization limitations of the data storage devices in the mill, the model can only be calibrated at

1Hz. Nevertheless, a frequency analysis indicates the models developed here will apply well at 10Hz as well, should faster sensors become available.

Another topic discussed in this chapter was determining the values of unmeasured process variables, yield strength and hardening coefficient of steel. These two variables are statistically modeled as functions of known variables. By substituting these two equations in places where the yield strength and hardening coefficient are used in Roberts' model, the output thickness can be calculated.

Sensitivity analysis can also be performed on this model to identify the sources of variation in the output thickness, and will be discussed in Chapter 5. This model cannot, however, predict the output thickness without values for the process variables. Chapter 6 will discuss controller models, which will predict values of the process variables.

Chapter 5: Variation Analysis

In Chapter 4, an integrated cold rolling model that predicts output thickness given the values of process variables. Even though this model still relies on the production data to calculate the output thickness, it explains the physics of the cold rolling process. Performing variation analysis on this model helps understanding the sensitivity between output thickness and each process variable. With this information, once can determine what are the major sources of variation.

There are several techniques to perform variation analysis. The most basic method is modeling overall variation as a sum of all variations in each process variable. A more complex method is modeling output variation as linear combination of variations in process variables. In this thesis, the relationships between output variation and the variation in the system are determined through Monte-Carlo simulation.

5.1 Related Works in Variation Modeling

Before discussing each technique, the basic ideas in variation analysis should be explained. A manufacturing system is composed of a series of operations. Each operation changes some characteristic properties of the workpiece, which can be geometrical or material. A schematic representation of an operation is shown in Figure 5.1, where F is the function mapping output vector $\bar{q}_2$ to input vectors $\bar{p}$ and $\bar{q}_1$.

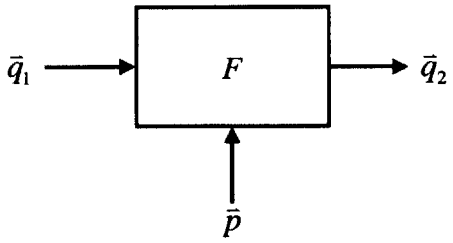

Figure 5.1 Schematic Representation of a Manufacturing Operation

Vector $\bar{q}_1$ contains information on material properties or geometrical characteristics of the workpiece. The workpiece can be either raw material or an output from previous

processes. The vector $\bar{p}$ contains values of process variables of this particular process. The output vector $\bar{q}_2$ describes important geometric characteristics and material properties of the workpiece as the result of this process. This can be expressed analytically with Equation 5.1.

$$\bar{q}_2 = F(\bar{p}, \bar{q}_1) \tag{5.1}$$

This equation describes the mapping between the input and output variables of the system at their nominal values, such as the models discussed in previous chapters. To describe the variation in the system, each input variable in $\bar{p}$ and $\bar{q}_1$ is considered a random variable with associated probability density function, *pdf*.

The average output variable is therefore the expected value of process F (Equation 5.2).

$$E(\bar{q}_2) = E(F(\bar{p}, \bar{q}_1)) = \int F(\bar{p}, \bar{q}_1) pdf(\bar{p}) pdf(\bar{q}_1) d\bar{p} d\bar{q}_1 \tag{5.2}$$

From this equation, the variance of the output vector $\bar{q}_2$ can be determined (Equation 5.3).

$$\sigma^2(\bar{q}_2) = \int (F(\bar{p}, \bar{q}_1) - E(F(\bar{p}, \bar{q}_1)))^2 pdf(\bar{p}) pdf(\bar{q}_1) d\bar{p} d\bar{q}_1 \tag{5.3}$$

The probability density distribution of a function $y = f(\bar{x})$, where $\bar{x}$ is a vector of random variables, can be calculated via a convolution integral of $\bar{x}$.

$$pdf_y(y) = \frac{d}{dy} \int_{-\infty}^{\infty} \cdots \int_{-\infty}^{\infty} pdf_x\left(x_1, \cdots, f_{x_i}^{-1}(y), \cdots, x_n\right) dx_1 \cdots dx_{i-1} dx_{i+1} \cdots dx_n \tag{5.4}$$

where $f_{x_i}^{-1}$ is the inverse function of f which returns a value of x_i given y while holding other values of x constant, and n is the number of elements in $\bar{x}$.

5.1.1 Linearization

Analytical expressions in the form of Equation 5.4 for a complex multivariate manufacturing systems are difficult to derive. Therefore, the process is often linearized based on the assumption that the system is operating linearly in the vicinity of the

operating point, $(\vec{p}^*, \vec{q}_q{}^*)$. Since manufacturing systems are rarely linear over large ranges, it is common to model their variation in a small range of operations using a linear model.

The general equation that describes the mapping between output and input variables, equation 5.1, can be linearized with Taylor series expansion.

$$\vec{q}_2 = \vec{F}(\vec{p}^*, \vec{q}_1{}^*) + \left(\frac{\partial \vec{F}}{\partial \vec{p}}\right)\Big|_{\vec{p}^*, \vec{q}_1^*} (\vec{p} - \vec{p}^*) + \left(\frac{\partial \vec{F}}{\partial \vec{q}_1}\right)\Big|_{\vec{p}^*, \vec{q}_1^*} (\vec{q}_1 - \vec{q}_1{}^*) + H.O.T., \tag{5.5}$$

where *H.O.T.* stands for higher-order terms, which are ignored in later analysis. The nominal term, $\vec{F}(\vec{p}^*, \vec{q}_1{}^*)$, and the partial derivatives, $\left(\frac{\partial \vec{F}}{\partial \vec{p}}\right)$ and $\left(\frac{\partial \vec{F}}{\partial \vec{q}_1}\right)$, are evaluated at the operating point, $\vec{p}(\vec{x}^*, \vec{q}_q{}^*)$. The resulting equation is as follows.

$$\vec{q}_2 = \vec{q}_2{}^* + [F_{\vec{p}}]_{\vec{p}^*, \vec{q}_1^*} \cdot (\vec{p} - \vec{p}^*) + [F_{\vec{q}_1}]_{\vec{p}^*, \vec{q}_1^*} \cdot (\vec{q}_1 - \vec{q}_1{}^*) \tag{5.6}$$

The equation is an approximation since *H.O.T.* is dropped. Defining the following new variables in Equation 5.7 enables rewriting Equation 5.6 into an equation based on deviations, and can eliminate the nominal values (Equation 5.8).

$$\Delta\vec{q}_1 = \vec{q}_1 - \vec{q}_1{}^* \tag{5.7a}$$

$$\Delta\vec{p} = \vec{p} - \vec{p}^* \tag{5.7b}$$

$$\Delta\vec{q}_2 = \vec{q}_2 - \vec{q}_2{}^* \tag{5.7c}$$

$$\Delta\vec{q}_2 = [F_{\vec{p}}]_{\vec{p}^*, \vec{q}_1^*} \Delta\vec{p} + [F_{\vec{q}_1}]_{\vec{p}^*, \vec{q}_1^*} \Delta\vec{q}_1 \tag{5.8}$$

The matrices $[F_{\vec{p}}]$ and $[F_{\vec{q}_1}]$ are also known as sensitivity matrices.

5.1.2 Root Sum Square (RSS)

The Root Sum Square technique is a simplified method to calculate variance. Instead of identifying a probability density for each random variable, all random variables are treated as normally distributed. The variance, σ^2, of each variable represents its variation. This technique applies to systems with independent input random variables. Based on the linearized model (Equation 5.8), the output variance is predicted with the following equation.

$$\bar{\sigma}_{\bar{q}_2}^{\,2} = \left[\bar{F}_{\bar{p}}^{\,2}\right]_{\bar{p}^*,\bar{q}_1^*} \cdot \bar{\sigma}_{\bar{p}}^{\,2} + \left[\bar{F}_{\bar{q}_1}^{\,2}\right]_{\bar{p}^*,\bar{q}_1^*} \cdot \bar{\sigma}_{\bar{q}_1}^{\,2} \tag{5.9}$$

This equation is known as the Root Sum Squares formula, mapping the variance of output variable to that of input variables.

5.1.3 Integrated System Model (ISM)

The Integrated System Model is composed of two layers of linked mathematical models of each operation in the manufacturing process. (Figure 5.2) The first layer is called the predictive model, which predicts nominal output values based on nominal input values, such as the models developed in chapters 4 and 5. These models can be either physically or statistically derived. The second layer of models is called the variation models. These variation models are derived from the predictive models through sensitivity analysis or Jacobians. Similar to RSS, ISM also uses variance to represent variation of each random variable, and assumes that variances of outputs are linear functions of that of inputs.

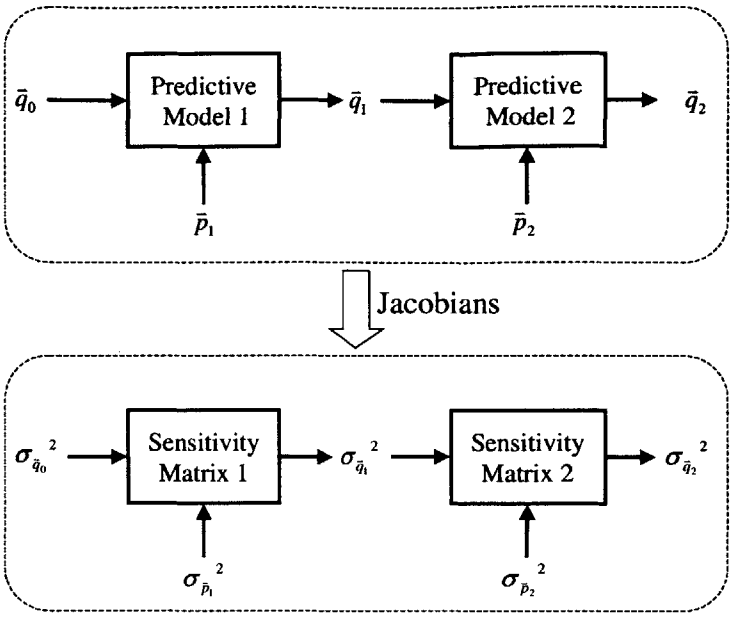

Figure 5.2 Variation Model

A general form of variance model is shown in Figure 5.3.

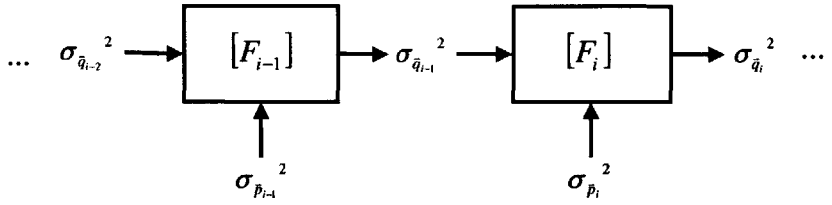

Figure 5.3 Integrate System Model by Linking Inputs and Outputs

The equation that predicts the output variance is shown below.

$$\bar{\sigma}_{\bar{q}_i}^2 = \left[F_{i,\bar{p}}^2\right]_{\bar{p}_i^*,\bar{q}_{i-1}^*} \cdot \bar{\sigma}_{\bar{p}_i} + \left[F_{i,\bar{q}_{i-1}}^2\right]_{\bar{p}_i^*,\bar{q}_{i-1}^*} \cdot \bar{\sigma}_{\bar{q}_{i-1}} \tag{5.10}$$

The term $\left[F_{w,z}^2\right]_{\bar{x}^*,\bar{y}^*}$ stands for the sensitivity matrix of operation w with respect to the variable z evaluated at the operating point $(\bar{x}^*, \bar{y}^*)$. The input variance $\bar{\sigma}_{\bar{q}_{i-1}}$ is a function of variances in previous operations. The general form of output variance at operation i is derived by substituting input variances as output of the previous operation.

$$\bar{\sigma}_{\bar{q}_i}{}^2 = \left[F_{i,\bar{p}_i}{}^2\right]_{\bar{p}_i^*,\bar{q}_{i-1}^*} \cdot \bar{\sigma}_{\bar{p}_i} + \sum_{m=0}^{i-1}\left(\prod_{n=0}^{m}\left[F_{i-n,\bar{q}_{i-n-1}}{}^2\right]_{\bar{p}_{i-n}^*,\bar{q}_{i-n-1}^*}\right)\left[F_{i-m-1,p_{i-m-1}}{}^2\right]_{\bar{p}_{i-m-1}^*,\bar{q}_{i-m-2}^*} \cdot \bar{\sigma}_{p_{i-m-1}}{}^2 + \left(\prod_{n=0}^{i-1}\left[F_{i-n,\bar{q}_{i-n-1}}{}^2\right]_{\bar{p}_{i-n}^*,\bar{q}_{i-n-1}^*}\right)\left[F_{1,\bar{q}_0}{}^2\right]_{\bar{p}_1^*,\bar{q}_0^*} \cdot \bar{\sigma}_{\bar{q}_0}{}^2 \tag{5.11}$$

Other than the linearization technique discussed above, an equation for σ^2 can also be analytically derived via convolution. Another way to determine the sensitivity matrix is via Response Surface Methods. This technique will result in an equation predicting output variances as linear functions of variances of input variables. The coefficients of these functions are statistically determined instead of being derived from predictive equations. This was the approach taken in Chapter 2.

The sensitivity matrix shows how sensitive the output is to variation in each variable. However, a more practical information is how much variation is caused by each variable. With the knowledge of sensitivity matrices, the contribution of each variable to the total output variation can be determined. The contribution is expressed as the ratio between the magnitude of each term in equation 5.12 over the total predicted variation, $\sigma_{\bar{q}_i}{}^2$. This information is critical for improving existing manufacturing systems because it identifies the major sources of variation.

5.1.4 Monte-Carlo Simulation

The previous techniques avoid deriving analytical expression by assuming linearity. Yet another way to determine the variation in the output variables is through numerical Monte-Carlo simulation. The simulation returns a distribution for each output variable formed by conducting many trials. Each trial calculates the output with the predictive model of the system, and values of input variables of this model are randomly selected from pre-determined random distributions. The larger the trial number, the more accurate the output distribution. The disadvantage of this approach is that the simulation tends to be computationally intensive. However, it allows an approximation of the probability

distribution of the output variable as shown in Equation 5.4 via the histogram of the trial results.

To approximate the *pdf* in Equation 5.4 with simulation, first construct a histogram with bin width Δx with the trial outputs. Second, define N_x to be the number of trial resulted in the range $\{x, x+\Delta x\}$. The probability that the output will be smaller than b can be calculated with the Equation 5.12.

$$P(x<b)=\frac{\sum_{i=x_{\min}}^{b} N_i \Delta x}{\sum_{i=x_{\min}}^{x_{\max}} N_i \Delta x} \tag{5.12}$$

where $x_{\min}$ is the smallest simulation trial result and $x_{\max}$ is the largest. The probability that the output value will fall in the range of $(a<x<b)$ can be calculated with Equation 5.13.

$$P(a<x<b)=P(x<b)-P(x<a) \tag{5.13}$$

A probability of x, $P(x)$, can be approximated from the histogram by setting $a=x-\Delta x$, $b=x$ in Equation 5.13. The expression for $P(x)$ is shown in Equation 5.14.

$$\begin{aligned} P(x) &= P(x-\Delta x<x<x) \\ &= \frac{N_x}{\sum_{i=x_{\min}}^{x_{\max}} N_i \Delta x} \end{aligned} \tag{5.14}$$

As the size of Δx decreases, the approximation becomes more accurate. Because it helps avoiding derivation of complex analytical expression for output *pdf*, Monte-Carlo simulation is used to identify the probability density function of the output variable in this thesis. Since all variables are treated as normally distributed random variables, the variation and standard deviation are synonymous from this point of the thesis.

The Monte-Carlo simulation is also useful for calculating the sensitivity matrix in ISM. The sensitivity values can be determined from the coefficient of correlation between each variable and the output. The equation for calculating the coefficient of correlation is shown in Equation 5.15.

$$C_{pq} = \frac{n\sum_{i=1}^{n} pq - \sum_{i=1}^{n} p \sum_{i=1}^{n} q}{\sqrt{n\sum_{i=1}^{n} p^2 - \left(\sum_{i=1}^{n} p\right)^2} \cdot \sqrt{n\sum_{i=1}^{n} q^2 - \left(\sum_{i=1}^{n} q\right)^2}} \tag{5.15}$$

In this formula, n is the number of trials, p and q are the input and output variables respectively. Correlation coefficients provide a measurement of the degree to which the input and output vary together. The coefficients range from -1 to +1. In the case of negative coefficients, the change in the input and output variables are in opposite directions. The larger the magnitude of the coefficient, the more correlated the input and output variables are. Commercially available software packages such as *Crystal Ball*© or *Matlab*© can quickly calculate these correlation coefficients via Monte-Carlo simulation.

5.2 Sensitivity Analysis on Cold Rolling Mill

Sensitivity analysis with Monte-Carlo simulation was performed using the predictive model. The outputs of one stand, including material and geometrical characteristics, serve as inputs to the next. (Figure 5.4)

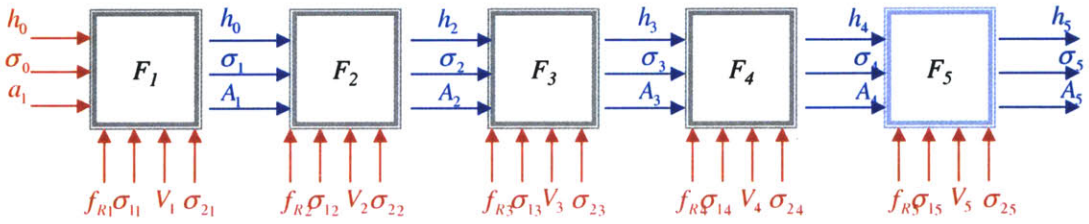

Figure 5.4 Random Variables in the Cold Rolling Mill Simulation

All input variables for each stand are treated as normally distributed random variables with the standard deviation calculated from the sampled 1Hz data. A schematic

representation of stand 1 model is shown in Figure 5.5. These input variables include roll force, input and exit tension, roll speed, and thickness measurements. The material properties, σ_0 and a_1, were also used in the simulation as inputs. The values of these two variables were solved for at each sampled point.

The sensitivity of the output thickness to each process variable was calculated based on Equation 5.12. Since the model was nonlinear, the contribution, λ, could not be calculated using the linearized method of section 5.1.1. Instead, an Monte-Carlo simulation was used, and the sensitivity of each variable calculated as the ratio between the square of the sensitivity of that variable over the sum of squares of all variables (Equation 5.16).

$$\lambda_{pq} = \frac{C_{pq}^{\ 2}}{\sum_{i=1}^{r} C_{iq}^{\ 2}} \tag{5.16}$$

In Equation 5.16, r is the total number of input variables and λ_{pq} is the contribution of input variable q to output variable p.

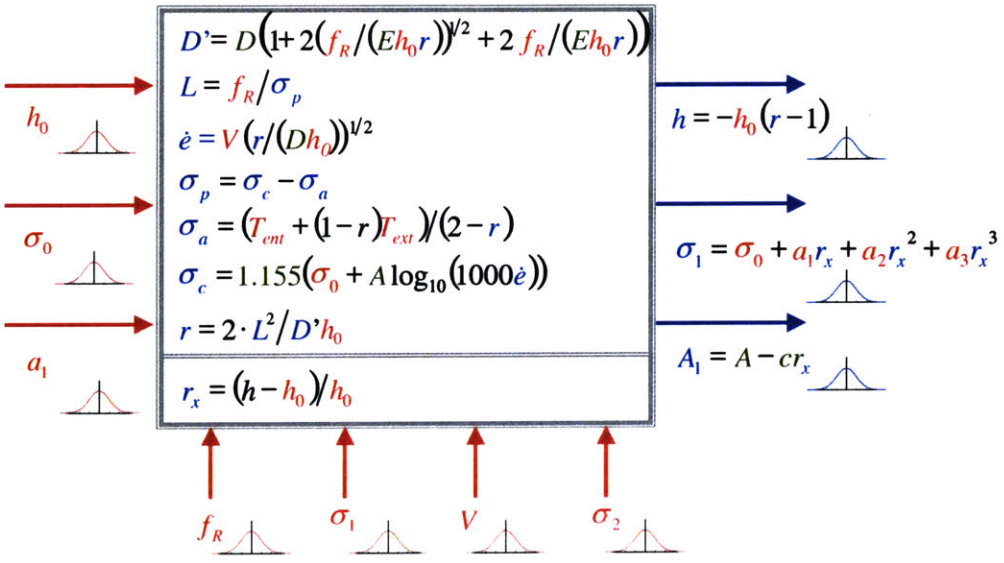

Figure 5.5 Random Variables and Equations for Stand 1 Simulation

For a Monte-Carlo simulation of 2000 trials, the resulting predictions are plotted as a histogram (Figure 5.6).

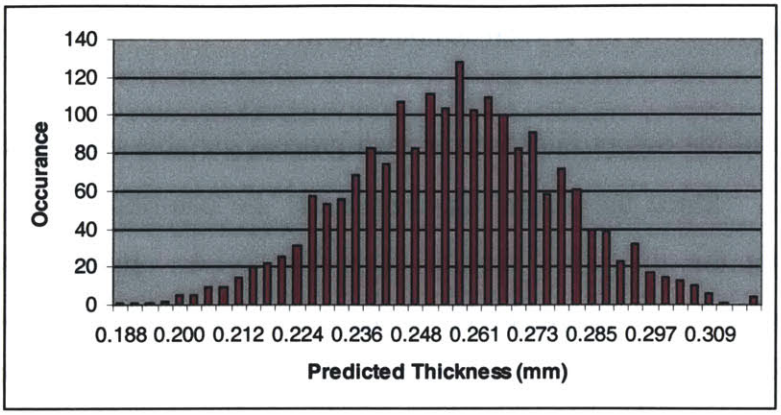

Figure 5.6 Simulated Output Thickness Variation

The distribution, which appeared very close to a normal distribution, had a mean of 0.2459mm and a standard deviation of 0.0213mm. A typical strip has mean of 0.3mm and standard deviation of 0.0005mm. The predicted standard deviation is off because the influences of controllers are not modeled in the simulation. The observed variation in each process variable is treated as disturbances in system, while significant portion of the variation is the controller's effort to attenuate input disturbances.

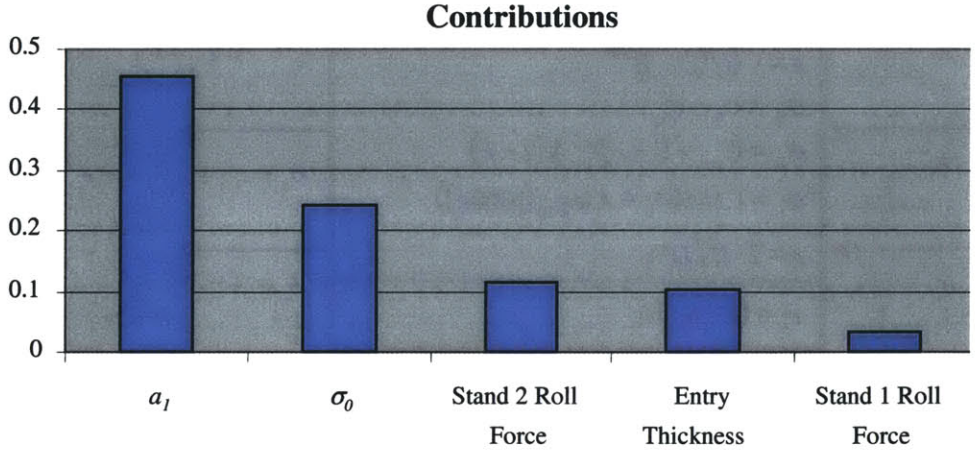

Figure 5.7 Contribution of Each Variable

The observed variation of the input variables was again a combination of control actions and noise. For example, the force was varied throughout the production of a coil because the force controller commanded the actuator to compensate for deviations in thickness. However, there was noise and disturbances in this force control and actuation system, which was part of the observed variation. In order to separate the random variation from the variation commanded by the controller, it is necessary to model how the controller responds to incoming strip thickness and material variations. On the other hand, it is useful to know which variables can have a large impact on thickness, and so require tight control.

The sensitivity analysis for the cold rolling mill identified the contribution of variation in each process variable to the output thickness variation (Figure 5.7). The output thickness variation has high sensitivity to material properties σ_0 and a_1. These two variables accounted for 70% of the total output thickness variation. Other significant sources of variations are second stand roll force, entry thickness, and first stand roll force, which accounted for 12%, 10% and 3% of the total variation respectively. All variations in other variables contributed to the remaining 5% of output variation.

5.3 Chapter Summary

In this chapter, Monte-Carlo simulation was applied to the integrated cold rolling model to identify the sensitivity between variation in output thickness and that in process variables. The material properties, yield strength and hardening coefficient, of the steel strip turned out to have the largest impact on the output thickness. While the simulation identified the relationship between variations in process variables and output variation, it overestimated the output variation because the controllers were not included. The variation in each variable was simulated as noises entering the mill. In reality, the variation in process variables could be results of control efforts, which were designed to reduce exit thickness variation.

It is necessary to separate the control actions from the noises in each variable for truly simulating the variation propagation in the mill. Including the controller model in the integrated mill model also enables prediction of process variables. With the knowledge of the process variables and the physical model that predicts output thickness, the output thickness can be predicted prior to actual production of the strip. The development of models for the controllers will be discussed in Chapter 6.

Chapter 6: Modeling Control Systems

In the previous chapter, the sensitivity of the output strip thickness to each process variable is calculated via Monte-Carlo simulation. From the sensitivity, the variation that each variable contributes to the final output variation is derived. However, this sensitivity is calculated with the observed variation in the process variable such as force, tension, and velocity, which are controlled variables. The changes in these variables may be results of control actions, which reduce instead of augment variation in the system. As a result, the simulation predicts more output variation that what is actually measured. The simulated output thickness has standard deviation 5.8 times of that measured. To accurately simulate the cold rolling process, it is necessary to model the controllers and separate the random variation in the system from control actions. This will enable a variation analysis that reflects the variation propagation in the cold rolling mill. From such an analysis, the contribution of variation in each process variable to the output thickness variation can be determined.

The controller models also predict the values of process variables, which are the inputs of the physical cold rolling mill model. The combination of the physical model and the controller model allows the prediction of output thickness before a strip is actually being processed. This helps avoiding processing steel strips that are likely to have high exit thickness variation.

6.1 Controllers in Manufacturing Systems

Modern manufacturing systems utilize computerized control systems to reduce variations in the processes. A control system consists of sensor, actuator, amplifier, and the manufacturing plant. The sensor measures a characteristic property of the workpiece or process variable. The measurement is compared against a reference, which is the desired value, and the difference is defined as error. The error is then amplified by multiplying a gain, which can be a constant or function of other process variables. The resulting product is the controller command, which specifies how the actuator will respond based

on the error. The output of the actuator is the process variable discussed in the previous chapter. However, the output of the actuator usually differ from what the controller commands intends to achieve. The cause of this discrepancy includes the model of actuator that the amplifier bases on to determine and the disturbances from the environment. The discrepancy is modeled as a noise added to the actuator output. A schematic representation is shown in Figure 6.1.

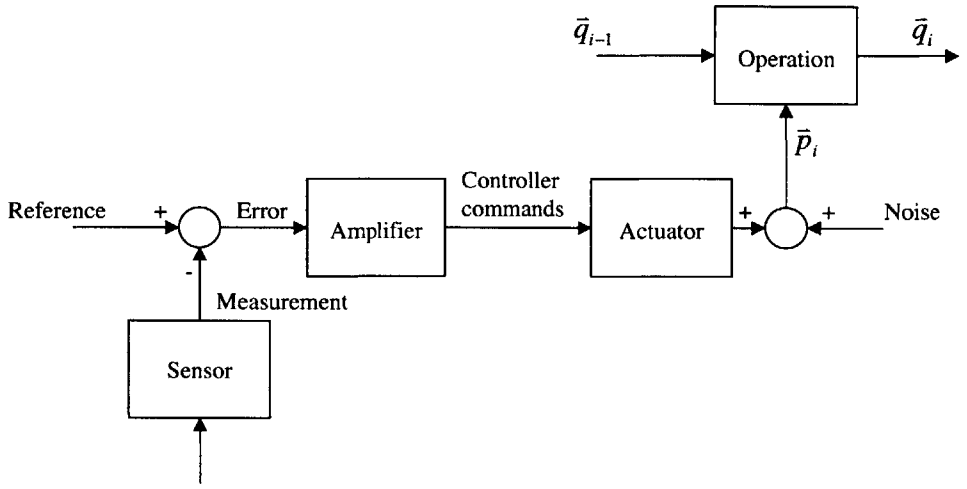

Figure 6.1 Controller in an Operation

The algorithm of the amplifier is the essence of all controllers. The value of gain determines if the overall system is stable, as well as how, and if, the output reaches the desired value. The stability and transient response of the system output can be calculated with modern control theories (Ogata 1990; Kuo 1995). This thesis focuses on modeling the variation in the manufacturing system. The measured process variables are treated as the sum of desired value and system noise. The transient behaviors of all process variables are ignored.

To model the control system in a manufacturing system, it is necessary to know what variables are measured and what are actuated. The actuated variables are outputs of the control system and the measured variables are the inputs. Control systems can be categorized into two types: Feedforward and Feedback, based on what is being measured.

6.1.1 Feedforward Control Systems

The Feedforward control systems measures the characteristic properties of workpiece prior to the operation. The schematic representation of Feedforward control system is shown in figure 6.2. For operation *i*, the algorithm for calculating the gain is expressed as H_i and the model for actuator is M_i. The error between the reference values, $\vec{R}_{i-1}$, and the sensors' measurements is defined as e_i. The product of e_i and H_i is the controller commands, $\vec{C}_i$, and the output of the actuator model is $\tilde{\vec{p}}_i$. Noise is added to $\tilde{\vec{p}}_i$ simulating the disturbances in the system and this leads to the process variables, $\vec{P}_i$, for the operation.

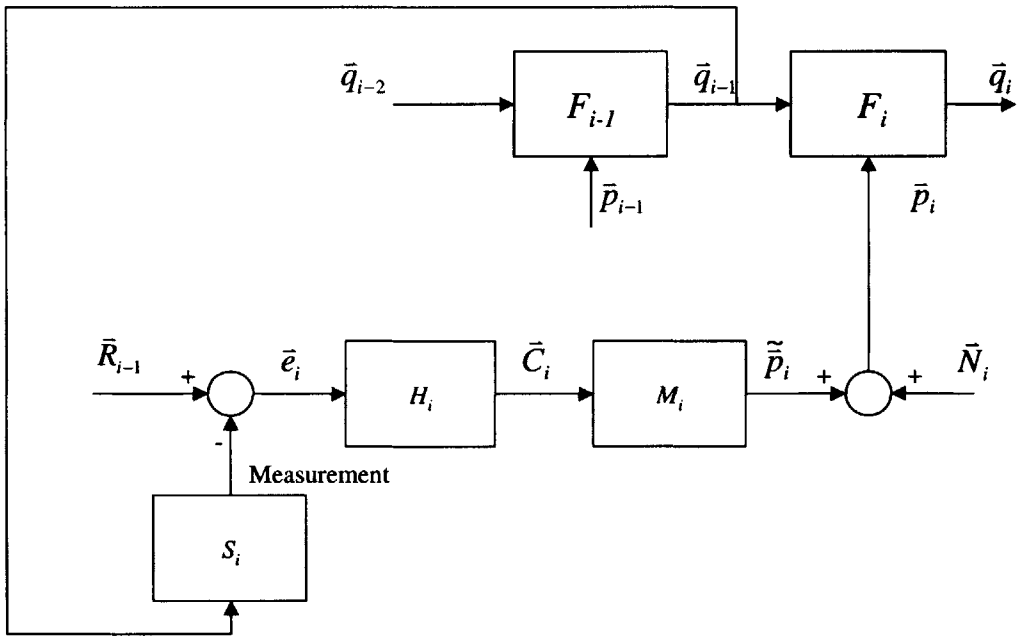

Figure 6.2 Feedforward Controller

Feedforward control systems allow the operation to be set the operating condition to compensate for variations observed in earlier stages. This prevents the variations from propagating through the manufacturing line. An analytical representation of a Feedforward control system is derived.

From the previous chapter, it is shown that the output vector $\vec{q}_i$ can be expressed as equation 6.1.

$$\vec{q}_i = F_i(\vec{p}_i, \vec{q}_{i-1}) \tag{6.1}$$

In the case that the process variables are controlled, the vector $\vec{p}_i$ is described in terms variables prior to operation i (Equation 6.2, 6.3).

$$\vec{p}_i = \tilde{\vec{p}}_i + \vec{N}_i \tag{6.2}$$

$$\vec{p}_i = M_i(\vec{C}_i) + \vec{N}_i = H_i(M_i(\vec{e}_i)) + \vec{N}_i \tag{6.3}$$

The error, $\vec{e}_i$, is the difference between the reference and the values measured by the sensors.

$$\vec{e}_i = \vec{R}_{i-1} - S_i(\vec{q}_{i-1}) \tag{6.4}$$

Substituting Equation 6.3 and 6.4 into equation 6.1 results in the following expression.

$$\vec{q}_i = F_i(H_i(M_i(\vec{R}_{i-1} - S_i(\vec{q}_{i-1}))) + \vec{N}, \vec{q}_{i-1}) \tag{6.5}$$

The above equation is useful when the controller model, H_i, and the actuator model, M_i, can be obtained separately. In the case that the model of the controllers needs to be experimentally determined from process data, $\vec{q}$ and $\vec{p}$, a model G_i that maps $\vec{Y}_i$ to $\vec{e}_i$ can be introduced. In that case, Equation 6.5 is rewritten as follows.

$$\vec{q}_i = F_i(G_i(\vec{R}_{i-1} - S_i(\vec{q}_{i-1})) + \vec{N}, \vec{q}_{i-1}) \tag{6.6}$$

6.1.2 Feedback Control Systems

Another common type of control system is the Feedback control system. Instead of being a function of process variables or characteristic measurements of workpiece in prior operations, the Feedback controller is a function of the output of current operation. The advantage of Feedback control system is that the control action takes place at the operation that directly influence the characteristic property that is being measured. The

controller adjusts values of $\vec{p}_i$ as the workpiece is being worked. On the other hand, the operation F_i system with Feedforward control is open loop, which means that there is no adjustment will be done even if $\vec{q}_i$ deviates from targets. The system relies on a precise model of F_i in order to determine a set of $\vec{p}_i$ for the operation to produce the output with desired specifications. The disadvantage of the Feedback control systems is that there is always a delay before the output reaches the desired target. The controller updates its gain based on the product that has past. Therefore, instead of setting the process to incorporate what is about to come, the controller uses the previous error $\vec{e}_i$ to predict what the process variables ought to be assuming $\vec{e}_i$ is same for the next moment. In the case when the input material properties change rapidly, the system is not able to adjust $\vec{p}_i$ quickly enough to achieve the target value.

A schematic drawing of the Feedback control system is shown in Figure 6.3.

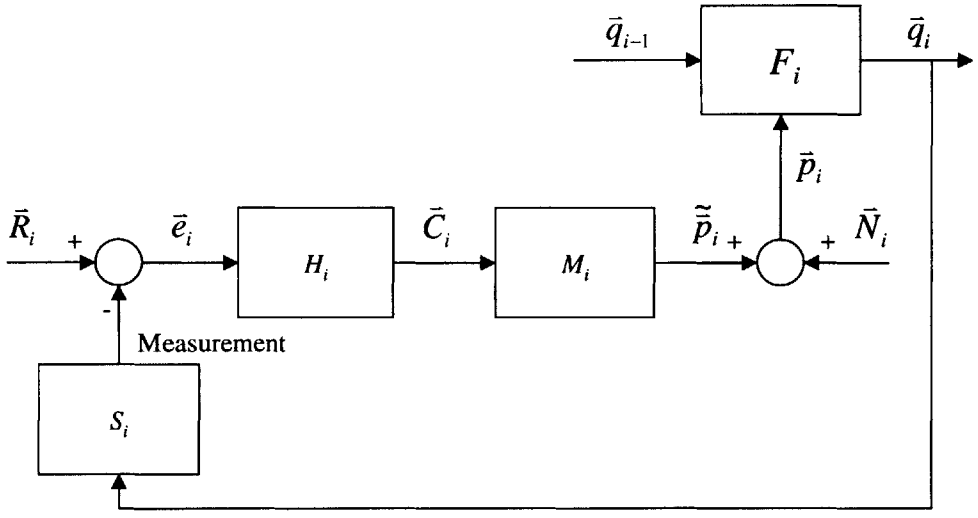

Figure 6.3 Feedback Controller

The analytical expression for this system is derived below. The output and process variables are expressed the same way as the Feedforward system (Equation 6.1, 6.3).

$$\vec{q}_i = F_i(\vec{p}_i, \vec{q}_{i-1}) \tag{6.1}$$

$$\vec{p}_i = M_i(\vec{C}_i) + \vec{N}_i = H_i(M_i(\vec{e}_i)) + \vec{N}_i \tag{6.3}$$

The error, on the other hand, is the difference between the reference values and the sensor measurements of the output of the operation *i*.

$$\vec{e}_i = \vec{R}_i - S_i(\vec{q}_i) \tag{6.7}$$

Therefore the output for operation with Feedback control system is as follows.

$$\vec{q}_i = F_i(H_i(M_i(\vec{R}_i - S_i(\vec{q}_i))) + \vec{N}, \vec{q}_{i-1}) \tag{6.8}$$

Again, a model G_i that maps $\vec{Y}_i$ to $\vec{e}_i$ can be introduced in the cases that the controller model, H_i, and the actuator model, M_i, cannot be obtained separately. The resulting expression for the output of the operation is shown below.

$$\vec{q}_i = F_i(G_i(\vec{R}_i - S_i(\vec{q}_i)) + \vec{N}, \vec{q}_{i-1}) \tag{6.9}$$

6.2 Model Control Systems in Cold Rolling Mill

In the cold rolling mill, velocity and force are adjusted to control the output thickness. Feedforward and Feedback control systems are found in both types of control systems. Each controller has a single output, and the sensor locations and process variables that the controller uses are identified. However, the control algorithm and the information on the actuators are not available. Therefore, functions mapping controller inputs to the control commands, G_i, are statistically determined. The control systems are modeled as linear combinations of characteristic measurements of the workpiece and process variables.

The controller takes input from some variables that are not measured. In practice, models are incorporated in the controllers to predict these values based on process variables and upstream process data are used to obtain these numbers. In this thesis, such variables are σ_0 and a_1. The values of these two variables are the number that allows the simultaneous equations to converge with minimum error. In this thesis, these values are considered as if they were actual measurements. Both σ_0 and a_1 are known to be

function of the steel's chemical compositions and the cooling history after hot rolling process. These models can be constructed and integrated into the existing models once the measurements of σ_0 and a_1 are available.

The control systems in the cold rolling mill is adaptive, which means that the coefficients are constantly changing based on the result of previous coil production. Therefore, a statistically obtained controller model will not validate on all production coils. The controller equation fit with a set of production data for one coil is only valid on the production of coil immediately after it. Of the available data, there are two coils manufactured back to back on one day and another three coils produced two days later. The first coil from each of these two bathes is used to regression fit the control models, which are validated on the following coils.

6.2.1 Velocity Controller

The speed controller is installed on Stand 1,2, and 4. The speed controller in stand one is a Feedforward system. The controller uses the information of input thickness, input strip speed, and yield strength of strip to calculate the gain for the controller. A schematic representation is shown in Figure 6.4, and the equation describing the process variable is in the following form.

$$V_1 = \beta_0 + \beta_1 h_0 + \beta_2 Vs_0 + \beta_3 \sigma_0 + N \tag{6.10}$$

h_0 is the input thickness, Vs_0 is the input strip speed, and σ_0 is the yield strength of the steel. The β_i are statistical coefficients and N is the noise, which is assumed to be normally distributed. The noise is a result of disturbances in the mill that the controller is not able to eliminate. Therefore, the value of N should stay constant with in a small batch of production. The regression process identifies a set of β_i that minimizes the error between the predicted V_1 and that measured, leaving the N term as lack of fit. The calibration and validation results for stand 1 speed controller are shown in Figure 6.5 and Figure 6.6.

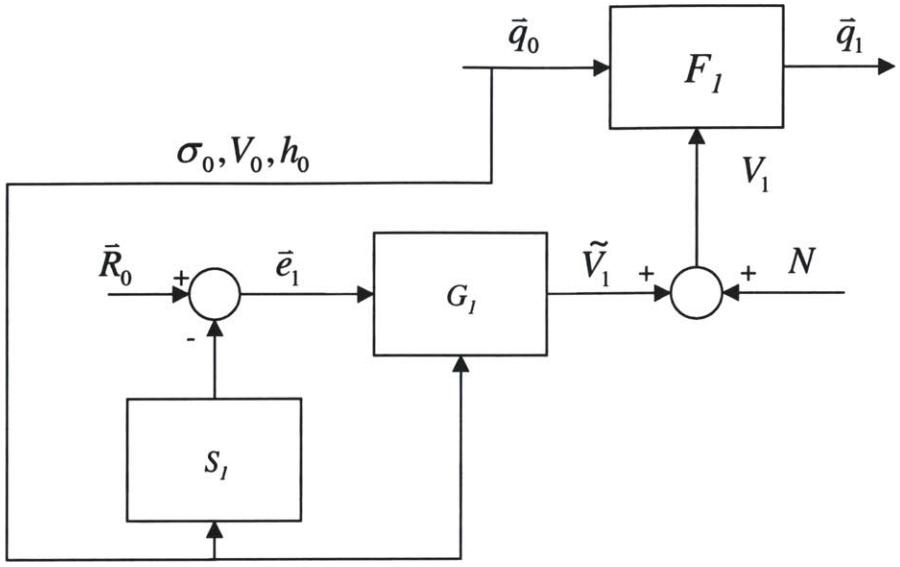

Figure 6.4 Stand 1 Speed Control Diagram

The regression for the first batch calibrated to r^2 of 0.81. Applied the same equation on the subsequent coil resulted in r^2 of 0.84. For the second batch, the model calibrated to r^2 of 0.84 and for validated to r^2 or 0.82 and 0.80 on the second and third coil respectively. The calibration and validation result for the first batch plotted below as an example.

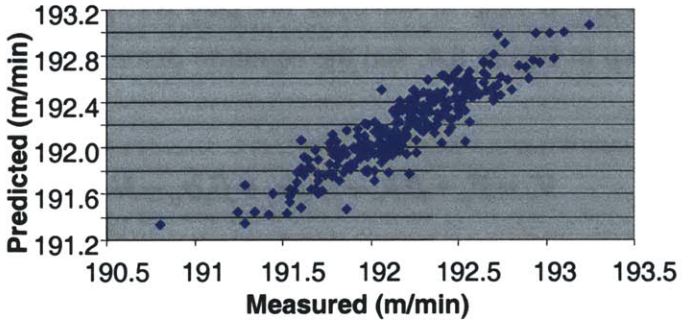

Figure 6.5 Calibration of Stand 1 Roll Speed Control Model

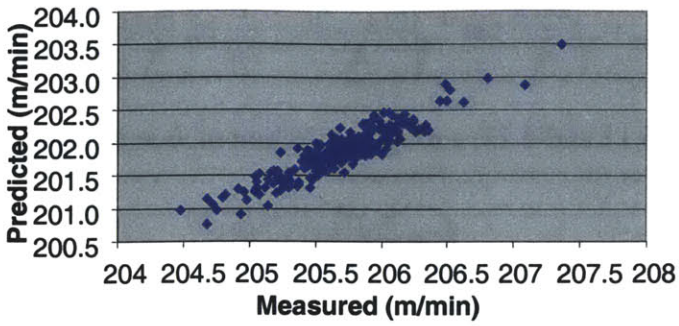

Figure 6.6 Validation of Stand 1 Roll Speed Control Model

Figure 6.6 showed that Stand 1 roll speed could be predicted from the statistically constructed controller equation. Bias was observed in the validation coils because each coil has a unique target thickness, and the process variables are set to operate at different nominal values. These nominal values were the β_0 coefficient in equation 6.10, and these nominal settings could be easily obtained in practice.

The roll-speed control system in stand 2 and 4 are more sophisticated. In addition to using the process variables and characteristic properties of workpiece, these controllers introduce a thickness prediction variable. Based on the conservation of mass, and the plane stress condition, i.e. constant strip width, the following relationship is derived.

$$h_{i-1}Vs_{i-1} = h_i Vs_i \tag{6.11}$$

Since the strip speeds between stands are not measurable, a forward slip ratio, f, is introduced to approximate the strip speed based on the measured roll speed, V_i.

$$Vs_i = (1+f_i)V_i \tag{6.12}$$

The forward slip ratio for each stand is calculated with the following equation prior to production based on material properties and mill settings. These values are constant through out the production of a coil.

$$f_i = \left\{ \tan\left(\frac{H_{ni}}{2} \sqrt{\frac{h_i}{D'/2}} \right) \right\} \tag{6.12}$$

H_n is known as the Neutral point function and is defined as the following.

$$H_{ni} = \sqrt{\frac{D'/2}{h_i}} \tan^{-1} \sqrt{\frac{h_{i-1} - h_i}{h_i}} - \frac{1}{2\mu} \ln\left(\frac{h_{i-1}}{h_i} \cdot \frac{\sigma_c - \sigma_2}{\sigma_c - \sigma_1} \right) \tag{6.13}$$

Based on Equation 6.11 and 6.12, a rough prediction of h_i is derived.

$$\hat{h}_i = \frac{h_{i-1} V_{i-1} (1 + f_{i-1})}{V_i (1 + f_i)} \tag{6.14}$$

This variable is used in speed controller in both stand 2 and stand 4. A diagram for speed control in stand 2 is shown in figure 6.7, and the controller model is in the following form.

$$V_2 = \beta_0 + \beta_1 \hat{h}_2 + \beta_2 V_1 + \beta_3 h_1 + N \tag{6.15}$$

Both V_1 and h_1 are measured, and $\hat{h}_2$ is calculated with Equations 6.14. Again, a set of β_i determined via regression, minimizing the error between predicted V_2 and that measured.

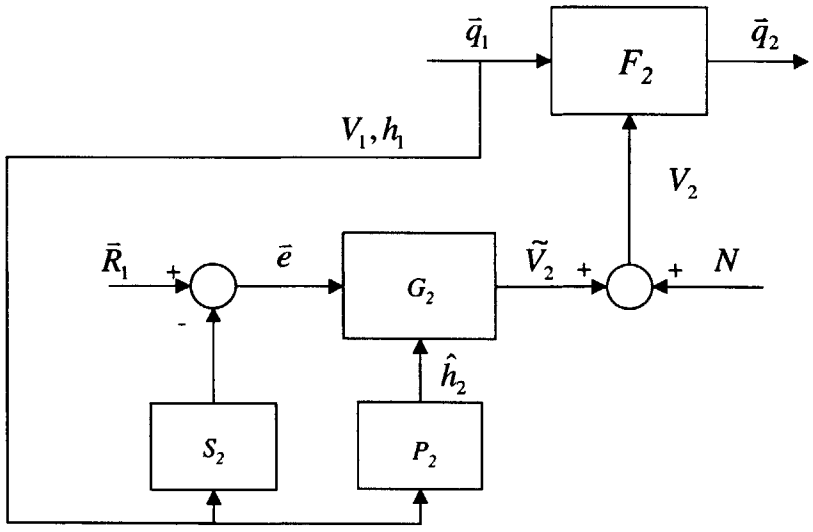

Figure 6.7 Stand 2 Speed Control Diagram

The model for stand 4 roll-speed controller is a Feedback loop. Figure 6.8 is a diagram for the controller, and the model for stand 4 roll-speed is as follows.

$$V_4 = \beta_0 + \beta_1 \hat{h}_5 + \beta_2 h_4 + N \tag{6.16}$$

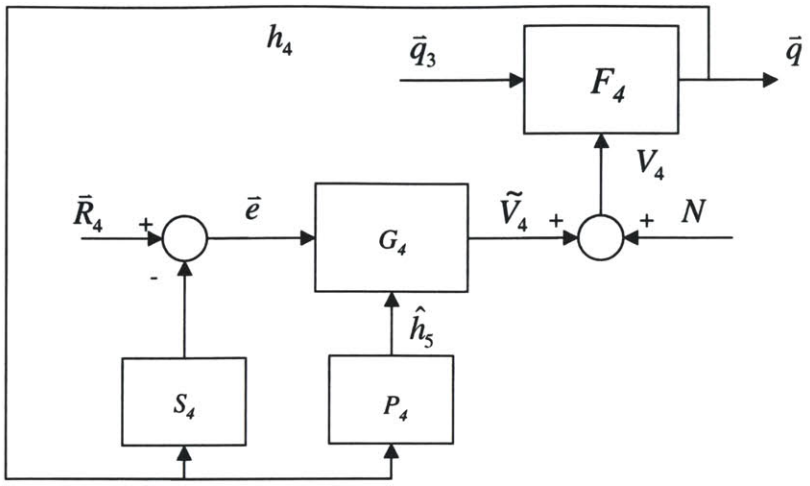

Figure 6.8 Stand 4 Speed Control Diagram

The model Calibration and validation of the model was performed the same way as stand 1 roll speed controller model. Both batch calibrated to r^2 of 0.99 and validated to r^2 of 0.99 excepted the last one in the second batch which validated to r^2 of 0.98. These high r^2 values suggested that the statistical model was what was very close to the actual control algorithm and the system disturbances in these variables were small.

The calibration and validation for the first batch is shown in Figure 6.9 through 6.12. Same as the stand 1 roll speed controller model, the biases in the validation are due to the difference in the mill's nominal operation settings. These biases do not affect the validity of these controller models.

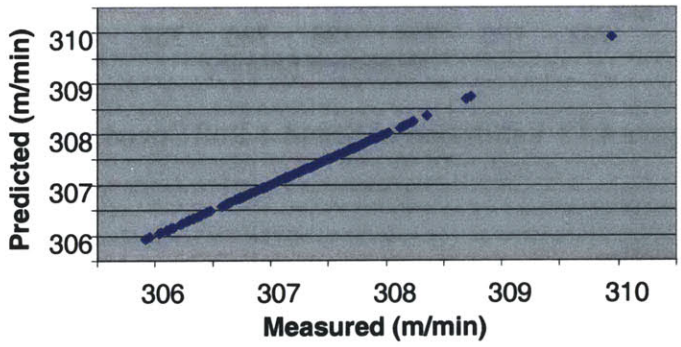

Figure 6.9 Calibration of Stand 2 Roll Speed Ctrl Model

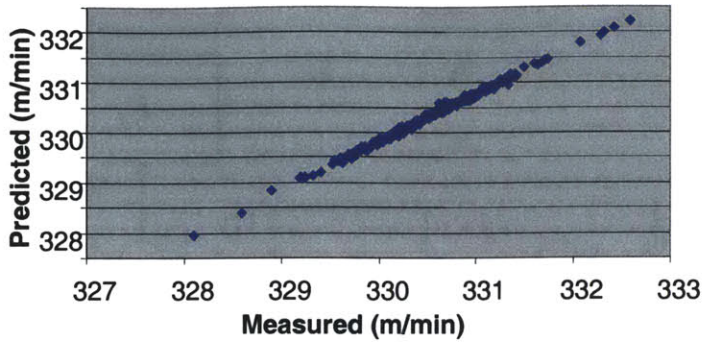

Figure 6.10 Validation of Stand 1 Roll Speed Ctrl Model

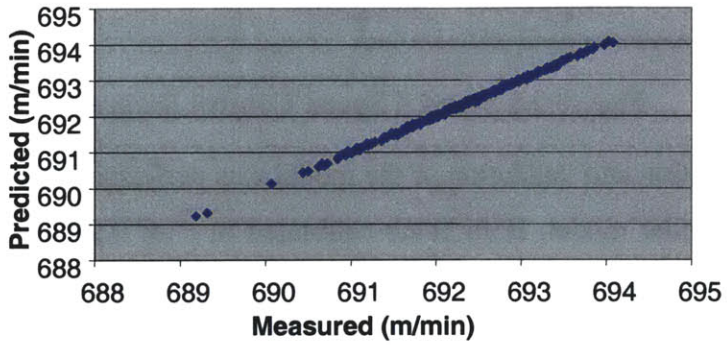

Figure 6.11 Calibration of Stand 4 Roll Speed Ctrl Model

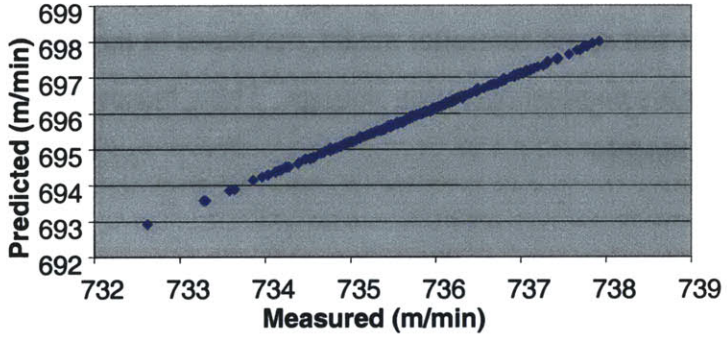

Figure 6.12 Validation of Stand 4 Roll Speed Ctrl Model

6.2.2 Force Controller

In the cold rolling mill, roll force control is active on Stands 1 through 4, each with a unique control algorithm. The stand 1 force is the controlled based on the input

thickness, input strip speed, and yield strength (Equation 6.17). Schematic of this controller is shown in Figure 6.13.

$$F_1 = \beta_0 + \beta_1 h_0 + \beta_2 V_0 + \beta_3 \sigma_0 + N \tag{6.17}$$

The equation regression fit to find the combination of β_i that leads to the least error between predictions and measurements. Same as the speed controller models, these roll-force models are adaptive, which means the coefficients keeps changing based on the production of previous coil.

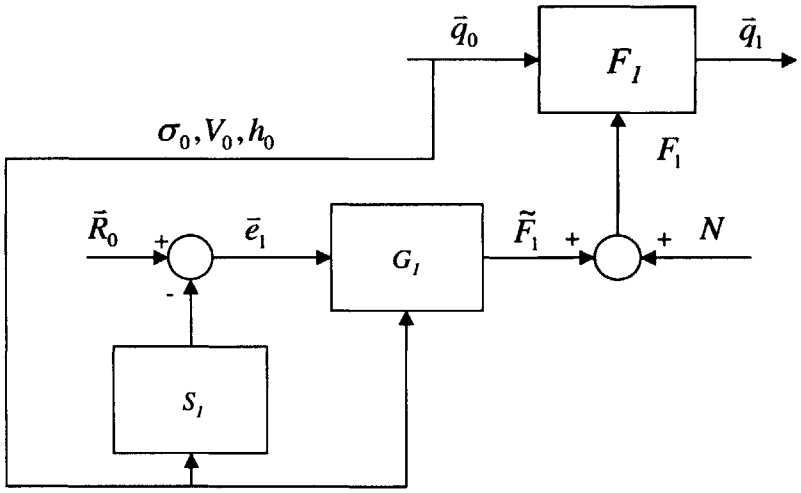

Figure 6.13 Stand 1 Force Control Diagram

The same batches of coil productions are used to calibrate and validate the roll-force models. The first batch calibrated to r^2 of 0.95 and validated also to r^2 of 0.95 (Figure 6.14, 6.15). The noise term, N, in 6.17 accounts for the lack of fit, and the magnitude of N is consistent. The second batch calibrated to 0.92 and validated on the second and third coil in this batch to 0.95 and 0.94 respectively. Again, bias was observed in the validation, but that is due to the nominal setting change in the mill, which could be easily adjusted in the model by updating β_0.

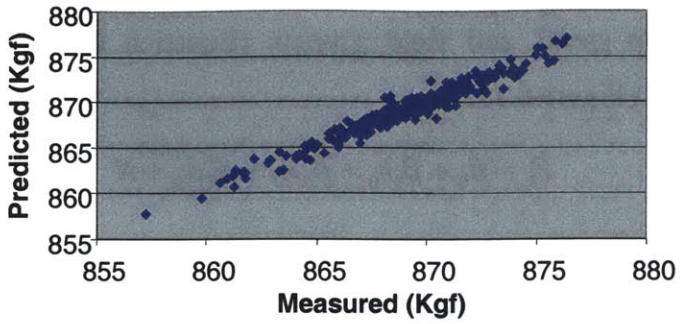

Figure 6.14 Calibration of Stand 1 Roll Force Ctrl Model

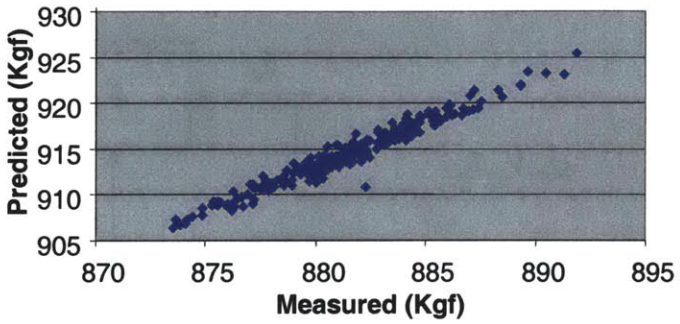

Figure 6.15 Validation of Stand 1 Roll Force Ctrl Model

The second roll-force is a function of the first roll-force, along with other variables such as stand 1 exit thickness, h_1, strip input yield strength, σ_0, and hardening coefficient, a_1 (Equation 6.18).

$$F_2 = \beta_0 + \beta_1 F_1 + \beta_2 h_1 + \beta_3 \sigma_0 + \beta_4 a_1 + N \tag{6.18}$$

The schematic of stand 2 roll-force controller is shown in Figure 6.16.

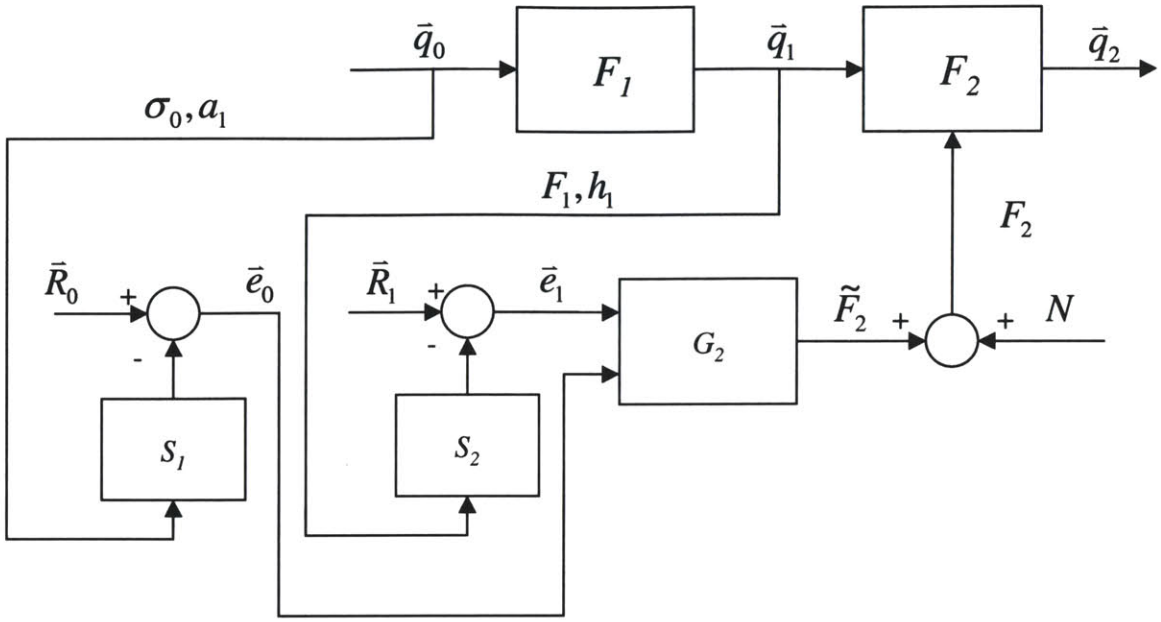

Figure 6.16 Stand 2 Force Control Diagram

The stand 2 roll-force model of calibrated on the first coil in the first batch to $r^2$of 0.97 and validated on the second coil in the same coil to r^2 of 0.93 (Figure 6.17, 6.18). That model calibrated on the first coil in the second batch fit to $r^2$of 0.89, and the model validated on the remaining coils to $r^2$of 0.91 and 0.89.

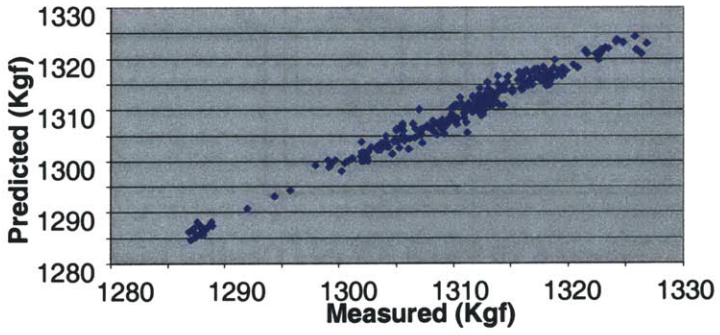

Figure 6.17 Calibration of Stand 2 Roll Force Ctrl Model

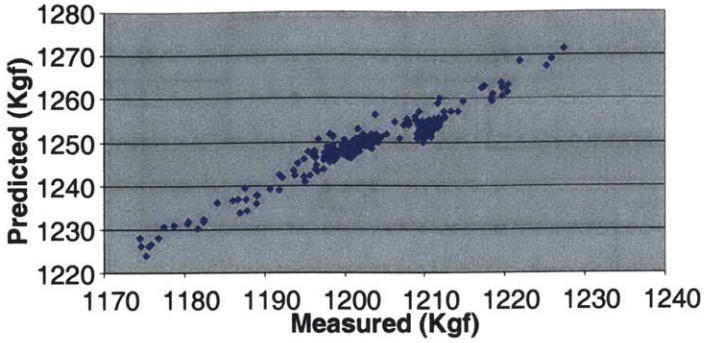

Figure 6.18 Validation of Stand 2 Roll Force Ctrl Model

Stand 3 force control model is based on roll-force in stand 1 and 2, along with stand 1 exit thickness, strip input yield strength, and hardening coefficient (Equation 6.19). The controller diagram is shown in Figure 6.19.

$$F_3 = \beta_0 + \beta_1 F_1 + \beta_2 h_1 + \beta_3 \sigma_0 + \beta_4 a_1 + \beta_5 F_2 + N \tag{6.19}$$

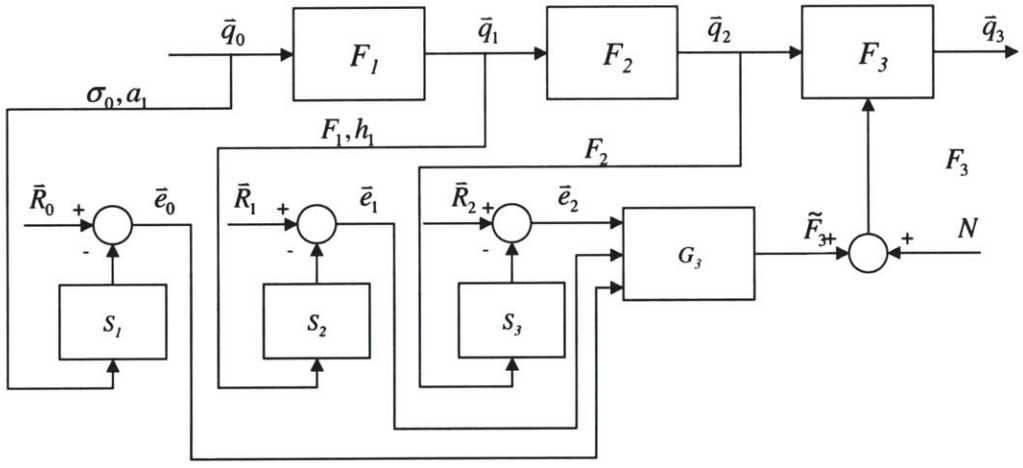

Figure 6.19 Stand 3 Force Control Diagram

The model was fit to production data from the same batches as previous models. The first model calibration had $r^2$of 0.57 and it validated on the second coil of the batch with $r^2$of 0.82 (Figure 6.20, 6.21). For the second production batch, the model was calibrated on the first coil to a $r^2$of 0.61, but it only validated on the following coils to $r^2$of 0.30 and $r^2$of 0.23.

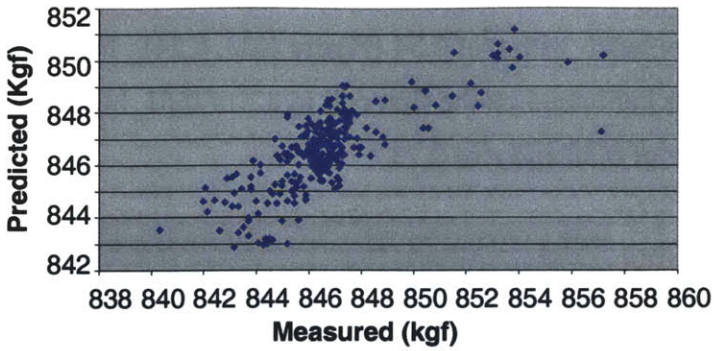

Figure 6.20 Calibration of Stand 3 Roll Force Ctrl Model

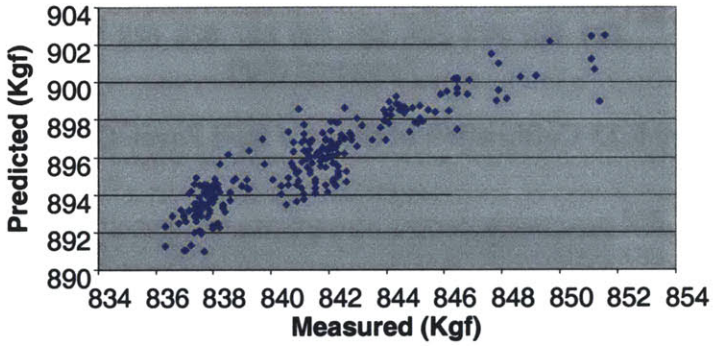

Figure 6.21 Validation of Stand 3 Roll Force Ctrl Model

The force controller in stand 4 is function of the roll force in stand 2 and 3, stand 1 exit thickness, strip input yield strength and the hardening coefficient (Equation 6.20). The schematic representation of force controller in stand 4 is shown in Figure 6.22.

$$F_4 = \beta_0 + \beta_1 F_2 + \beta_2 h_1 + \beta_3 \sigma_0 + \beta_4 a_1 + \beta_5 F_3 + N \tag{6.20}$$

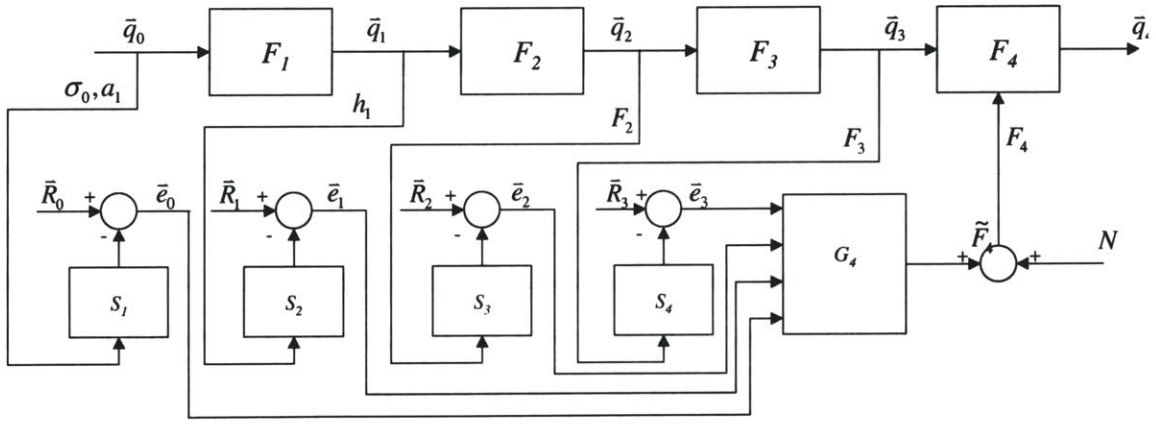

Figure 6.22 Stand 4 Force Control Diagram

This model calibrated to $r^2$of 0.65 on the first coil of the first batch, and it validated on the second coil of the batch with $r^2$of 0.34 (Figure 6.23, 6.24). For the second production batch, the model was calibrated on the first coil to a $r^2$of 0.61, but it only validated on the subsequent coils to $r^2$of 0.30 and $r^2$of 0.23.

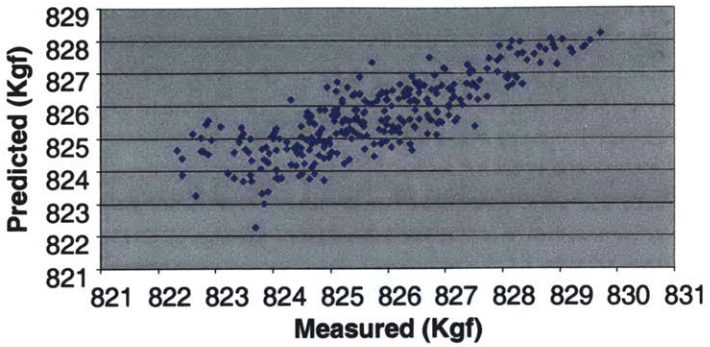

Figure 6.23 Calibration of Stand 4 Roll Force Ctrl Model

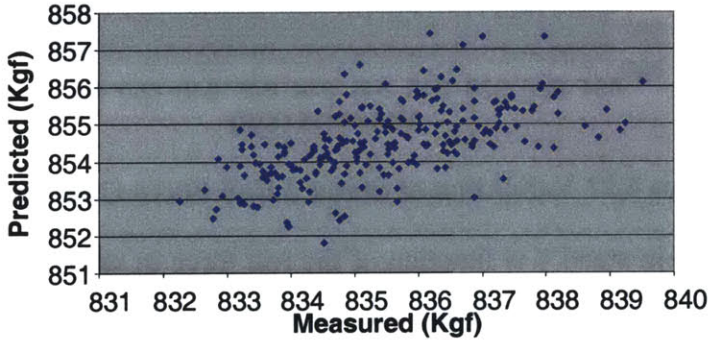

Figure 6.24 Validation of Stand 4 Roll Force Ctrl Model

Most of the controllers modeled in this thesis predict the process variable accurately. The force controller model for stand 3 and 4 are less accurate in comparison. One reason can be that the actual control algorithm is nonlinear and the linear model is not valid. Another possibility is that a prediction variable is introduced in the actual controller, such as the case for the speed controller in stand 2 and 4. Without the knowledge on this prediction variable, an accurate model for the controller cannot be constructed. Modeling these controllers is trivial once the original controller algorithm is made available. This thesis is intended to shows the importance and the techniques for modeling complex multi-operation manufacturing systems for variation analysis.

6.3 Chapter Summary

In Chapter 6, the models of the on-line controllers are constructed. These controllers are designed to removed variations in the exit thickness. Their values are determined by the geometric and material properties of incoming strip, along with the process variables of previous stands. By combining the models of the controllers with the physical cold rolling model, the output thickness of a strip can be predicted without being processed.

The sensitivity analysis of this model can separate the variations in process variables into control actions and system disturbances. The variations in the system that were compensated by the controllers would not appear in the output thickness. This allows the variation analysis to correctly identify the sources of variation in the output thickness.

Chapter 7: Cold Rolling Model with Control Systems

In chapter 6, the simple variation propagation analysis resulted in larger output thickness variations than the actual values. This was due to the lack of controller model. The observed variations in the cold rolling mill, such as force and speed, do not directly propagate through the system and cause quality loss. Instead, most of the observed variations of these variables are results of control actions intended to reduce the final output variation.

The algorithms of these controllers were derived in Chapter 6. In this chapter, the control algorithms are now incorporated in the cold rolling model and a complete, large scale virtual cold rolling mill simulation is constructed and explored. Since this complete model simulates the behavior of the cold rolling mill, the output thickness of a steel strip can be predicted prior to production, given only its geometric and material properties. A variation analysis on this model separates the noises from control actions in each process variable and identifies the sources of variations in exit thickness.

7.1 Virtual Cold Mill Simulation

In chapter 6, the inputs of each model are upstream workpiece properties and process variables. In chapter 7, it is shown that some of the process variables are results of control actions that comply with specified algorithms. By expressing these controlled variables with the control algorithms, a virtual mill can be constructed. The schematic representation of this cold rolling mill model is shown in figure 7.1.

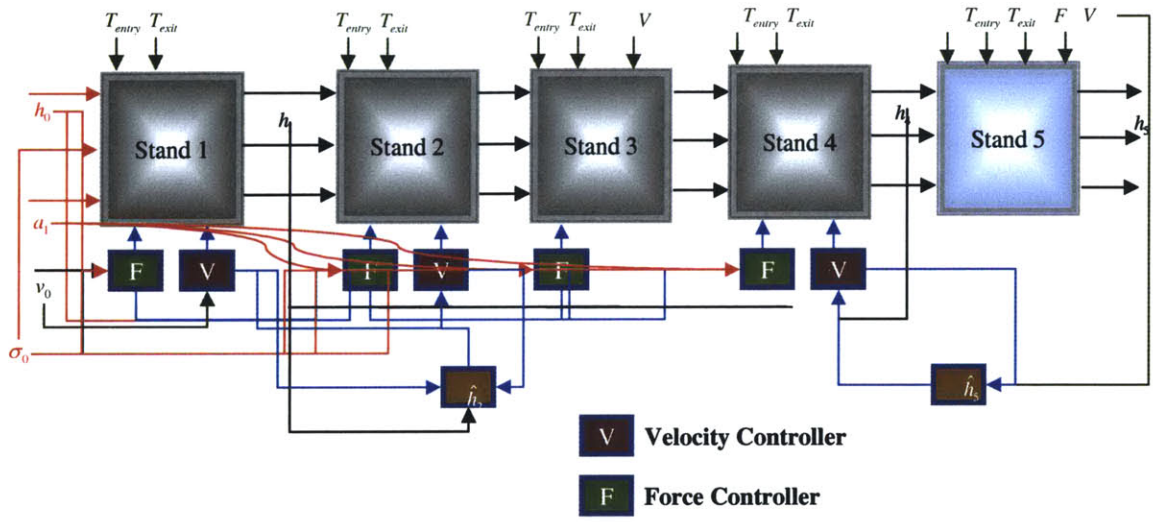

Figure 7.1 Schematics of the Complete Cold Rolling Mill Model

As discussed in the previous chapter, the control algorithms are constantly adaptive, based on the production of the previous coil. Therefore, the statistically derived model is only valid on the coil produced immediately after the calibration coil. The same batches of coils in Chapter 6 are used in this chapter to demonstrate the techniques for simulating variation propagation in a complex manufacturing system.

Similarly as in previous chapters, the cold rolling mill is split into three models: Stand 1, Stand 2-3-4, and Stand 5. Each model is discussed in the following sections. After being validated individually, these models are integrated to form a model that simulates the behavior of the cold rolling mill based on the steel strip's input geometrical and material properties. Sensitivity analysis is then performed to determine the contribution of variation in each process variable.

7.1.1 Stand 1 Simulation

The Stand 1 simulation model is based on the model discussed in chapter 4. The values of roll forces and roll speed are now predicted based on the control models derived in chapter 6, instead of using the measured values, which are not know a priori. The noises in these two variables are normally distributed random variables. The magnitude of the

noise is tuned so that the simulated output thickness has the same variance as the measured output thickness. The amount of these noises, which propagate through the manufacturing system, depends on the effectiveness of the controllers. Therefore, the amount of variation calibrated on one coil should be valid on the subsequent coil production. In this thesis, the variations in these controllers are calibrated on the first coil of each batch. These variations are then validated with the following coils in the batch.

The uncontrolled variables, such as entry and exit tension, are treated as constant in the simulation. The entry thickness is measured prior to processing, and the values of σ_0 and a_1 are determined from the statistical Equations 4.14. Practically, there are models underway to determine σ_0 and a_1 prior to production through chemistry and the temperature history of the strip. The schematic of stand 1 simulation is shown in Figure 7.2.

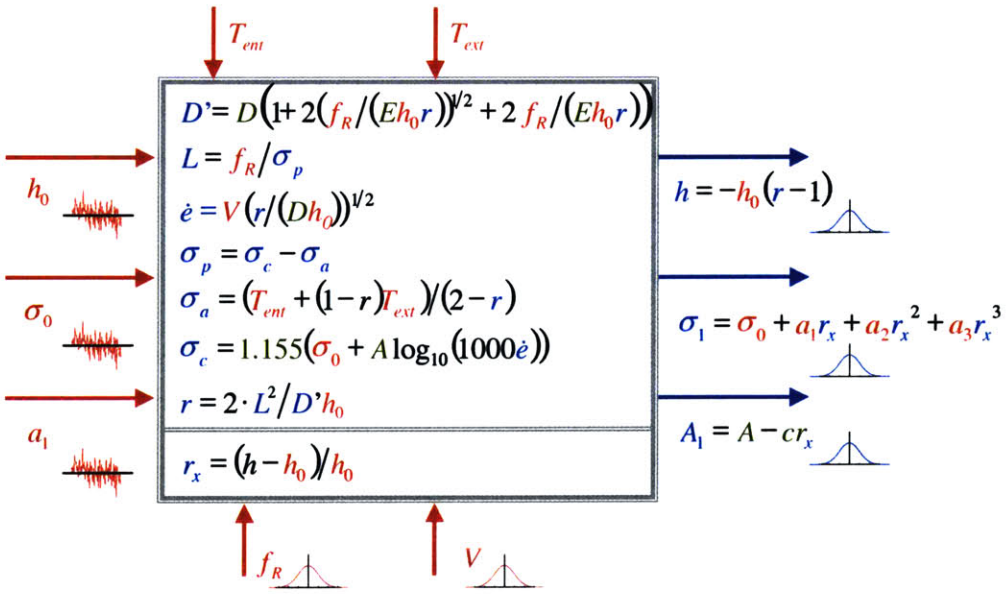

Figure 7.2 Random Variables and Equations for Stand 1

Since some noise is randomly generated, this simulation is not intended to compare the thickness measurements at each sampled point down the strip. Instead, the goal is to predict the mean, standard deviation, and histogram of the output based on the information on the input variables. In both batches, the noise in stand 1 force is

calibrated to be a normally distributed variable with variance of 0.061%, and the variance for the noise variable in roll speed is 0.013% of its nominal value, determined experimentally. The calibration and validation results of the first batch are shown below as an example. The histograms of the actual measurement and simulation result of stand 1 exit thickness of the first coil are shown in Figures 7.3. The difference in the standard deviations between these two distributions is 2.5%, and the mean offset is 0.0057%.

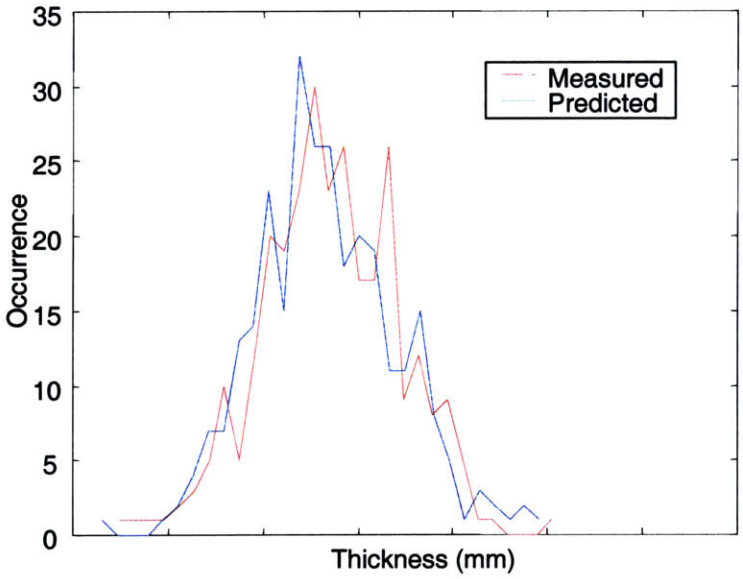

Figure 7.3 Stand 1 Exit Thickness Distribution of a Calibrated Coil

The noise and control algorithms calibrated on this coil are validated on the subsequent coil in this batch. There are 250 samples in the second coil and the simulated output thickness has standard deviation 0.6% from that measured, and the mean offset is 0.0017%. The histograms of the measured and predicted output thickness of the second coil are shown in Figure 7.4.

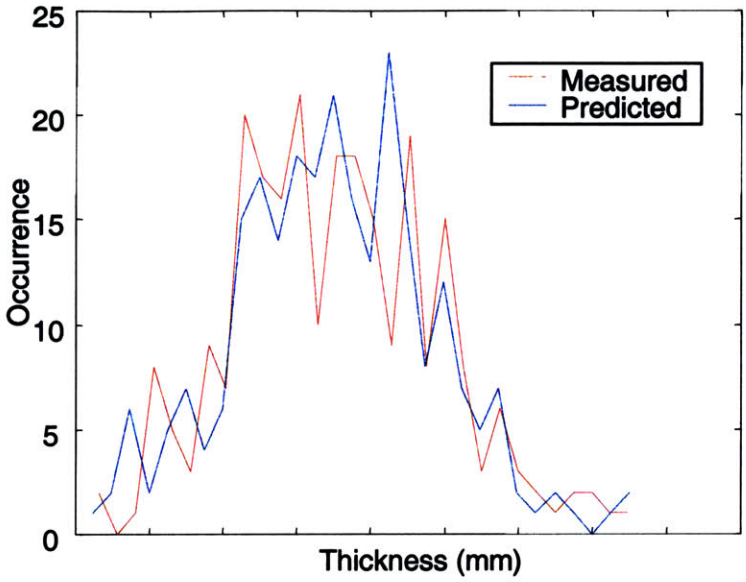

Figure 7.4 Measured Stand 1 Exit Thickness Distribution of a Validated Coil

In the second batch, the difference between predicted and measured stand 1 output thickness standard deviation for the first coil is 0.1%, with a mean offset is again insignificant (0.0034%). The mean offsets between measured and predicted thickness distributions are negligible, and therefore not mentioned in the remaining of this section. The noise and control algorithms calibrated on this coil are validated on the two subsequent coils. The simulated stand 1 output thickness for these two coils have standard deviations of 5.3% and 1.8% from the measured values respectively. Given these results, one can conclude that an effective simulation of cold mill stand can be done, given only the incoming material properties, localized in time.

7.1.2 Stand 2-3-4 Simulation

Stands 2, 3, and 4 are combined into one model because of the lack of inter-stand gauge measurements after stand 2 and 3. The Stand 2-3-4 model is based on the Roberts' model discussed in chapter 5. The input thickness is the measured stand 1 exit thickness. The input hardened yield strength, σ_1, and strain rate sensitivity, A_1, are calculated using the models discussed in chapter 5. The controlled variables, roll forces in stands 2 through 4 and roll speed in stands 2 and 4, are modeled as described in chapter 7. The uncontrolled

variables, such as tensions and stand 3 roll speed, are held constant. The standard deviation of the noise added into each controlled variable is modeled as a constant ratio of the variable's nominal value. (Equation 7.1)

$$\sigma N_{P_i} = \left(\overline{P}_i\right) \times R \tag{7.1}$$

The ratio R is tuned to minimize the error between the predicted and measured variation using the data from the first coil in each batch. The value is then validated on preceding coils. The value of R should be consistent in a short time span, when little has changed in the operation settings. A schematic representation of the model is shown in Figure 7.5.

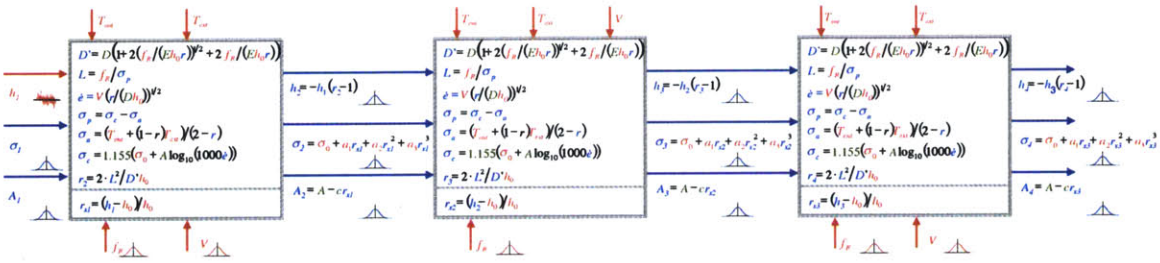

Figure 7.5

The controller algorithm and variation ratio, R, is validated on the first coil of each batch. For the first batch, R is experimentally found to be 0.0009%; the measured and calibrated stand 4 output thickness distribution for the first batch is shown in Figures 7.6. Even though the value of R seems small, the outcomes of simulations were sensitive to changes in R.

During the simulation of this sample coil, a small perturbation was necessary for the model for Stand 2-3-4 to converge. A small perturbation of +0.18% was added to the Stand 2 force to help convergence. This contributed to the mean offset observed in Figure 7.6.

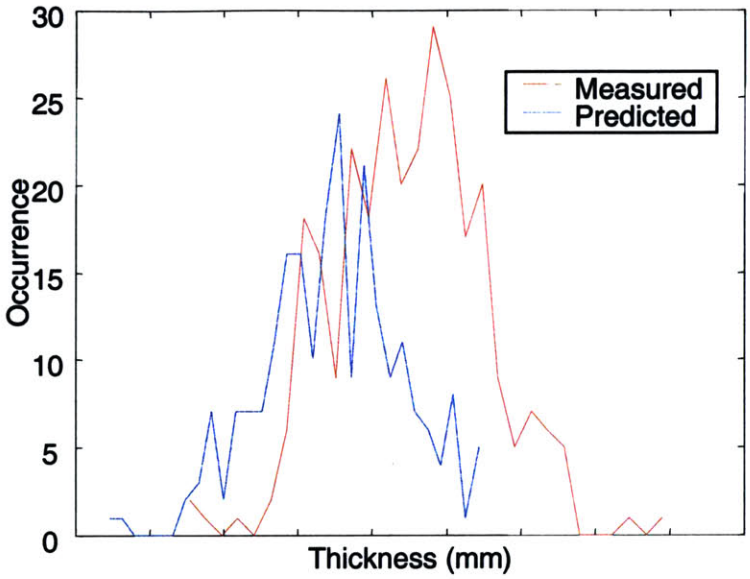

Figure 7.6 Stand 4 Exit Thickness Distribution of the Calibrated Coil

The difference between the standard deviation of the measured and calibrated distributions of the stand 4 output thickness is 6.4%, with mean offset of 0.1%. The controller models and R are validated on the next coil and the resulting difference in standard deviations is 2.5%, the mean offset between measurement and prediction is 0.06% (Figure 7.7).

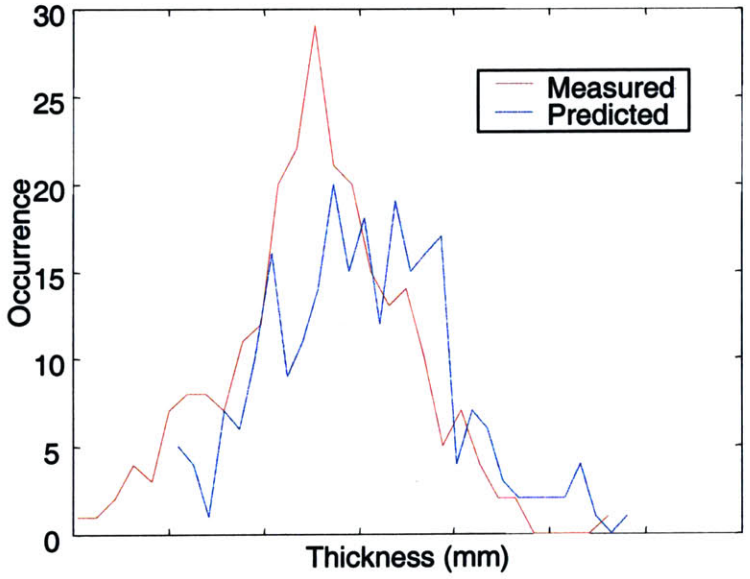

Figure 7.7 Stand 4 Exit Thickness Distribution of the Validated Coil

The error between standard deviations of measured and simulated thickness for the calibration coil in the second batch is 2.2%. For the two validation coils, this number is 7.8% and 7.6%. Here, one can see larger errors than Stand 1. This is expected, since 3 rolling stands are compounded into one model.

7.1.3 Stand 5 Simulation

Since there are no controllers installed in Stand 5, all process variables are designed to stay at their setup value. Therefore, the value of each input variable is held constant, and the stand 5 output can be calculated based on conservation of volume. (Equation 7.2)

$$h_i Vs_i = h_{i-1} Vs_{i-1} \tag{7.2}$$

where Vs is the strip speed.

The strip speed is the product of forward slip ratio, f, and the roll speed, V. The roll speed can be determined from the setup value, but the forward slip ratio is a complex function of the operating conditions, such as friction and roll radius. Since the operating conditions are relatively stable within a short period of time, the forward slip ratio calculated from one coil is close to the preceding coil, given the operation setups are similar.

The resulting expression for the stand 5 model is as follows.

$$h_5 = \frac{h_4 Vs_4}{Vs_5} = \frac{h_4 f_4 V_4}{f_5 V_5} \tag{7.3}$$

The slip ratios are calculated from the first coil of each batch. The roll speed is the setup value for each coil. The input strip thickness of this model is the measured exit thickness at stand 4. Again, the forward slip ratios are calibrated on the first coil of each batch and used for validation on following coils. The measurement and calibration result for the first batch is shown in Figures 7.8. The difference in standard deviation is 0.8%.

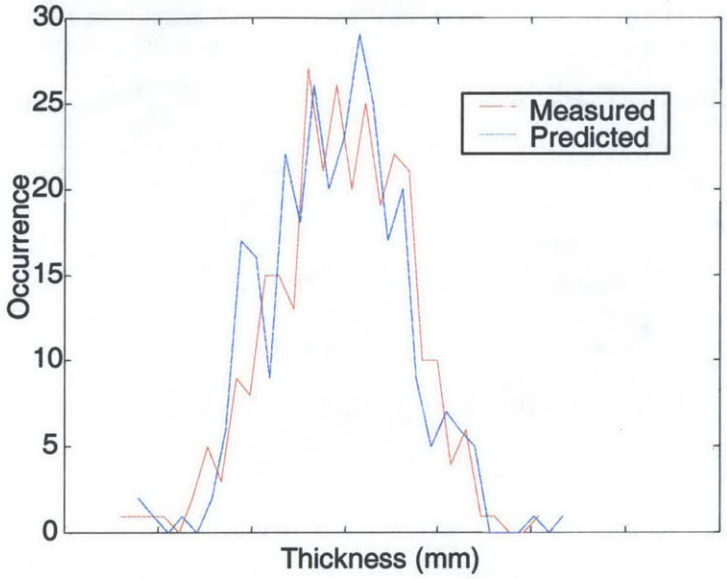

Figure 7.8 Stand 5 Exit Thickness Distribution of the Calibrated Coil

The forward slip ratio calibrated on this coil is substituted in Equation 7.3 to predict the thickness output on the following coil. The difference between the measured and predicted standard deviation of the output thickness is 0.8%, and mean offset of 0.007%. For the second batch, the error between measured and predicted output thickness variation is 13% for the calibration coil. A special variation, which is not monitored, might have occurred at Stand 5 during the production of this coil. On the other hand, the two validation coils predict the output thickness variation to within 1% and 6.3% error from that measured.

These results show that each stand, with physical stand and control models, can predict the nominal value of the output thickness very accurately, and the output thickness variation to within 13%. A summary of the error between predicted and measured thickness variations is shown in Table 7.1.

		Error between measured variation and variation predicted by individual model		
Batch	Coil	Thickness	Thickness	Exit
1	Calibration	2.5%	6.4%	0.8%
1	Validation	0.6%	2.5%	2.7%
2	Calibration	0.1%	2.2%	13.0%
2	Validation #1	5.3%	7.8%	1.0%
2	Validation #2	1.8%	8.6%	6.3%

Table 7.1 Thickness Variation Prediction Results

7.1.4 Five-Stand Virtual Mill

In the previous sections, each stand model was calibrated and validated individually. The thickness measurement at exit of stand 1 is one of the inputs for Stand 2-3-4 model, and the thickness measurement at exit of stand 4 is used in Stand 5 model. It is desired to predict the final output thickness variation for the entire mill solely based on the geometrical and material properties of the strip prior to the production. Therefore, the output thickness predicted by the Stand 1 model is fed into the Stand 2-3-4 model, whose thickness prediction then becomes the input of the Stand 5 model.

The integrated model uses the same calibrated values obtained in the previous sections, such as the magnitude of each noise variable and the forward slip ratios. Since the thickness prediction of each model becomes the input of the next model, error in the models is compounded. This leads to larger error in the prediction of thickness at Stands 4 and 5.

As an example, the measured thickness and the integrated model's simulation results of the validation coil in the first batch are shown below. The measured thickness and simulated Stand 1 thickness of the integrated model are shown in Figures 7.9.

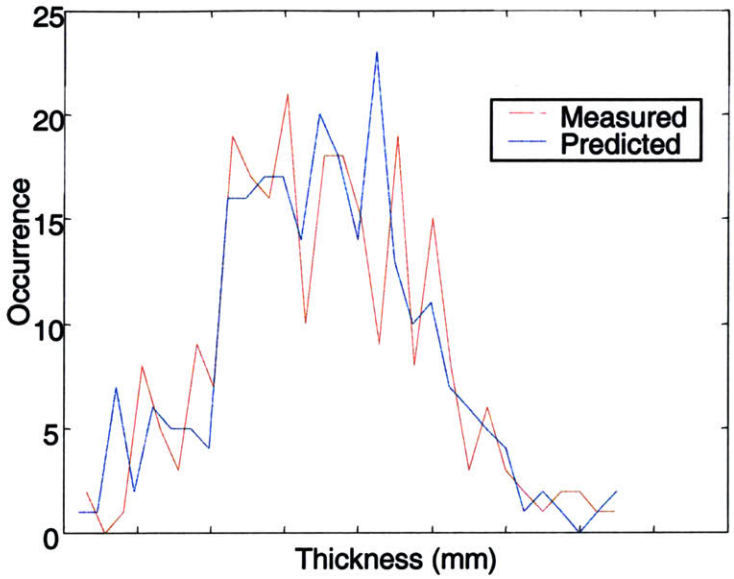

Figure 7.9 Stand 1 Exit Thickness Distribution of the Validation Coil

Figures 7.10 is the measured thickness and the thickness predicted by the integrated model at exit of Stand 4. Figures 7.11 is the thickness distributions of the measured Stand 5 thickness and the thickness predicted by the same model. The variation of Stand 4 output thickness prediction is 9.7% different from that of measured thickness, and the mean offset is 0.05%. This error for Stand 5 output thickness prediction is 11.2%, with mean offsets of 0.03%.

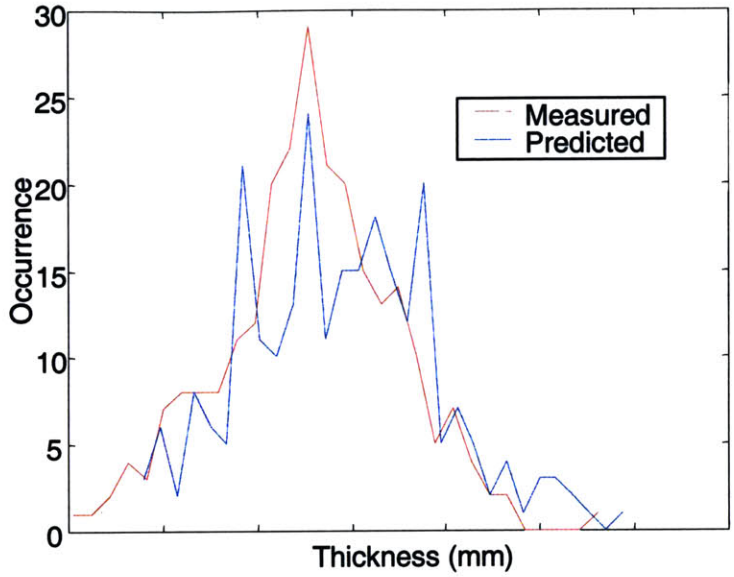

Figure 7.10 Measured Stand 4 Exit Thickness Distribution of the Validation Coil

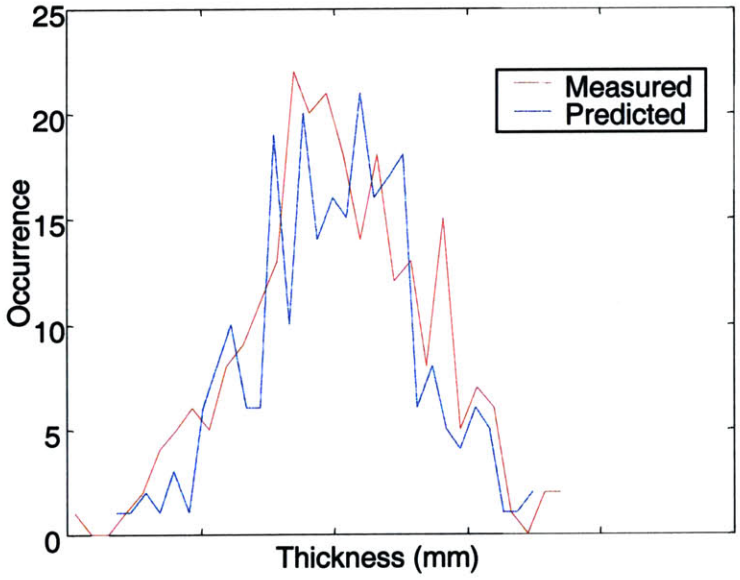

Figure 7.11 Stand 5 Exit Thickness Distribution of the Validation Coil

Table 7.2 compares the error between thickness variation calculated from data and that predicted by both individual and integrated models. The error in thickness prediction at Stand 4 and Stand 5 are significantly larger for the integrated model since the error in the upstream model is compounded in the downstream model.

In summary, a complete cold mill simulation was developed and tested. Generally, given no more information that strip geometry and materials, final gauge of the entire mill can be predicted to within 15%. This is all for variations below 1 Hz.

		Standard Deviation Difference			Mean Offset		
Batch	Coil	h1	h4	h5	h1	h4	h5
1	Calibration	2.3%	11.6%	10.7%	0.00%	0.16%	0.17%
1	Validation	4.5%	9.7%	11.2%	0.00%	0.05%	0.03%
2	Calibration	4.3%	13.4%	11.3%	0.00%	0.40%	0.93%
2	Validation	8.2%	7.8%	7.0%	0.00%	0.08%	0.48%
2	Validation	5.4%	5.1%	0.9%	0.03%	1.55%	1.76%

Table 7.2 Thickness Variation Prediction Results with Integrated Model

7.2 Sensitivity Analysis on Virtual Cold Mill

Sensitivity analysis is performed on the integrated model with the methods discussed in Chapter 6. The preliminary analysis in Chapter 6 has determined that output thickness is insensitive to tension. Therefore, sensitivity analysis in this chapter focuses on the relationship between the variation in output thickness and the variation in each controlled variable and input strip's characteristic properties.

The sensitivity analysis described in Chapter 5 is repeated with this integrated model with on-line controllers. The sources of variation in output thickness are identified, and the results are shown in Figure 7.13.

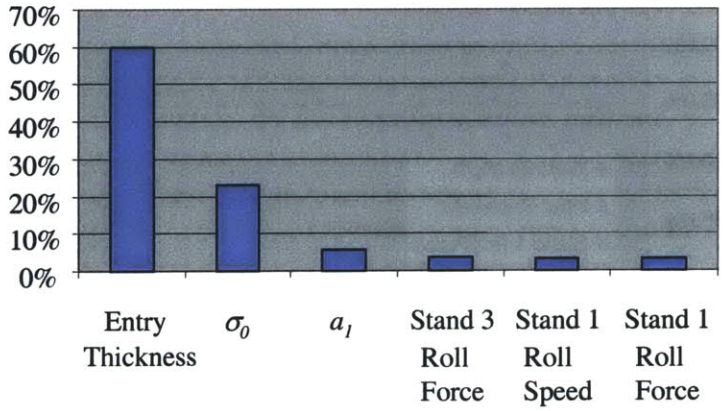

Figure 7.12 Percent Contribution of Variation in Output Thickness

Contrary to the results in Figure 5.7, the analysis shows that most of the output thickness is most sensitive to the variations in input thickness, which contributes 60% of the observed output thickness variation, given the cold mill control system. The second largest contributor is the yield strength variation, which accounts for 23% of the observed output variation, given the cold mill control system. From this, one can conclude that the cold mill, with its current control system, does not add in variation, and that all output variation is primarily due to remaining input coil variation. This statement is valid for data averaged at 1Hz. The difference between Figure 5.7 and Figure 7.13 is that the analysis in this chapter included the influences of controllers. The variations in σ_0 and a_1 are removed by the controllers and the entry thickness variation propagates through the mill.

7.3 Simulating Various Scenarios

It is logical to reduce variations in the variables to which output thickness is sensitive. The integrated model is used to simulate the amount of reduction in thickness variation based on the reduction in input variables. Figure 7.24 shows the reduction in output thickness in the cases that variations in entry thickness, input yield strength, and Stand 1 roll force are reduced from 0 to 50%.

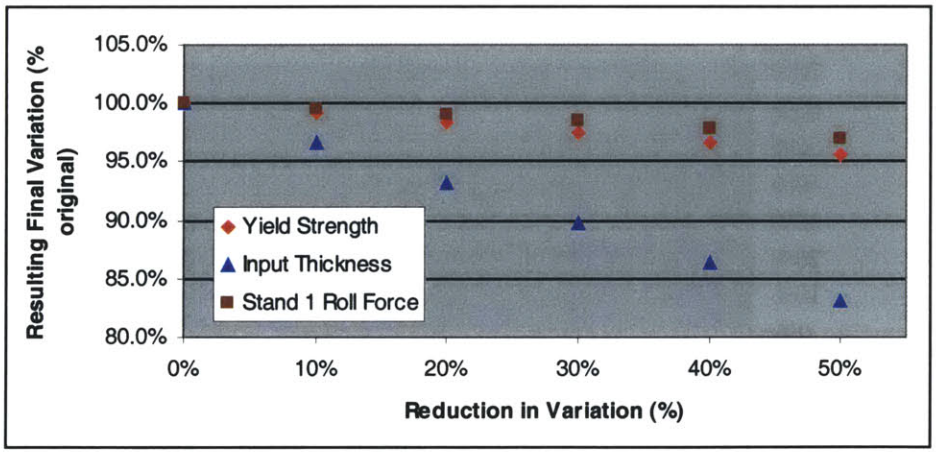

Figure 7.13 Output Thickness Variation Reduction by Improving Input Strip

As predicted by the sensitivity analysis, the reduction in entry thickness variation has the most significant improvement on the output of the mill. Since both yield strength and input thickness are determined at the hot rolling stage, it should be possible to reduce their variations at the same time. Figure 7.25 shows the resulting variation reduction when variations in entry thickness and yield strength are reduced from 0 to 40%.

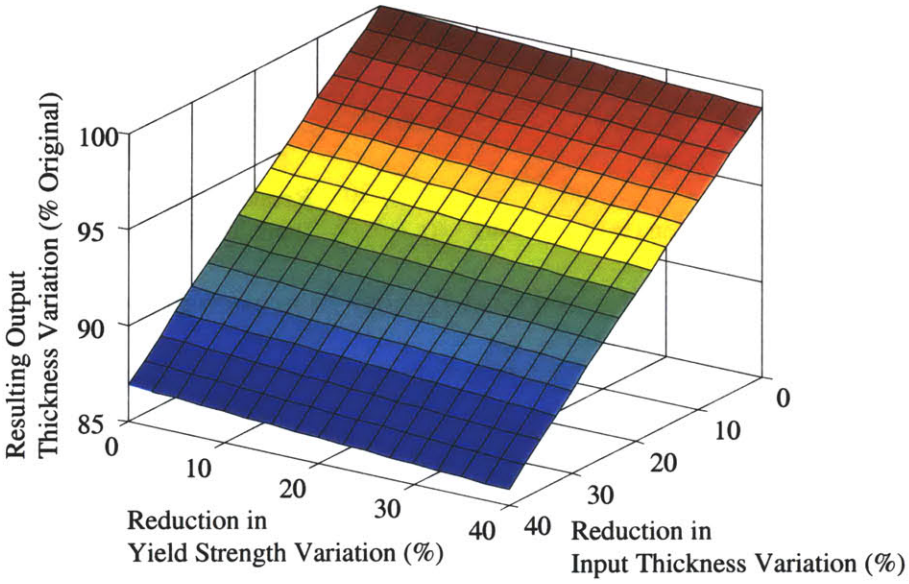

Figure 7.14 Output Thickness Variation Reduction by Reducing Entry Thickness and Yield Strength Variation

The conclusion from this analysis enables engineers to determine the most efficient way to reduce the variation in the system. If the cost to reduce variation in each input variable is known, an optimum point can be calculated that utilizes the least cost to achieve the most variation reduction. A matrix C can be introduced as the product of the new resulting variation and the cost required.

Figure 7.26 is generated with a quadratic expression for cost. The x-axis is the reduction in entry thickness variation, and the y-axis is the reduction in yield strength. The z-axis is the value of C. The values of this curve are normalized so that C for the original condition, 0% variation reduction in each input variable, is unity.

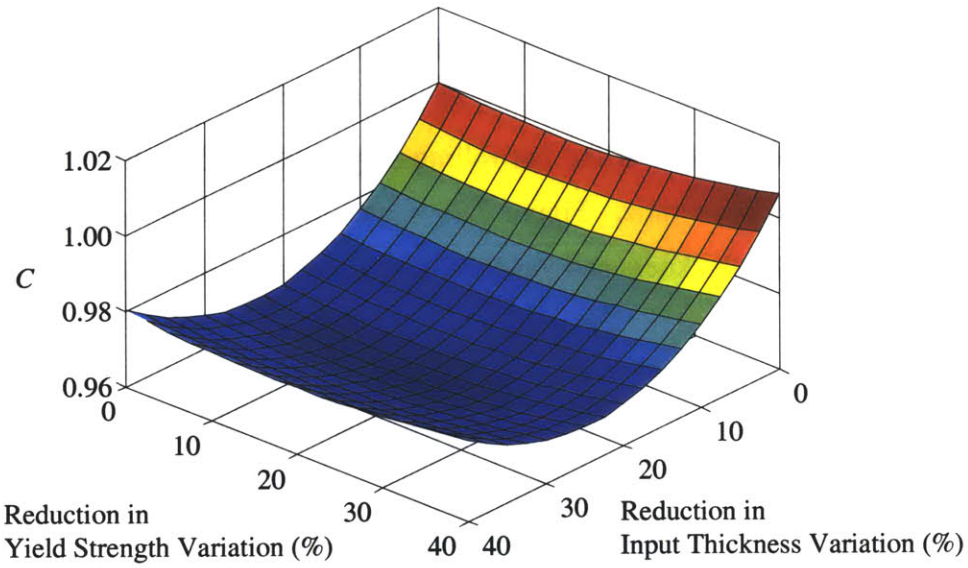

Figure 7.15 Normalized Cost-Quality Improvement Surface

The minimum point of this curve is the optimum improvement of the mill.

7.4 Chapter Summary

This chapter has shown that by combining the controller models and the physical stand models, the strip output thickness can be predicted from the geometric and material properties of incoming strips. Monte-Carlo simulation is used to identify the sources of variation and perform sensitivity analysis. The sensitivity analysis suggests that the entry thickness variation contribute the most to the output thickness variation, followed by the yield strength and hardening coefficient variation. Confirming the sensitivity analysis, reducing input thickness variation results in the best improvement in output thickness variation in the simulation.

Chapter 8: Conclusion

This thesis has developed techniques for modeling variations in complex continuous manufacturing systems. The techniques have been successfully applied to cold rolled steel manufacturing. The sensitivities between output thickness variation and variations in process variables were determined through Monte-Carlo simulation in this thesis. A limiting factor for continuous controlled manufacturing systems is that often statistical models cannot be used to predict output since the values of the on-line controlled process variables cannot be obtained prior to actual production. Therefore, physical simulation models must be constructed to predict output. In this thesis, the thickness variation of a cold rolling mill was done based solely on the input steel strip's geometrical and material properties. This simulation model includes both the physics of cold rolling, and models of the on-line controllers in the cold mill.

To construct simulation models, the concept of an Integrated System Model is utilized, linking up the inputs and outputs of individual operation models in the entire manufacturing system. An aspect of continuous systems is that the measured data streams must be split into bins so that high frequency sensor noises and unmodeled system vibrations are masked from the data. On the other hand, one cannot discard real data that impacts the output. A novel information content preserving algorithm is developed to judge sufficiency of a sample size.

A second issue in determining sampling frequency occurs with parallel measured data streams. The offset errors between the data streams must also be considered. In the considered cold mill, there were significant offset errors.

Due to the clock offsets in data storage devices, the finest bin size that is achievable with currently available data is one second. The output thickness variation in the binned data stream is 36% of the sufficiently observed variation, which is determined using the method developed in Chapter 4. As was shown, roll eccentricity is the primary cause of

the remaining high frequency variation, which can be readily modeled. Roll eccentricities cause the remaining 64% of the measured variation.

To analyze for sources of variation within complex continuous manufacturing systems, Monte Carlo analysis can be applied. For the considered cold mill, within the 36% of the measured variation the sensitivity analysis has shown that remaining input thickness variation is the dominant contributor to output thickness variation. For continuous controlled manufacturing systems, sensitivity analysis must be performed through Monte-Carlo simulation. In previous non-continuous system work, sensitivity coefficients were derived from linearized physical models through Taylor series expansion. The approach here extends these thoughts to more complex controlled systems.

Through simulation models, the output distribution can be predicted for a complex controlled continuous manufacturing system, given the input distributions. With the predicted output distribution, the expected c_p and c_{pk} can be calculated prior to the actual production. This enables operators to determine the likelihood of the product meeting the design specifications. Furthermore, the virtual mill can predict the final variation for scenarios with different magnitudes of variations in input variables. By combining the simulation results and the cost required to achieve that scenario, engineers can determine what is the optimum improvement that can be applied to the system.

As a further study in this thesis, statistical models were explored for use in describing complex controlled continuous manufacturing systems. Such models map output variation directly to process variations without frequency considerations. Such analyses can serve as tools for quickly calculating the output variation parameters when the process variables are not on-line controlled. Furthermore, since a statistical variation model is a linear combination of variation in process variables, the coefficients for each term is a good indication of the sensitivity of the output thickness to that process variable.

In summary, this work has developed analyses for studying variation in complex controlled continuous manufacturing systems. It was shown that physical models of the system could be combined with controller models to predict output parameters, given input measurements, for large complex controlled systems.

References

Bentz, R. J. and W. L. Roberts (1966). "Speed Effects in the Second Cold Reduction of Steel Strip." Mechanical Working and Steel Processing: 193-222.

Blahut, R. E. (1987). Principles and Practice of Information Theory, Addison-Wesley.

Bodner, S. R. (1965). Strain Rate Effects in Dynamic Loading of Structures. Behavior of Materials Under Dynamic Loading. N. J. Huffington. Chicago.

Bolbrinker, A. K. (1992). Steel Manual. Dusseldorf, Verein Deutscher Eisenhuttenleute.

Boning, D. S. M., P.K. (1993). DOE/Opt: A System for Design of Experiments, Response Surface Modeling, and Optimization using Process and Device Simulation. Dallax, Semiconductor Process and Design Center, Texas Instruments.

Box, G. (1957). "Evolutionary Operation: A Method for Increasing Industrial Productivity." Applied Statistics **6**: 81-101.

Carlton, A. J., W. J. Edwards, et al. Formulae for Cold Rolling Analysis. Newcastle, N.S.W. Australia, Research and Technology Centre, John Lysaght (Australia) Limited: 223-248.

Chen, C. P., Shyu, A., Liou, P., Leu, R.Q., Huang, K., Lin, J.Y., Yang, T.H., Liu, H.C., Ting, M.I., Shih, Y.C. (1998). A Novel Methodology of Critical Dimension Statistical Process Control. International Workshop on Statistical Metrology Technical Papers.

Cory, J. F. J., Puckett, S.J., Nessler, G.L (1990). "Roll eccentricity monitoring for strip quality control." Iron and Steel Engineer(February): 24.

Crowder, S. V. (1989). "Design of Exponentially Weighted Moving Average Schemes." Journal of Quality Technology **21**(3).

DeVor, R. E., Chang, T.-H., Sutherland, J.W. (1992). Statistical Quality Design and Control: Contemporary Concepts and Methods. New York, Macmillan Publishing Company.

Dunteman, G. H. (1989). Principal Components Analysis. Newbury Park, CA, Sage Publications, Inc.

Egan, S. J., Fryer, C.A., Lubomirski, M.S., Reeve, P.J. (1996). "Flatness modeling and control for a continuous tandem cold mill." Iron and Steel Engineer(March): 38.

Fleck, N. A., Johnson, K.L., Mear, M.E. , and Zhang, L.C. (1992). "Cold Rolling of Foil." Proc Instn Mech Engrs **206**: 119.

Ford, H., Ellis, F., Bland, D. R. (1951). "Cold Rolling with Strip Tension." J.I.S.I. **168**: 57-72.

Frey, D. D., Otto, K.N., Taketani, S. Manufacturing Block Diagrams and Optimal Adjustment Procedures. Cambridge, MA, Engineering Design Research Laboratory, Massachusetts Institute of Technology.

Fuller, M. A. (1969). The Modelling of Roll Gap Relationships in COld ROlling. Imperial College. London.

Ginzburg, V. (1989). Steel-Rolling Technology Theory and Practice.

Guo (1996). "Optimal Profile and Shape Control of Flat Sheet Metal Using Multiple Control Devices." IEEE Transactions on Industry Applications **32**(2): 449.

Hu, S. J. (1997). "Stream-Of-Variation Theory for Automotive Body Assembly." Annals of the CIRP **46**(1).

Ishikawa, N., Kobayashi, Y., Tsukada, K., Maenaka, H., Toyoda, M. (1996). "Effect of Strain Rate on Deformation and Fracture Properties of Structural Steels." Journal of Constructional Steel **4**.

John, E., Geddes, M., Oistlethwaite, I. (1998). "Improvements in Product Quality in Tandem Cold Rolling Using Robust Multivariable Control." IEEE Transactions on Control Systems Technology **6**(2): 257.

Kalpakjian, S. (1991). Manufacturing Processes for Engineering Materials. Reading, MA, Addison Wesley.

Kalpakjian, S. (1995). Manufacturing Engineering and Technology. Reading, MA, Addison Wesley.

Kamada, S., Iyama, S., Hamada, R., Hashimoto, S. Hayashi, K., Kajihara, T. (1996). "Edge profile control using Pair Cross mill in cold rolling." Iron and Steel Engineer(June): 20.

Khan, A. S., Huang, S. (1995). Continuum Theory of Plasticity. New York, NY, John Wiley & Sons, Inc.

Kuo, B. C. (1995). Automatic Control Systems. Englewood Cliffs, NJ, Prentice-Hall Inc.

Lei, J., Lima-Filho, P., Styblinski, M.A. (1998). Quadratic Propagation of Variance (QPOV) in Statistical Circuits Design. International Workshop on Statistical Metrology Technical Papers, IEEE.

Lin, C. C. Y. A., M. (1996). Comparison of Three Cold Mill Rolling Force Models: (1) The Modified Bland and Ford Model, (2) The Roberts Model, and (3) The Stone Model. 2nd International Conference on Modeling of Metal Rolling Process.

Lindholm, R. S. (1965). Dynamic Deformation of Metals. Behavior of Materials Under Dynamic Loading. N. J. Huffington. Chicago.

Lubrano, M., Bianchi, J.H. (1996). A Simple Model for On-Line Control of Skin Pass From Finite Element Analysis of Rolling Deformation. 2nd International Conference on Modelling of Metal Rolling Process, London, UK.

Lynn, J. B., Mayrosh, T.M., Neith, D.O., Santiago, J.G. (1991). "Quality and productivity gains in a structural rolling mill through statistical process control." Iron and Steel Engineer(January): 49.

MacAlister, A. F. (1989). "Modeling and adaptive techniques for rolling mill automation." Iron and Steel Engineer(December): 38.

Manjoine, M. J. (1944). "Influence of Rate of Strain and Temperature on Yield Stresses of Mild Steel." Journal of Applied Mechanics: A-211 - A-216.

Mantripragada, R. W., D.E. (1999). "Modeling and Controlling Variation Propagation in Mechanical Assemblies Using State Transitional Models." IEEE Transactions on Robotics and Automation **15**(1).

Marsh, K. J., Campbell, J.D. (1963). "The Effect of Strain Rate on the Post-Yield Flow of Mild Steel." Journal of the Mechanics and Physics of Solids **11**: 49-63.

Nessler, G. L., Cory, J.F. Jr. (1993). "Identification of chatter sources in cold rolling mills." Iron and Steel Engineer(January): 40.

Nieb, J. R., Nicolas, V.T. (1991). "Automated monitoring and control of vibration and chatter in rolling processes." Iron and Steel Engineer(July): 33.

Ogata, K. (1990). Modern Control Engineering. Englewood Cliffs, Prentice Hall.

Orowan, E. The Calculation of ROll Pressure in Hot and Cold Flat Rolling.

Painter, C., Frey, D.D., Otto, K.N. Key Inspection Characteristics. Cambridge, Massachusetts Institute of Technology.

Pinkowski, J. W., Andjelich, M. (1996). "Tandem mill roll marks: Source, cause and corrective action." Iron and Steel Engineer(June): 27.

Richards, S. J. (1992). "Vibration analysis of ratating equipment in a mill environment." Iron and Steel Engineer(June): 33.

Roberts, W. (1987). Flat Processing of Steel.

Roberts, W. L. (1978). Cold Rolling of Steel. New York, Marcel Dekker, Inc.

Sachs, E., Hu, A., Ingolfsson, A. (1995). "Run by Run Process Control: Combining SPC and Feedback Control." IEEE Transactions on Semiconductor Manufacturing **8**(1).

Shim, M. and N.-S. Park (1998). "Strip Gage Analysis System Using Frequency Analysis." SEAISI Quarterly **July**: 71-79.

Smith, T. H. B., D.S. An Artifical Neural Network EWMA Controller for Semiconductor Processes. Cambridge, Microsystems Technology Laboratories, Massachusetts Institute of Technology.

Suri, R. and K. Otto Evaluating Variation Reduction Process Control Strategies through System Modeling. Cambridge, MA, Engineering Design Research Laboratory
Department of Mechanical Engineering
Massachusetts Institute of Technology: 1-16.

Thornton, A. (1996). "Key Characteristics." Target **12**(5): 14-19.

Wei, Y.-F. T., A.C. (2000). Tube Production and Assembly Systems: The Impact of Compliance and Variability on Yield. Design Engineering Technical Conferences, Baltimore, MD.

Wold, S., K. Esbensen, et al. (1987). "Principal Component Analysis." Chemometrics and Intelligent Laboratory Systems(2): 37-52.

Wusatowski, Z. (1969). Fundamentals of Rolling.

Appendix A: Correlation Matrix from Spike Analysis over the Entire Length of a Strip

	bin	5XTHKX	1ESS	1ETHK	1ET	1RF	1RSS	1TQ	1XTHK	1_2SS	1_2T	2RF	2RSS	2TQ	2_3SS	2_3T	3RF	3RSS	3TQ	3_4SS	3_4T	4RF	4RSS	4TQ	4XTHK	4_5SS	4_5T	5RF	5RSS	5TQ	5XT	5XSS
bin	100%																															
5XTHKX	-12%	100%																														
1ESS	-12%	32%	100%																													
1ETHK	15%	-5%	39%	100%																												
1ET	1%	-4%	-4%	-6%	100%																											
1RF	18%	-4%	11%	5%	17%	100%																										
1RSS	-15%	29%	96%	37%	-4%	9%	100%																									
1TQ	-7%	20%	80%	43%	-7%	5%	73%	100%																								
1XTHK	18%	-4%	-6%	7%	-4%	16%	-7%	-6%	100%																							
1_2SS	-14%	28%	97%	39%	-6%	9%	99%	74%	-7%	100%																						
1_2T	17%	-2%	-3%	-3%	-2%	-2%	-3%	16%	-2%	-3%	100%																					
2RF	24%	6%	22%	31%	-4%	3%	22%	22%	74%	22%	-2%	100%																				
2RSS	-15%	29%	97%	36%	-4%	9%	100%	74%	-7%	99%	-3%	22%	100%																			
2TQ	-13%	33%	77%	29%	-6%	2%	69%	83%	3%	71%	-3%	19%	70%	100%																		
2_3SS	-14%	31%	98%	37%	-6%	9%	99%	76%	-6%	99%	-3%	21%	99%	73%	100%																	
2_3T	1%	28%	48%	5%	-7%	38%	44%	30%	20%	45%	-3%	16%	47%	53%	48%	100%																
3RF	4%	12%	67%	38%	18%	27%	66%	40%	11%	64%	-3%	34%	67%	33%	65%	34%	100%															
3RSS	-15%	29%	97%	37%	-4%	9%	99%	73%	-7%	99%	-3%	22%	99%	72%	99%	47%	65%	100%														
3TQ	-5%	25%	85%	49%	-6%	5%	77%	91%	-5%	80%	7%	23%	78%	92%	81%	46%	42%	79%	100%													
3_4SS	-16%	29%	98%	38%	-4%	10%	99%	76%	-6%	99%	-3%	22%	99%	74%	99%	47%	66%	99%	82%	100%												
3_4T	-15%	-6%	6%	-1%	-6%	37%	7%	-2%	35%	5%	-3%	27%	7%	5%	6%	18%	19%	7%	-4%	6%	100%											
4RF	1%	26%	64%	34%	12%	14%	58%	40%	2%	60%	-3%	29%	59%	31%	60%	30%	67%	58%	47%	61%	-6%	100%										
4RSS	-15%	28%	96%	38%	-4%	9%	99%	72%	-6%	99%	-3%	22%	100%	69%	99%	46%	66%	99%	78%	99%	6%	58%	100%									
4TQ	-7%	29%	77%	38%	-6%	3%	70%	86%	3%	72%	-3%	24%	71%	98%	74%	50%	35%	73%	95%	75%	-1%	37%	71%	100%								
4XTHK	23%	14%	8%	7%	-5%	-2%	13%	4%	-4%	13%	-2%	4%	15%	1%	17%	25%	30%	9%	6%	9%	-6%	17%	16%	3%	100%							
4_5SS	-14%	27%	96%	39%	-6%	9%	99%	76%	-6%	99%	-3%	22%	99%	75%	99%	48%	64%	99%	83%	99%	5%	57%	99%	77%	16%	100%						
4_5T	-3%	13%	35%	-4%	-3%	10%	36%	13%	24%	32%	-2%	24%	36%	16%	34%	13%	49%	35%	4%	33%	40%	3%	34%	7%	7%	31%	100%					
5RF	19%	-2%	13%	-2%	-3%	79%	14%	0%	32%	14%	-2%	15%	15%	2%	14%	50%	24%	13%	-1%	13%	42%	18%	14%	0%	16%	12%	26%	100%				
5RSS	-16%	33%	97%	38%	-5%	8%	99%	79%	-6%	99%	-3%	21%	98%	77%	99%	44%	61%	98%	84%	99%	5%	57%	98%	78%	10%	99%	33%	12%	100%			
5TQ	-8%	6%	77%	45%	-6%	4%	79%	81%	-6%	80%	-3%	19%	79%	68%	81%	19%	40%	79%	81%	79%	-2%	44%	80%	74%	15%	83%	6%	2%	83%	100%		
5XT	24%	42%	-1%	-4%	-3%	-3%	-3%	-4%	-3%	-3%	-1%	-3%	-1%	4%	3%	11%	11%	-5%	-4%	-4%	-4%	16%	-1%	-4%	73%	-1%	24%	11%	-2%	-1%	100%	
5XSS	-11%	31%	96%	42%	-7%	6%	96%	79%	-6%	96%	-4%	20%	96%	79%	97%	44%	57%	96%	85%	97%	2%	54%	96%	80%	8%	97%	28%	9%	98%	82%	-6%	100%

Appendix B: Correlation Matrix from Spike Analysis over Constant Velocity Section of a Strip

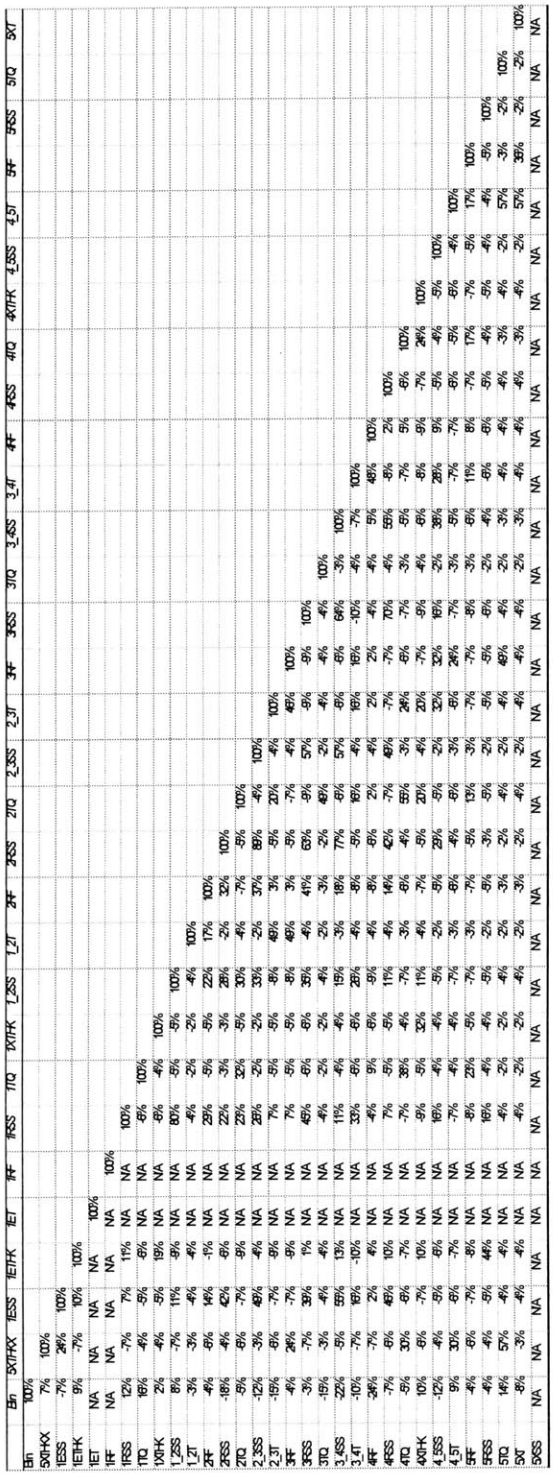

Note: N/A indicates that no spike was observed in least one of the data streams.